Extraplastidial Cytidinediphosphate Diacylglycerol Synthases of *Arabidopsis thaliana*

Von der Fakultät für Mathematik, Informatik und Naturwissenschaften der Rheinisch-Westfälischen Technischen Hochschule Aachen zur Erlangung des akademischen Grades eines Doktors der Naturwissenschaften genehmigte Dissertation

vorgelegt von

Master of Science
Yonghong Zhou
aus
Guangxi, China

Berichter:
Universitätsprofessorin Dr. rer. nat. M. Frentzen
Universitätsprofessor Dr. rer. nat. R. Panstruga

Tag der mündlichen Prüfung: 26. August 2013

To my wife and parents

Part of this work have been published in *Plant Journal* with a title of

Extraplastidial Cytidinediphosphate Diacylglycerol Synthase Activity is Required for Vegetative Development in *Arabidopsis thaliana*

The Plant Journal (2013) **75**, 867-879, DOI: 10.1111/tpj.12248.

Part of this work have been orally presented in the 6th European Symposium on Plant Lipids (07-10 July 2013, Bordeaux, France) with a title of

Extraplastidial Cytidinediphosphate Diacylglycerol Synthases of *Arabidopsis thaliana*

Table of contents

ABBREVIATIONS

35S	35S promoter from Cauliflower Mosaic Virus
aa	amino acid
ATP	adenosine-5'-triphosphate
bp	base pair
BSA	bovine serum albumin
cDNA	complementary DNA
CDP-DAG	cytidinediphosphate diacylglycerol
CDS	cytidinediphosphate diacylglycerol synthase
Ci	Curie
CL	cardiolipin
CLS	cardiolipin synthase
DAG	diacylglycerol
DGDG	digalactosyldiacylglycerol
DGK	diacylglycerol kinase
DGPP	DAG pyrophosphate
DNA	deoxyribonucleic acid
dNTP	deoxyribonucleotide, dATP, dCTP, dGTP, dTTP
DTT	1, 4-dithiothreitol
EDTA	ethylenediaminetetraacetic acid
ER	endoplasmic reticulum
EST	expressed sequence tags
G-3-P	glycerol-3-phosphate
GFP	green fluorescent protein
GPAT	glycerol-3-phosphate acyltransferase
kb	1000 base pairs
LB	T-DNA left border sequence
LPA	lyso-phoshpatidic acid
LPAAT	lysophosphatidic acid acyltransferase
LPP	lipid phosphate phosphatase
MGDG	monogalactosyldiacylglycerol
MLCL	monolysocardiolipin
NPC	non-specific phospholipase C
OD	optical density
PA	phosphatidic acid
PAK	phosphatidic acid kinase
PAP	phosphatidic acid phosphohydrolase
PC	phosphatidylcholine
PCR	polymerase chain reaction

PE	phosphatidylethanolamine
PG	phosphatidylglycerol
PGP	phosphatidylglycerolphosphate
PGPS	phosphatidylglycerolphosphate synthase
PGS	phosphatidylglycerol synthase
PI	phosphatidylinositol
PIS	phosphatidylinositol synthase
PLA_2	phospholipase A_2
PLD	phospholipase D
PS	phosphatidyserine
PSS	phosphatidylserine synthase
RB	T-DNA right border sequence
RFP	red fluorescent protein
RNA	ribonucleic acid
RNase	ribonuclease
rpm	rotations per minute
RT-PCR	reverse transcription polymerase chain reaction
SDS-PAGE	sodium dodecylsulfate polyacrylamide gel electrophoresis
SQDG	sulfoquinovosyldiacylglycerol
TAZ	Tafazzin gene
T-DNA	transferred DNA
TMD	transmembrane domain
UTR	untranslated region
WT	wild type

ABSTRACT

Cytidinediphosphate diacylglycerol synthase (CDS) catalyzes the transfer of a cytidylyl group from CTP to phosphatidic acid so that CDP-diacylglycerol, an important intermediate in glycerolipid biosynthesis of prokaryotic and eukaryotic organisms, is formed. It serves as precursor of anionic phosphoglycerolipids such as phosphatidylinositol, phosphatidylglycerol and cardiolipin. In plant cells CDS isozymes are located in the envelope membranes of plastids, in the inner mitochondrial membranes and microsomes, especially the ER. These CDS isozymes are encoded by a small gene family that comprises five members in *Arabidopsis thaliana,* two of which have previously been shown to code for the plastidial isoforms and be essential for the biosynthesis of plastidial phosphatidylglycerol.

In this work the focus have been on the extraplastidial CDS, encoded by *CDS1*, *CDS2* and *CDS3*. These enzymes were demonstrated to be the integral membrane proteins of the ER and possess similar enzymatic properties. Unlike the *CDS3* gene, the expression of which was only detectable during the generative growth phase, *CDS1* and *CDS2* genes are constitutively expressed. Single Arabidopsis mutants lacking either *CDS1* or *CDS2* showed a wild type phenotype whereas disruption of both genes led to a seedling lethal phenotype, which can be complemented by functional expression of either *CDS1* or *CDS2* cDNA in the mutants. Hence these genes have redundant but indispensible functions. Analyses of *cds1cds2* showed that the cell division and expansion were arrested in the mutant. Based on data from phospholipid labeling and steady state lipid composition, the dramatic accumulation of phosphatidic acid and the decrease of phosphatidylinositol are probably the reasons for the severe consequence of Arabidopsis losing the microsomal CDS functions.

1 INTRODUCTION

1.1 Structure and distribution of membrane phospholipids in plant cells

Biological membranes form hydrophobic barriers and separate the cell and its compartments from the environment, providing a crucial space for life (Somerville *et al.*, 2000). As the major structure components of biological membranes, lipids include a wide variety of compositions, of which the glycerolipids serve as the dominating part. Structurally, glycerolipids consist of a central glycerol molecule, to which fatty acids esterified at *sn1* and *sn2* position, and a hydrophilic group (head) attached to *sn3* position directly (e.g. glyceroglycolipids) or via a phosphate (e.g. phospholipids, Fig. 1.1).

In biological membranes, the fatty acid chains arranged in two layers, serve as a hydrophobic core, keeping the membranes impermeable for polar molecules. The fatty acids vary in the length of carbon chain and the number and position of double bonds. These variations of fatty acids can influence the properties of biological membrane. For example, double mutants of *fad2fad6* lacking polyunsaturated fatty acids in membrane lipids, were not capable of autotrophic growth and produced extremely chlorotic cotyledons and leaves (McConn and Browse, 1998). In addition, certain fatty acids show a positional specific distribution at the glycerol backbone, such as a 3-trans-hexadecenoate, which exist specifically at the sn-2 glycerol carbon of PG (Browse *et al.*, 1985; Gao *et al.*, 2009). The variations of fatty acids can also influence the interaction of lipids and the embedded proteins, hence the biological functions of membranes. A severe disease, the Barth syndrome, is caused by mutations of the *tafazzin* gene, which is involved in the remodeling of the newly synthesized mitochondrial cardiolipin in skeletal muscle and heart: replacing the fatty acids to exclusive linoleic acids forming $(18:2)_4$-CL (Valianpour *et al.*, 2002). Based on analysis of CL species from various organelles, Schlame *et al.* (2005) provided evidence that restriction of the number of fatty acid species rather than the selection of a certain fatty acid (e.g. 18:2), is typical of eukaryotic cardiolipins. In that way, the number diversity of CL species is limited and CL species with symmetric fatty acid distributions are preferentially created.

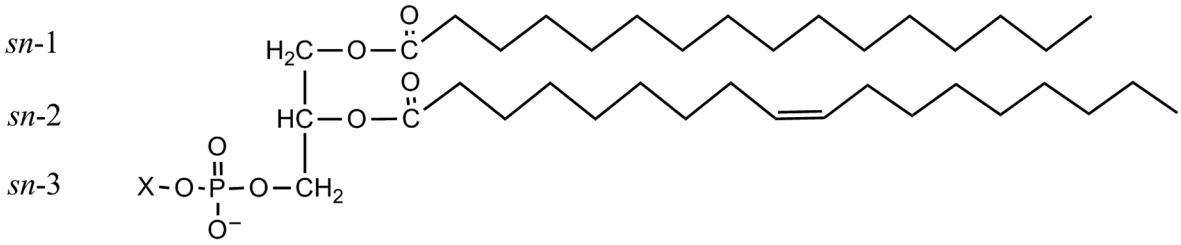

Name of phospholipid	- X
Phosphatidic acid (**PA**)	$-H$
Phosphatidylcholine (**PC**)	$-CH_2CH_2\overset{+}{N}(CH_3)_3$
Phosphatidylethanolamine (**PE**)	$-CH_2CH_2\overset{+}{N}H_3$
Phosphatidylserine (**PS**)	$-CH_2\underset{\overset{+}{N}H_3}{C}HCOO^-$
Phosphatidylglycerol (**PG**)	$-CH\underset{OH}{C}HCH_2OH$
Phosphatidylinositol (**PI**)	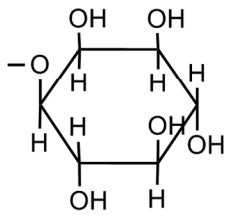
Cardiolipin (**CL**)	$-CH_2CH(OH)CH_2-$

Figure 1.1 Structure of major phospholipid classes. The general structure of a phospholipid is shown at the top. The glycerol backbone is esterified with fatty acids at *sn1* and *sn2* position and is attached with a polar head group at *sn3* position. The structure of the head group of each phospholipid class is given. In cardiolipin (CL), two phosphatidate moieties were attached to a glycerol moiety at *sn1* and *sn3* position.

In contrast to the fatty acid chains, the hydrophilic groups which define the classes of glycerolipids, contact with the aqueous outer environment and inner matrix. The classes and structures of phosphoglycerolipids and the corresponding alcohols are shown in Fig. 1.1. They include the residues of choline in PC, ethanolamine in PE, serine in PS, glycerol in PG, *myo*-inositol in PI and phosphatidylglycerol in CL. The head group is critical for the properties

of glycerolipids: on the one hand, it determines the charge of the membrane lipids, such as PC and PE are zwitterionic lipids, while PG, PI and PS are anionic lipids; on the other hand, the size of head group determines overall shape of the membrane lipids, the protein interaction at the water-lipid interface, and plays an important role in the formation of contact site in comparison to glyceroglycolipids.

The variation of head group and fatty acids provides numerous options of combination, and actually hundreds of lipids are found from various biological membranes with different abundance. Table 1.1 demonstrates the distributions of membrane glycerolipids in plant cells. Extraplastidial membranes contain high amount of PC and PE, especially the latter is excluded from plastids. PG, an anionic lipid, shows a wide range of distribution, with a higher portion in chloroplast membranes. Similar to PG, PI also distributes in all membranes, but with lower abundance in chloroplast membranes. PS and PA are minor phospholipids which are restricted in endomembranes in plant cells. Significant different from other lipids, CL is exclusively present in inner membrane in mitochondria. The glycolipids (MGDG, DGDG and SQDG) are only present in chloroplast membranes.

Table 1.1 Membrane glycerolipid distributions in plant cells[a], adapted from Moreau *et al.* (1998) and Jouhet *et al.* (2007). Full names of glycerolipids are given in the list of abbreviation.

Membrane		PC	PE	PG	PI	PS	PA	CL	MGDG	DGDG	SQDG
Endomembranes	ER + Golgi	43-48	23-26	6	6	3	1[b]				
	Topoplast	15-28	15-28	2	5-9	2	2				
	Plasma membrane	8-36	9-32	1-5	1-6	1-10	5-20				
Chloroplasts	Outer membrane	32		10	5				17	30	6
	Inner membrane			9	1				55	30	5
	Thylakoids			7	1				58	27	7
Mitochondria	Outer membrane	52	22	3	10						
	Inner membrane	37	33	2	4			11			

[a](mol% of total)

[b]ER

The combination of diverse lipids gives an optimal environment for membrane proteins and membrane functions. Therefore, it is critical for learning the cellular activities and processes to understand the properties, biosynthesis and regulation of membrane lipids. In this research, we

have focus on biosynthesis and functions of extraplastidial cytidinediphosphate diacylglycerol, an important intermediate for the biosynthesis of phospholipids.

1.2 *De novo* biosynthesis pathway of membrane glycerolipids in plants

The enzymes and genes for the phospholipid biosynthesis pathway have been studied extensively in prokaryotes and eukaryotes. According to the research scope, we will focus on the results in plants. Fig. 1.2A shows a simplified scheme of the *de novo* biosynthesis of membrane glycerolipids in plants.

The first step of glycerolipid biosynthesis is the acylation of glycerol-3-phosphate (G-3-P) at the *sn1* position catalyzed by glycerol-3-phosphate acyltransferase (GPAT) using acyl-ACP (acyl carrier protein) or acyl-CoA (Coenzyme A) to form lysophosphatidic acid (Fig. 1.2 A). Plant cells contain three types of GPATs, which are located in the chloroplasts, mitochondrial and cytoplasm, respectively (Murata and Tasaka, 1997). The plastidial isoform, also named as ATS1, is a soluble stroma enzyme and prefer to utilize acyl-ACP as acyl donor (Frentzen *et al.*, 1983; Joyard and Douce, 1977; Ishizaki *et al.*, 1988; Nishida *et al.*, 1993). ATS1 is involved in prokaryotic pathway of phospholipid biosynthesis, contributing to the plastidial PG biosynthesis in all plants (Xu *et al.*, 2006). The *ats1* (early termed *act1*) mutant defective in plastidial GPAT showed an alternation of the fatty acid composition of the leaf membrane lipids, increasing the synthesis of lipids by the cytoplasmic pathway (Kunst and Somerville, 1988). A more severe growth phenotype - small green plants and reduced seed set was observed when the RNA level of *ATS1* in T-DNA insertion mutants of *ats1* was reduced by RNAi, but the content of PG was not altered, pointing to the compensation from extraplastidial GPAT (Xu *et al.*, 2006). Unlike plastidial GPAT, the mitochondrial and cytoplasmic isoforms are membrane-associated enzymes and use acyl-CoA as the acyl donor (Frentzen *et al.*, 1990; Murata and Tasaka, 1997). There is a gene family encoding the extraplastidial GPAT in Arabidopsis, and several members involved in multiple functions are identified. For instance, AtGPAT1 and AtGPAT6 have been shown to be essential for tapetum differentiation and male fertility in Arabidopsis (Zheng *et al.*, 2003; Li *et al.*, 2012).

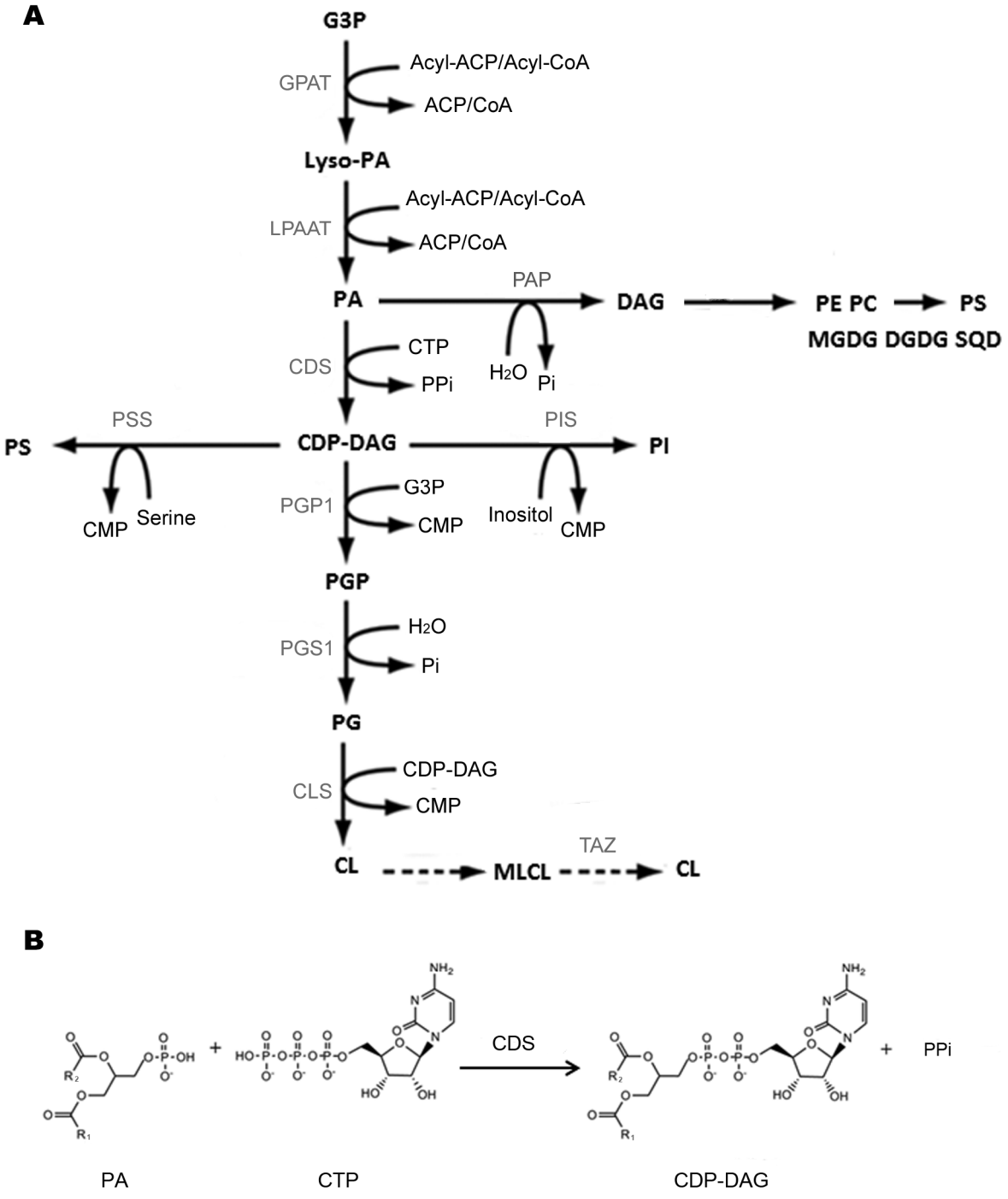

Figure 1.2 A simplified scheme for phospholipid biosynthesis in plants.

A. Scheme focusing on the CDP-DAG dependent phospholipid biosynthesis pathway. These enzymes are involved: GPAT, glycerol-3-phosphate acyltransferase; LPAAT, lysophosphatidic acid acyltransferase; PAP, phosphatidic acid phosphohydrolase; CDS, cytidinediphosphate diacylglycerol synthase; PIS, phosphatidylinositol synthase; PSS, phosphatidylserine synthase; PGP, phosphatidylglycerol phosphate synthase; PGS, PGP phosphatase; CLS, cardiolipin synthase; TAZ, tafazzin.

B. Highlight on CDS catalyzing the formation of CDP-DAG from PA and CTP.

In the second step, a lysophosphatidic acid acyltransferase (LPAAT) catalyzes the acylation reaction at the sn2 position of LPA to form PA, which is a central intermediate in the glycerolipid biosynthesis. Similar to GPAT enzymes, plants possess a single plastidial isoform and multiple extraplastidial isoforms of LPAAT enzymes. The plastidial LPAAT, known as ATS2, localized in the envelope of chloroplasts, preferred utilizing acyl-ACP as substrate and showed a high specificity for palmitoyl group (Joyard and Douce, 1977; Frentzen *et al.*, 1983; Andrews and Mudd, 1985; Bourgis *et al.*, 1999). The *in vitro* assay showed that the plastidial isoform heterologously expressed in bacterium had a preference for 16:0-CoA compared to 18:0-CoA (Kim and Huang, 2004). In Arabidopsis, the plastidial isoform ATS2 is essential for the embryo development. Loss function of *ATS2* led to an embryo lethality and mutant embryos were arrested at the globular stage (Kim and Huang, 2004; Yu *et al.*, 2004). Unlike the plastidial isoform, the endoplasmic reticulum-associated isoform LPAAT2 of Arabidopsis had higher activity with 18:1-CoA than 16:0-CoA (Kim *et al.*, 2005). Except for LPAAT2, Arabidopsis possesses further extraplastidial LPAAT, such as LPAAT3 to 5 (Kim *et al.*, 2005). In addition, Ghosh *et al.* (2009) revealed a soluble LPAAT encoded by At4g24160, which may play a role in PA biosynthesis.

PA is a crucial phospholipid in all eukaryotes, involved in membrane glycerolipid biosynthesis and signal transduction (Fig. 1.3), for the latter, PA acts as a second messenger, rapidly responding for various biotic and abiotic stresses. As a messenger, it is not formed by de novo glycerolipid biosynthesis but from phospholipids by phospholipase C or D, the former in combination with diacylglycerol kinase (Munnik, 2001; Qin and Wang, 2002; Nakamura *et al.*, 2005; Testerink and Munnik, 2005, 2011). Except for channeling into DAG and CDP-DAG for biosynthesis of membrane lipids, PA can also be phosphorylated by PA kinase (PAK) to form diacylglycerol pyrophosphate (DGPP) (van Schooten *et al.*, 2006), or deacylated to lyso-PA (LPA) through PLA_2 activity (Meijer *et al.*, 2001).

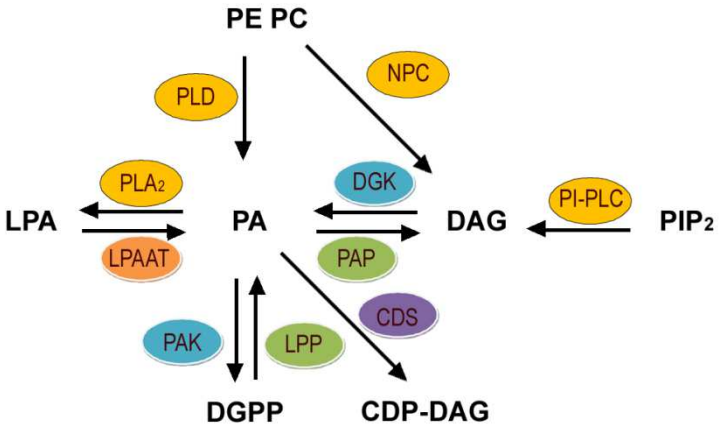

Figure 1.3 Pathway of PA formation and degradation in plants, including both glycerolipid metabolism and signaling pathway, adapted from Testerink and Munnik, 2011. PLA_2, phospholipase A_2; PLD, phospholipase D; NPC, non-specific phospholipase C; PI-PLC, PIP_2 phospholipase C; PAK, phosphatidic acid kinase; DGK, diacylglycerol kinase; LPP, lipid phosphate phosphatase; DGPP, DAG pyrophosphate.

Here, we will focus on the role of PA in the glycerolipid biosynthesis. On one hand, PA is dephosphorylated by phosphatidic acid phosphatase (PAP) to produce diacylglycerol (DAG, Fig. 1.2 A). The chloroplast PAP activity was located on the inner envelope membrane (Joyard and Douce, 1977; Block *et al.*, 1983), and its activity was inhibited when the membrane was enriched in DAG (Malherbe *et al.*, 1992). Three plastidic PAPs in Arabidopsis were identified and characterized to belong to a distinct lipid phosphate phosphatase subfamily with prokaryotic origin (Nakamura *et al.*, 2007). In ER two Mg^{2+}-dependent PAP, named phosphatidic acid phosphohydrolase 1 and 2 (PAH1 and PAH2) act redundantly to repress phospholipid biosynthesis at endoplasmic reticulum (ER). The double mutant *pah1pah2* contains a higher level of phospholipids and exhibits gross changes in ER morphology and massive membrane overexpansion (Eastmond *et al.*, 2010). The formed DAG serves as a precursor for the synthesis of galactolipids in the plastids including monogalactosyldiacylglycerol (MGDG), digalactosyldiacylglycerol (DGDG), and a sulfolipid, sulfoquinovosyl diacylglycerol (SQDG), and the main eukaryotic phospholipids PC and PE in the ER (Fig. 1.2 A). The galactolipids are the most common nonphosphorous lipids and account for 80 % of membrane lipids in green plant tissues (Härtel *et al.*, 2000). In Arabidopsis, there are two types of MGDG synthases based

on the N-terminal portion, located in chloroplasts: type A (MGD1) and type B (MGD2 and MGD3). *MGD1* is abundantly expressed in green tissues, along plant development and essential for photosynthesis and photoprotection in Arabidopsis leaves (Jarvis *et al.*, 2000; Awai *et al.*, 2001; Kobayashi *et al.*, 2004; Aronsson *et al.*, 2008), while the expression levels of *MGD2* and *MGD3* were higher in nongreen tissues (Awai *et al.*, 2001; Kobayashi *et al.*, 2004). Utilizing MGDG and UDP-galactose, DGD1 and DGD2 catalyze the production of DGDG at the outer envelope membrane of chloroplasts and play a role in the proper assembly and maintenance of the photosynthetic apparatus (Härtel *et al.*, 1997; Froehlich *et al.*, 2001; Guo *et al.*, 2005). Disruption of *DGD1* in the *dgd1* mutant resulted in a 90 % reduction of the DGDG content, which can be alleviated by *DGD2* under phosphate deprivation (Härtel *et al.*, 1997, 2000). These data revealed that *DGD1* is responsible for the synthesis of the bulk of DGDG found in chloroplasts, which can be transported from the plastids to other subcellular compartment, while *DGD*2 apparently is involved in the synthesis of DGDG under phosphate starvation (Kelly *et al.*, 2002). SQDG is exclusively located in the plastidial membranes and plays an important role in enabling photosynthesis under phosphate-limiting conditions (Frentzen, 2004). The main eukaryotic phospholipids, PC and PE are *de novo* synthesized via the Kennedy pathway, from DAG with CDP-choline and CDP-ethanolamine, respectively (Gibellini and Smith, 2010). In addition, PC and PE are involved in PS biosynthesis catalyzed by base-exchange-type PS synthase PSS1, which is required for microspore development in Arabidopsis (Yamaoka *et al.*, 2011). Moreover, PS decarboxylases convert PS into PE. In plants, however, these decarboxylases contribute to a minor part of PE production only (Nerlich *et al.*, 2007).

On the other hand, PA is channeled into CDP-DAG, catalyzed by CDS (Fig. 1.2 A). CDP-DAG, the topic of this thesis, is an important intermediate for the biosynthesis of PS, PI and PGP. PS is a relatively minor phospholipid in Arabidopsis, accounting for less than 2 % of total phospholipids (Devaiah *et al.*, 2006). Different from the PSS1 of Arabidopsis (Yamaoka *et al.*, 2011), there are experimental evidences for CDP-DAG dependent PS synthesis activity in plants. A wheat cDNA *TaPSS1* encodes a phosphatidylserine synthase, which shows homology to PSS from both bacteria and yeast, but differs from the base-exchange type PSS in animals (Delhaize *et al.*, 1999). The biosynthesis of phosphatidylinositol (PI) and its polyphosphorylated derivatives, however, depends on microsomal CDP-DAG (Lykidis and Jackowski, 2000; Löfke

et al., 2008; Gillaspy, 2011). In Arabidopsis, PI is produced by two microsomal enzymes PIS1 and PIS2 encoded by two genes (Collin *et al.*, 1999; Xue *et al.*, 2000; Löfke *et al.*, 2008). PI is an important component of biomembranes, contributing more than 20 % of the phospholipids in nonphotosynthetic plant membranes (Devaiah *et al.*, 2006), but very low levels in chloroplasts (Roughan and Slack, 1982; Devaiah *et al.*, 2006). Furthermore, the phosphorylated derivates of PI play an important role in signal transduction by mediating temporal and spatial information to downstream effectors (Gillaspy, 2011).

Differing from PS and PI, PG is mainly distributed in photosynthetic tissues (Devaiah *et al.*, 2006). As depicted in Fig 1.2, PG is synthesized from CDP-DAG and G-3-P forming PGP, which is subsequently dephosphorylated by a phosphatidylglycerolphosphate phosphatase (PGS) so that PG is formed. Arabidopsis possesses two PGP synthase genes (*PGP1* and *2*), which encode enzymes closely related to the bacterial PGP synthases, but unrelated to the mitochondrial enzymes of yeast and mammals (Müller and Frentzen, 2001). PGP2 represents the microsomal isoform whereas PGP1 is a preprotein that is targeted not only to plastids but also to mitochondria (Babiychuk *et al.*, 2003). Plastidial PG has been shown to be indispensable for the development and function of thylakoid membranes (Kruse *et al.*, 2000; Sato *et al.*, 2000). This was reflected in the phenotype of *pgp1* mutant of Arabidopsis lacking plastidial PG. The mutant developed pale yellow leaves and required sucrose for growth (Hagio *et al.*, 2002; Babiychuk *et al.*, 2003). These and further mutants defective in plastidial membrane lipid biosynthesis revealed that thylakoid membranes require a defined level of anionic membrane lipids PG and SQDG for proper function (Xu *et al.*, 2002; Yu and Benning 2003; Babiychuk *et al.*, 2003). In this regard SQDG can partially substitute for PG, but a defined level of PG is indispensable for photoautotrophic growth.

In eukaryotes, PG and CDP-DAG at the inner mitochondrial membrane are involved in the formation of the mitochondrial marker lipid CL (Schlame and Greenberg, 1997; Schlame and Hostetler, 1997). Interestingly, mutants with an inactivated *PGP1* provided evidence that mitochondria can compensate for their defect in PG biosynthesis for CL biosynthesis, likely by importing microsomal PG formed by the activity of PGP2 (Babiychuk *et al.*, 2003). In Arabidopsis, a mitochondrial CL synthase was identified and characterized (Katayama *et al.*, 2004; Nowicki *et al.*, 2005). Its amino acid sequence resembles those of bacterial and plant PGP

synthases. Furthermore, based on the results that *de novo* synthesized CL in yeast and human requires a remodeling of its fatty acid composition catalyzed by tafazzin (TAZ, Vaz *et al.*, 2003; Houtkooper *et al.*, 2009), a remodeling pathway for CL may exist in plants as well.

1.3 Biosynthesis of CDP-DAG in prokaryotes and eukaryotes

As shown in Fig. 1.2, cytidinediphosphate diacylglycerol (CDP-DAG) is an important branch point intermediate in the glycerolipid biosynthesis. Its activity was originally discovered in microsomal preparations from pig liver (Carter and Kennedy, 1966), but it is now known to be ubiquitous in prokaryotic and eukaryotic organisms. Structurally, CDP-DAG is a liponucleotide, consists of cytosine 5'-diphosphate attached to diacylglycerol via a phosphodiester bond (Fig. 1.2 B), which provides the chemical energy in diphosphate for the downstream biosynthesis reaction of PG, PS, PI and CL. In that way, it is different from the biosynthesis reactions of PC, PE, MGDG, DGDG and SQDG, in which the head groups but no diacylglycerol are phosphorylated, and provide energy for the reactions.

CDS of bacteria is associated with the cytoplasmic membrane (Bell *et al.*, 1971; White *et al.*, 1971; Icho *et al.*, 1985; Sparrow and Raetz, 1985). The cytoplasmic fraction showed the highest specific activity of CDS, while the specific activity in the outer membrane fraction was very low (Bell *et al.*, 1971). Moreover, *CDS* of *E. coli* was cloned, and the respective protein was purified and characterized, showing a high substrate specificity: utilize only CTP and PA with long chain fatty acids(Icho *et al.*, 1985; Sparrow and Raetz, 1985).

In yeast, purification and characterization of CDS *in vitro* showed that CDS required Mg^{2+} and Triton X-100 for activity, and had a pH optimum of 6.5 (Kelley and Carman, 1987). CDS in yeast is encoded by only one gene, the disruption of which will lead to incapability of spore germination and vegetative growth of cells (Shen *et al.*, 1996). CDS activity involves in the regulation of the biosynthesis of PS and PI (Shen and Dowhan, 1997).

Drosophila possesses one *CDS* gene like yeast, but forms two CDS isoforms by alternative RNA splicing namely the constitutively isoform and the photoreceptor specific isoform. The latter serves as key regulator of phototransduction. Its activity is required for the regeneration of PIP_2,

thus regulate PI-mediated signaling cascade in Drosophila. It was demonstrated that *cds* mutants cannot sustain a light-activated current as a result of depletion of PIP_2, while overexpression of *CDS* in photoreceptor cells increased the amplitude of light response (Wu *et al.*, 1995). Vertebrates including human possess two *CDS* genes, the amino acid sequence of which shows high similarity to Drosophila eye CDS (Lykidis *et al.*, 1997; Halford *et al.*, 1998; Heacock *et al.*, 2002). Expression of the human cDNA in a null *cds1* mutant yeast strain complements its growth defect and shows CDS activity. Transfection of this cDNA of *CDS1* into mammalian cells leads to increased CDS activity in the membrane fractions of *CDS* transfectants (Weeks *et al.*, 1997; Heacock *et al.*, 2002). Northern blot showed *CDS* was expressed at distinctly different levels in various human tissues (Lykidis *et al.*, 1997). *CDS1* shows a high level of expression in the photoreceptor layer of adult retina, while *CDS2* is highly expressed in the differentiating neuroblasts of the neural retina and in the central nervous system during embryonic development (Volta *et al.*, 1999). In addition, Pan *et al.* (2012) showed that zebrafish CDS2 activity was involve in regulation of vascular endothelial growth factor A (VEGFA) signaling and vascular morphogenesis, via regulation of PIP_2 availability.

Different from animals, plants possess multiple forms of CDS. Enzymatic assays using different plant materials have shown multiple localizations of CDS in plants, including ER, mitochondria, chloroplasts and plasma membrane (Andrew and Mudd, 1985; Kleppinger-Sparace and Moore, 1985; Hanenberg *et al.*, 1993). In the inner envelope membrane of pea chloroplasts, the synthesis of CDP-DAG using PA and CTP, followed by PG using CDP-DAG and G-3-P was proved by Andrew and Mudd (1985). In the assay using subcellular fractions from castor bean endosperm, CDS activity was detected in ER and mitochondrial membranes. CDS in the ER had a pH optimum of 6.5 and preferred Mn^{2+} for activity, which was inhibited by Triton X-100, while the mitochondrial CDS had a pH optimum of 6.0 and preferred similar divalent cations as the ER isoform for activity, which were stimulated by Triton X-100 (Kleppinger-Sparace and Moore, 1985). Also, the genes of *StCDS1* in potato and *AtCDS1* in Arabidopsis were cloned and showed high similarity. Both proteins belong to the eukaryotic CDS proteins and contain eight predicted TMD. *In vitro* assay of *StCDS1* expressed in *E. coli* resulted in a CDS activity (Kopka *et al.*, 1997). In *Arabidopsis thaliana*, CDS isoforms are encoded by a small gene family that comprises five members (Beisson *et al.*, 2003). These genes termed *CDS1* to *CDS5* were

functionally expressed in yeast cells and rescued the lethal phenotype of the mutant strain carrying a disrupted *CDS1* gene. CDS1, CDS2 and CDS3 protein sequences are very similar to each other and each protein possesses the same pattern of predicted transmembrane domains (Haselier *et al.*, 2010). They resemble CDS proteins of vertebrates (Wu *et al.*, 1995; Volta *et al.*, 1999; Pan *et al.*, 2012) but differ in sequence and structure from the closely related CDS4 and CDS5 proteins, which show highest sequence similarity to cyanobacterial proteins (Sato *et al.*, 2000). CDS4 and CDS5 have been shown to represent the plastidial isoforms located in the envelope membranes of plastids (Froehlich *et. al.*, 2003; Haselier *et al.*, 2010). Analysis of Arabidopsis *cds4cds5* mutants provided clear evidence for the importance of plastidial PG for photoautotrophic growth (Haselier *et al.*, 2010), in line with results obtained with an Arabidopsis mutant deficient or defective in the plastidial phosphatidylglycerolphosphate synthase gene (Hagio *et al.*, 2002; Xu *et al.*, 2002, 2006; Babiychuk *et al.*, 2003).

1.4 Goal of the research

The research described in this thesis focused on extraplastidial cytidinediphosphate diacylglycerol synthases of *Arabidopsis thaliana*, termed CDS1, CDS2 and CDS3. Firstly, these CDS enzymes should be studied using membranes of yeast cells expressing one of the *CDS* genes as enzyme source and PA as well as radioactivity labeled CTP as substrates. After optimizing the assay conditions, the enzymatic properties of the three CDS proteins should be determined and compared with the plastidial isoforms (CDS4 and CDS5).

Secondly, it was planned to investigate the subcellular localization of the CDS proteins by fusing a full or partial CDS sequence with a fluorescence proteins and expressing the fusion constructs in plant cells.

To learn the biological functions of individual extraplastidial *CDS* gene, different T-DNA insertion lines should be identified and analyzed on the transcription and product level. Phenotype of *CDS* knock out mutants will show whether for instance *CDS1* and *CDS2* have redundant functions, like the plastidial isoforms, *CDS4* and *CDS5*. To create double mutants by crossing experiments with single mutants are planned. Subsequently, the mutants should be

investigated by multiple approaches, such as complementation assay, microscopic analysis, *in vivo* phospholipid labeling, and lipid composition analysis.

In summary, it is planned to get an overall view of extraplastidial CDSs of Arabidopsis helping us to understand the biosynthesis and functions of CDP-DAG and its importance in regulation the metabolism of glycerolipids in plants.

2 MATERIALS AND METHODS

2.1 Instruments

Table 2.1 Instruments used in this work

Name	Producer
Centrifuge 5417 C	Eppendorf
Centrifuge 5417 R	Eppendorf
Centrifuge 5810 R	Eppendorf
Centrifuge Sorvall RC-5B	Thermo Scientific
Ultracentrifuge Optima L60	Beckman
Thermocycler Mastercycler Gradient	Eppendorf
Thermocycler Primus 96	MWG
Plant clean bench	Cleaner
Bacterial clean bench	Gelaire
Thermomixer	Eppendorf
Dounce Homogenisator	B.Braun
Radioactive contaminate monitor FHT 111M	ESM
Spectrophotometer SmartSpec 3000	Bio-Rad
Spectrophotometer NanoDrop 2000c	Thermo Scientific
pH-Meter HI9321	Hanna inst.
Fluorescence Microscope BZ-9000	Keyence
Fluorescence Microscope DMR	Leica
Confocal laser scanning microscope	Leica
Electron microscope EM10	Zeiss
Bioimager FLA-3000	Fujifilm
GelDoc XR+ imaging system	Bio-Rad
MicroPulser electoporator	Bio-Rad
HPLC-Chip/MS system 1200 series	Agilent
LS6500 Multi-Purpose Scintillation Counter	Beckman Coulter

2.2 Chemicals, consumables and kits

Chemicals and kits

Table 2.2 reagents and kits used in this work

Catalogue	Name	Manufacturer
Antibiotics	Carbenicilin disodium	Duchefa

	Cefotaxim sodium	
	G418 disulfate	Duchefa
	Gentamycin	
	Glufosinate Ammonium	
	Hygromycin	
	Kanamycin monosulfate	
	Rifampicin	
	Spectinomycin	
	Streptomycin sulfate	
	Tetracycline	
Probes	Mito Tracker Red	Invitrogen
	Mito Tracker Green	
	ER Tracker Green	
DNA markers	GeneRuler^{TM} 1k DNA ladder	Fermentas
	GeneRuler^{TM} 100 bp Plus	
Phospholipid standards	Phosphatidylcholine	Sigma
	Phosphatidylethanolamine	
	Phosphatidic acid	
	Phosphatidylglycerol	
	Phosphatidylinositol	
	Phosphatidylserine	
	Cardiolipin	
Medium	MS medium B5 vitamin	Duchefa
	Gamborg B5 medium	
	MS basal salt mixture	
Kits	innuPREP DOUBLEpure Kit	Analytik Jena
	innuPREP plasmid Mini Kit	
Enzymes	Zymolyase 20T	MP Biomedicals
	DNA restriction enzymes	Fermentas
	Phusion DNA polymerase	New England Biolabs
	SupraThermo Taq DNA polymerase	Genecraft
	M-MLV Reverse transcriptase	Promega
	DNase I	Fermentas
	RNase	Fermentas
Radioactive materials	[33P] phosphoric acid	Hartmann analytic
	[3H] CTP	Perkin Elmer
	[14C] G-3-P	Perkin Elmer
	β-estradiol	Sigma
	TLC plates SIL G25	Macherey & Nagel

Oligonucleotides

Oligonucleotides used for amplification and sequencing were synthesized by Eurofins MWG Operon, and the sequences were shown in Appendix (Table. A1).

Plasmids

Table 2.3 Plasmids used in this work

Name	Source or reference
pAgrikola*	Agrikola Consortium
pENTR/SD/D-TOPO	Invitrogen
pH7WG2.0	Karimi *et al.*, 2002
pH7FWG2.0	Karimi *et al.*, 2002
pK7RWG2.0	R. Tsien
pMDC7	Zuo *et al.*, 2000
	Curtis and Grossniklaus, 2003
pSOUP**	Hellens *et al.*, 2000
pTRAkc-rbcs1-cTP	Maclean *et al*., 2007
pTRAkc-ERH	Maclean *et al.*, 2007
pWatergate	CSIRO plant industry
pYES-DEST52	Invitrogen

The structures of plasmids are shown in Appendix (Fig. A1 – A7).

*pAgrikola was constructed by cloning the NotI fragment from Hellsgate 12 containing the 35S promoter and twin Gateway™ cassettes into pGreen 0229.

** The original helper plasmid for pGreen, which will not replicate in Agrobacterium if pSOUP is not present.

2.3 Organisms and their cultivation

Table 2.4 Organisms used in this work

Species	Strain	Source or reference
Escherichia coli	DH5α	Bethesda Research Laboratories
	Top10	Invitrogen
	BL21AI	Invitrogen
	DB3.1	Invitrogen
Agrobacterium tumefaciens	GV3101::pMP90RK	Koncz and Schell (1986)
	GV3101::pMP90	Koncz and Schell (1986)
Saccharomyces cerevisiae	BY4743 YBR029c::KanMX (*cds1*)	Euroscarf

Nicotiana tabacum	BY2	Nagata *et al.* (1992)
	SR1	Maliga *et al.* (1973)
Arabidopsis thaliana	Col-0	-

2.3.1 *Escherichia coli*

The cultivation of *Escherichia coli* was carried out at 37 °C in LB medium or on LB Agar plates (Roth, Table 2.5) in thermal constant room. The medium was autoclaved for 15 min, and after cooling down, antibiotics were added for selection if needed. For mini-preparation, *E. coli* was cultivated in 5 ml test tubes and rotated on inclined plate at 60 rpm, and for large preparation, culture was shaken horizontally at 140 rpm. *E. coli* strains with/without a plasmid were stored in 40 % glycerol at -80 °C.

Table 2.5 LB medium and LB-agar for *E. coli* and agrobacteria

Components	**Concentration**
Tryptone	10 g/l
Yeast extract	5 g/l
NaCl	10 g/l
pH 7.0	
Agar (for plates)	15 g/l
ddH_2O	to 1 liter
Autoclave at 121 °C for 15 min	

2.3.2 *Agrobacterium tumefaciens*

A. tumefaciens strain GV3101 containing pMP90RK (GV3101::pMP90RK) has three resistance genes: rifampicin on genomic DNA, gentamycin and kanamycin on the Ti-plasmid. GV3101::pMP90RK was used almost in all of the transformations of plants in this work, except transformation of pAgrikola, which harbors a kanamycin-resistant gene. GV3101::pMP90 was used for pAgrikola, because pMP90 has gentamycin-resistant gene only. Before transformation of pAgrikola, GV3101::pMP90 was first transformed with a helper vector pSOUP containing a tetracycline resistance gene, giving rise to GV3101::pMP90::pSOUP. Both strains were cultivated in LB medium or LB-Agar plates at 28 °C in a thermal constant room with suitable

antibiotics: rifampicin, 20 mg/l; gentamycin, 50 mg/l; kanamycin, 50 mg/l; spectinomycin, 100 mg/l; streptomycin, 300 mg/l; carbenicilin, 50 mg/l; tetracycline, 10 mg/l. The verified strains with/without a destination vector were stored in 40 % glycerol at -80 °C.

2.3.3 *Saccharomyces cerevisiae*

Yeast was incubated in YPD (Table 2.6) or minimal medium SC-U (Table 2.7), shaken at 100 rpm at 28 °C in a thermal constant room. Antibiotic G418-containing and uracil-lacking medium was used for selection of genomic and plasmid marker, respectively. The verified strains with/without a destination vector were stored in 40 % glycerol at -80 °C.

Table 2.6 YPD medium for yeast

Components	**Concentration**
Yeast extract (Duchefa)	10 g/l
Peptone (Duchefa)	20 g/l
D-glucose (Roth)	20 g/l
Autoclave at 121°C for 15 min	

Table 2.7 Minimal medium (SC-U) for yeast

Components	**Concentration**
YNB without ammonium sulfate (MP Biomedicals)	1.7 g/l
CMS-Leu-Ura (MP Biomedicals)	0.68 g/l
Ammonium sulfate (Merck)	5 g/l
Glucose (without induction)	20 g/l
Galactose (induction)	20 g/l
Agar (for solidified plates)	10 g/l
ddH_2O	to 1 liter
Autoclave at 121 °C for 15 min	

2.3.4 *Arabidopsis thaliana*

The T-DNA insertion mutants of *cds1* and *cds2* (SALK_088268 and SALK_011704, Alonso *et al.*, 2003) were obtained from the European Arabidopsis Stock Centre (The University of Nottingham, UK). Seeds were surface sterilized and sown on 0.8 % agar-solidified MSG medium (MS medium including Gamborg B5 vitamins; Duchefa) containing 2 % sucrose. After

stratification in the dark at 4 °C for 2 days, seeds were germinated by incubation in short day conditions (8-h-light/16-h-dark, 22 °C). Two-week-old seedlings were transferred to potting soil. To induce flowering, plants were cultivated under long day conditions (16-h-light, 23 °C/8-h-dark, 21 °C).

For inducing callus from seedlings of Arabidopsis, the cotyledons, hypocotyls and radicles from 5-day-old seedlings were harvested and transferred to callus inducing medium (CIM, Table 2.8). For inducing expression of *CDS* in pMDC7 in Arabidopsis, 10 µM β-estradiol was applied to callus inducing medium. After incubation at 26 °C in the dark for 3 weeks, the emerged calluses were further cultivated on callus inducing medium under the same conditions, and transferred to fresh medium each week.

Table 2.8 Callus inducing medium for Arabidopsis

Components	**Concentration**
Gamborg B5 medium (Duchefa)	3.16 g/l
Sucrose (Roth)	30 g/l
Plant agar (Duchefa, for plates)	8 g/l
Kinetin (Duchefa)	0.05 mg/l
2, 4- Dichlorophenoxyacetic acid (Duchefa)	0.5 ml/l
pH to 5.7 by KOH, autoclave at 121 °C for 15 min	
β-estradiol (for inducing *CDS* expression)	10 µM

2.3.5 *Nicotiana tabacum*

Tobacco BY-2 cells (Nagata *et al.*, 1992) were cultivated on MSBY plates at 26 °C and transferred to fresh plates every two weeks, or in MSBY medium (see recipe below), shaken at 140 rpm at 26 °C, and transferred to fresh medium each week.

Table 2.9 MSBY medium for BY-2 cells

Components	**Concentration**
MS basic salts (Duchefa)	4.3 g/l
Sucrose (Roth)	30 g/l
2, 4-Dichlorophenoxyacetic acid (Duchefa)	0.2 mg/l
Thiamine (Sigma)	1.0 mg/l
myo-Inositol (Duchefa)	100 mg/l

Plant agar (Duchefa, for plates)	8 g/l
pH to 5.7 by KOH, autoclave at 121 for 15 min	

2.4 Transformation

2.4.1 *Escherichia coli*

Preparation of electrocompetent cells of *E. coli* Transformation of *E. coli* was performed by electroporation, an efficient transforming method including preparation of electrocompetent cells and electroporation. To prepare competent cells, firstly *E. coli* was cultivated overnight in LB medium and subsequently inoculated 500 ml LB medium with antibiotics if needed. The cells were grown at 37 °C at 140 rpm to an OD600 of 0.7 (mid-log phase). The culture were chilled on ice for 20 min. The culture, containers and solutions were kept as close to 0 °C as possible in the subsequent steps. The cells were harvested by spinning down at 4000 x g for 15 min at 4 °C, resuspended in 500 ml of ice-cold 10 % glycerol, then centrifuged again at 4000 x g for 15 min at 4 °C. Repeat the washing step with 250 ml then 20 ml ice-cold 10 % glycerol. The cell pellet was finally resuspended in 2 ml of ice-cold 10 % glycerol. The cell suspension were separated into aliquots (40 µl per aliquot), frozen in liquid nitrogen, and stored at -80 °C.

Transformation of *E. coli* For electroporation, the *E. coli* aliquot was thawed on ice and mixed with 100 to 200 ng of DNA (1 – 2 µl) which should be in distilled water or low salt solution like TE buffer. After 1 min incubation on ice, the mixture was transferred into a 0.2 cm pre-cooled cuvette (note: dry the surface) and electroporated once by MicroPulser (Bio-Rad, Ec2 program, 2.5 kV, 5 msec). The suspension in the cuvette was immediately mixed with 1 ml of LB medium without antibiotic, transferred into a 1.5 ml tube and shaken at 1000 rpm at 37 °C for 1 hour. Different volumes of suspension were spread on LB plates with suitable antibiotics. After overnight incubation, positive colonies would be appeared and were analyzed by colony PCR, followed by plasmid isolation and restriction analysis.

2.4.2 *Agrobacterium tumefaciens*

Transformation of *A. tumefaciens* was similar to that of *E. coli*, except some modifications in cultivation and electroporation: For competent cell preparation, the agrobacterial cells were

cultivated at 28 °C and grow slower than *E. coli*. Overnight incubation for large culture was needed to reach mid-log phase. For transformation, "Agr" program (2.2 kV, 5 msec) was used to electroporate cells. Before the suspension was spread on selection plates, it should be incubated in LB medium at 28 °C for 3 hours. After cells were spread on selection plates, it took 36 to 48 hours to obtain the positive colonies. The putative plasmid in agrobacterium was isolated and retransformed into *E. coli* for verification by restriction analysis, because of the low copy number in agrobacterium.

2.4.3 *Saccharomyces cerevisiae*

Preparation of competent *S. cerevisiae* cells 20 ml of YPD medium was inoculated with one yeast colony, and incubated at 28 °C for 24 hours. 200 ml of YPD medium was inoculated with 100 µl 24 h preculture and incubated overnight at 28 °C. On the coming morning, the culture was chilled on ice for 20 min, divided into 4 of 50 ml falcon tubes. The cells were harvested by centrifugation at 2000 x g for 15 min at 4 °C. Each pellet was resuspended in 50 ml ice-cold sterile distilled water and centrifugation was carried out again at 2000 x g for 15 min at 4 °C. The washing step was repeated with 50 ml ice-cold sterile distilled water and then with 10 ml ice-cold sterile 1 M sorbitol. All of the suspensions were combined and centrifugated. The cell pellet was finally resuspended in 200 µl of 1 M ice-cold sorbitol solution. The competent cells were ready for transformation and could not be frozen for long time storage.

Electroporation of *S. cerevisiae* cells 2 µl plasmid DNA (up to 120 µg) was transferred into 40 µl competent cells and incubated on ice for 5 min. The mixture was transferred into a 0.2 cm cuvette. The electroporation was carried out by Electroporator (Bio-Rad) with program Sc2 (1.5 kV, 5 msec). 1 ml of 1 M ice-cold sorbitol solution was added, mixed, and transferred to a 1.5 ml tube. The cells were spun down by centrifugation at 12000 rpm for 1 min. After pouring out the supernatant, the cells were resuspended in the rest solution and spread on a selective minimal medium plate (SC-U). The plates were incubated at 28 °C for 2-3 days to obtain positive colonies which would be confirmed by PCR. The putative transformed plasmid would be isolated and retransformed into E. coli for restriction analysis.

2.4.4 *Arabidopsis thaliana*

Arabidopsis was transformed with destination vectors via the floral dip method (Clough and Bent, 1998). In brief, agrobacterium containing destination vector was cultivated in 500 ml LB medium with suitable antibiotics at 28 °C. Until OD_{600} reached 1, the cells were harvested by centrifugation at 6000 rpm for 10 min at 4 °C, washed once with ddH_2O, subsequently resuspended in 500 ml 5 % sucrose solution containing 0.04 % Silwet L-77. Arabidopsis inflorescences were inverted dipped into agrobacterium suspension for 3 min, 3 times. After the infiltration, Arabidopsis plants in a covered container were incubated at about 12 °C for 24 hours and transferred to a long day room (16 hour light, 23 °C / 8 hour dark, 21 °C). Seeds with some transformants were harvested and selected.

2.4.5 *Nicotiana tabacum*

Transformation of tobacco BY2 cells The transient transformation of BY2 cells was performed according to Sack *et al.* (2007). Firstly, recombinant Agrobacterium GV3101::pMP90RK cells containing GFP or RFP construct were harvested, washed once with sterile ddH_2O and MSBY medium, consecutively. After measurement of OD_{600}, a suitable volume of Agrobacterium was added to 3 ml of 4-day-old BY2 suspension culture in a petri dish to a final OD_{600} of 0.05. To get higher transformation efficiency, acetosyringone was added to a final concentration of 200 µM. After 2 - 3 days of incubation at 26 °C, transient transformed cells were searched and observed by fluorescence microscopy.

For stable transformation, the 3-day-old co-culture of BY2 and Agrobacterium was transferred onto solidified MSBY medium supplemented with 50 mg/l kanamycin (select BY2 transformants) and 200 mg/l cefotaxime (kill remained agrobacterium). After drying of liquid medium, the plates were sealed with parafilm and incubated at 26°C. Kanamycin-resistant BY2 calluses after 4 weeks incubation were genotyped by PCR, subsequently cultivated in suspension. The suspension culture was transferred to fresh medium each week and observed by fluorescence microscopy at 3 – 5 days after transferring.

Transient expression in tobacco leaf epidermal cells Tobacco SR1 (Maliga *et al.* , 1973) plants were grown at 16-h-light, 23 °C/8-h-dark, 21 °C and used for studying subcellular

localization of fusion proteins using a rapid transient expression method according to Sparkes *et al.* (2006). Agrobacterium tumefaciens GV3101::pMP90RK containing GFP or RFP constructs of interest were grown in LB medium with appropriate antibiotics overnight, at 28 °C, 140 rpm. The OD600 of culture was measured and the cells were harvested and washed once with water to remove salts and antibiotics. After resuspending in infiltration medium (Table 2.10), medium with agrobacteria was infiltrated into tobacco leaves. The 1-3 apical leaves and the leaves close to root should not be selected, because apical leaves are hard to be infiltrated and leaves close to root show a low transformation rate. To infiltrate the epidermal cells, a syringe with suspension and without needle was gently rubbed on the abaxial side of leaves and the suspension was injected into the mesophylar air spaces of the cells. After injection, the infiltrated area was marked, and tobacco plants were incubated in the dark overnight and grown at 16-h-light, 23 °C/8-h-dark, 21 °C for 48 hours. For fluorescence microscopy, the infiltrated areas of leaves were cut out and observed using a confocal laser microscope (Leica).

Table 2.10 Infiltration medium

Components	**Concentration**
D-glucose (Roth)	5 g/l
MES (Roth)	50 mM
$Na_3PO_4 \bullet 12H_2O$ (Roth)	2 mM
Acetosyringone (Sigma-Aldrich)	200 µM
Prepare freshly before use, and not need to be autoclaved	

2.5 Isolation of DNA from plant materials

Arabidopsis leaves (5 – 10 mg) were harvested in 2 ml eppendorf centrifuge tubes containing about 20 ceramic beads, and quick frozen in liquid nitrogen. The tubes were quickly transferred to a box and thoroughly shaken to pulverize the leaves. 500 µl of extraction buffer (Table 2.11) was added and mixed by vortexing. 100µl of chloroform was added and vortexed again. The mixture was shaken in an Eppendorf thermomixer at 1250 rpm at 25 °C for 10 min, subsequently centrifuged by an Eppendorf table centrifuge at 12 000 rpm at room temperature for 10 min. 250 µl of the clear upper phase was transferred to a fresh 1.5 ml tube. The DNA was precipitated by adding 1 volume of isopropanol and mixing by inverting the tube. For better precipitation,

mixture was incubated at – 20 °C for 15 min. A centrifugation at 14 000 rpm at 4 °C for 10 min was performed to spin down the DNA. After removing the supernatant, the DNA pellet was washed with 500 µl of 70 % ethanol. Another centrifugation at 14 000 rpm at 4 °C for 5 min was carried out to collect the DNA. After completely removing the ethanol solution, the DNA pellet was air dried at room temperature for 5 min. DNA were dissolved by addition of 50 µl ddH_2O. After incubation at 37 °C for 5 min and mixing by vortexing, the DNA solution was ready for genotyping and stored at – 20 °C.

Because the growth of double mutant *cds1cds2* are arrested (Fig. 3.14), the individual plants is not sufficient to isolate DNA as described upper. We used two ways to solve this problem. First, a mini preparation modified from upper protocol was used for one *cds1cds2* seedling. The volume of reagents and solutions in mini preparation was 1/5 of that in the upper protocol and finally DNA was eluted in 8 µl ddH_2O. The DNA extraction should be competent for routine PCR. Second, a rapid protocol for DNA extraction was used according to Kasajima *et al.* (2004). A seedling of *cds1cds2* was harvested in a 1.5 ml centrifuge tube containing 10 µl 10-time-diluted TE buffer (TE buffer: 10 mM Tris-HCl (pH8) and 1 mM EDTA), and crushed by a yellow pipette tip against the tube wall until the solution become slight green. The DNA dissolved in buffer is suitable for PCR analysis. Two notices for this protocol: first, excess crushing must be avoided, because it would inhibit the following PCR amplification; second, the DNA solution should be chilled on ice, used freshly, and cannot be stored for next usage.

The procedure of DNA isolation from Arabidopsis calluses or tobacco BY2 cells was similar to that from Arabidopsis leaves, except some modification, such as more initial plant material was used, 20 – 30 mg. After quick frozen by liquid nitrogen, the calluses were crushed by mortar and pestle, and transferred to 2 ml tube. After that the isolation steps were started.

Table 2.11 DNA extraction buffer

Components	**Concentration**
Tris-HCl, pH8.0 (Roth)	200 mM
NaCl (Roth)	240 mM
EDTA, pH 8.0 (Duchefa)	25 mM
SDS (Roth)	1 %

2.6 Polymerase chain reaction

The polymerase chain reaction (PCR) is a method to amplify a specific DNA fragment from a few copies to millions copies by multiple repeating of denaturation, annealing and extension (Mullis *et al.*, 1986). For a specific target sequence and a special purpose, optimal reaction conditions had to be set up, considering polymerase, primers, template, reaction buffer, annealing temperature, extension duration, and number of cycles.

2.6.1 Routine PCR

Routine PCR was used for determining the genotype of plant materials of which the DNA was extracted in advance. Since the DNA extracted by rapid method is low abundance and usually contaminated with proteins, salts, and even some ethanol residual, the polymerase used must be able to tolerate these disadvantage. SupraTherm^{TM} Taq DNA polymerase (Genecraft) we used is competent for this work. Mg^{2+} is required for the polymerase and supplemented in the buffer. The Oligonucleotides were designed in a melting temperature range of 52 – 60 °C. The annealing temperature in the PCR thermal cycles was set as (T_m – 3) °C, but in the range of 52 – 60 °C. The following reaction mixture (Table 2.12) and thermal cycling conditions (Table 2.13) for routine PCR was used in this work. The amplification products were separated and visualized by agarose gel electrophoresis described below in section 2.8.

Table 2.12 Routine PCR mixture setup

Component	Volume (µl)	Final concentration
H_2O	7.2	
10X PCR buffer (Genecraft)	1	1X, 1.5 mM Mg^{2+}
10 mM dNTP (Fermentas)	0.2	0.2 mM for each dNTP
Primer forward (Eurofins)	0.2	0.2 µM
Primer reverse (Eurofins)	0.2	0.2 µM
Taq DNA polymerase (Genecraft)	0.2	0.1 U/µl
DNA template	1	
Total volume	10	

Table 2.13 Routine PCR thermal cycles

Step	Temperature (°C)	Time	Number of cycles
Initial denaturation	95	3 min	1

Denaturation	95	30 sec	
Primer annealing	Tm – 3, 52 – 60	30 sec	35
Extension	72	1 min/1 kb*	
Final extension	72	5 min	1
Keep	8	∞	1

*The time for extension depends on the length of target sequence.

2.6.2 Colony PCR

Colony PCR was used for amplifying sequences of genomic DNA or plasmid DNA in bacteria and yeast. It is an ease and rapid method that omits the DNA isolation steps. The DNA template in cells is released at the initial denaturation step. Because there are a lot of components in bacterial and yeast cells which could inhibit polymerase reaction, it is important that only a small amount of cells are added in the reaction. To the end, a yellow tip attached to a pipette was applied to touch the colony once and pipette up and down to mix in PCR mixture. Except that the DNA template volume in routine PCR is treated as 0 and substituent with water, the mixture and thermal program of colony PCR is similar to routine PCR. The amplification products were separated and visualized by agarose gel electrophoresis described below in section 2.8.

2.6.3 High fidelity PCR

To amplifying sequence for cloning and sequencing, high fidelity PCR was used to avoid errors of base pair. Phusion™ high fidelity DNA polymerase (New England Biolabs, NEB) possesses 5’ → 3’ DNA polymerase activity and 3’ → 5’ exonuclease activity, and generates long templates with a high speed and low error rate which is approximately 50-fold lower than that of Taq DNA polymerase and 6-fold lower than that of Pfu DNA polymerase (Frey and Suppmann, 1995). Phusion™ high fidelity DNA polymerase generates blunt ends amplification products, which is suitable for GATEWAY™ direct entry cloning. The following reaction mixture (Table 2.14) and thermal cycling conditions (Table 2.15) for high fidelity PCR were used in this work. The amplification products were separated and visualized by agarose gel electrophoresis described below in section 2.8. For restriction analysis, cloning or sequencing, the products were purified according to section 2.9.

Table 2.14 High fidelity PCR mixture

Component	Volume (µl)	Final concentration
H_2O	to 50	
5X PCR buffer (NEB)	10	1X
10 mM dNTP (Fermentas)	1	0.2 mM for each dNTP
Primer forward (Eurofins)	2.5	0.5 µM
Primer reverse (Eurofins)	2.5	0.5 µM
Phusion™ DNA polymerase (NEB)	0.25	0.01 U/µl
DNA template	3 – 5*	
Total volume	50	

*DNA extracted by mini preparation or DNA synthesized by RT-PCR was used as a template, the volume added depended on the concentration.

Table 2.15 High fidelity PCR thermal cycling conditions

Step	Temperature (°C)	Time	Number of cycles
Initial denaturation	98	30 sec	1
Denaturation	98	10 sec	
Primer annealing	60	15 sec	35
Extension	72	15-30 s/1 kb*	
Final extension	72	5 min	1
Keep	8	∞	1

*The time for extension depends on the length of target sequence and is calculated with amplification speed.

2.7 Isolation of RNA and RT-PCR

2.7.1 Purification of total RNA

All solutions and tubes used should be RNase free. About 100 mg of Arabidopsis rosette leaves were quickly frozen by liquid nitrogen in 2 ml Eppendorf tube containing 20 – 30 ceramic beads. The leaves were pulverized by shaking tubes in a box. After adding 1.0 ml Trizol, the tube was vortexed briefly and incubated at RT for 5 min. Centrifugation was performed at 14 000, 4 °C for 10 min, to sediment the leaf debris. The supernatant was transferred to a fresh 2 ml tube, added with 100 µl bromchloropropane, shaken vigorously, and incubated at RT for 5

min. To separate phases, centrifugation was carried out at 14 000 rpm, 4 °C for 10 min. 200 µl of the upper phase containing RNA was transferred to a new 1.5 ml tube without disturbing the semi-solid inter-phase containing DNA. 1 volume of isopropanol was added, vortexed briefly and incubated at RT for 10 min. The RNA was spun down by centrifugation at 14 000, 4 °C for 10 min and washed once with 75 % ethanol. The RNA pellet was air dried for 5 min, and dissolved in 150 µl ddH_2O. The concentration and the quality of RNA were detected by agarose gel electrophoresis and Nanodrop 2000C. The RNA was stored at - 80 °C, or directly used for cDNA synthesis and RT-PCR.

2.7.2 RT-PCR for transcript level

First strand cDNA was synthesized by M-MLV Reverse Transcriptase (Promega). To remove residual DNA, 1 µg of total RNA was mixed with reaction buffer and DNase I, and incubated at 37 °C for 30 min. The DNase was inactivated by adding 1 µl of 25 mM EDTA and incubating at 65 °C for 10 min. For RT-PCR, 0.5 µg RNA was mixed with 2 µl of 10 µM gene specific primer or oligo$(dT)_{18}$ and filled up with H_2O to 13 µl. The mixture was incubated at 70 °C for 5 min. After that, the mixture was quick cooled down on ice. The following components were added to the primer/template mixture: 4 µl of 5X M-MLV buffer, 2 µl dNTP, 1 µl of 200 units/µl M-MLV RT, and finally RNase free H_2O to 20 µl. The reaction was carried out at 42 °C for 60 min and stopped by incubating at 70 °C for 15 min. The first strand cDNA was further used as template for end-point PCR.

For semi-quantitative PCR, each primer pair spans at least one intron. 1 µl of first strand cDNA reaction was used for subsequent PCR using routing PCR protocol by amplifying 25, 30 cycles. PCR products were separated on 1 % agarose gel, stained with ethidium bromide and visualized by UV. Quantification of the signals was carried out by Bio-rad software (Image Lab).

2.8 Agarose gel electrophoresis

Agarose gel electrophoresis was used to determine the size and amount of DNA for PCR products, purified fragments, restriction analysis, plasmid isolation, and RNA extraction. The

migration of nucleic acid during electrophoresis is related to voltage, the concentration of agarose, the fragment size which is indicated by co-migration of DNA or RNA markers of known fragment sizes. For preparing agarose gel, 1 % - 2 % agarose (Roth) was melted in 1 x TAE buffer (Table 2.16) using a microwave oven. Ethidium bromide was added to a final concentration of 0.3 µg/ml. After cooling down to 60 °C, the gel was poured into a gel chamber with comb. After gel solidification, the comb was removed and the gel was placed in a horizontal electrophoresis tank containing 1 x TAE buffer. DNA or RNA with added tracking dyes was loaded into the wells and separated by applying an electric field. After electrophoresis is complete, nucleic acids were visualized and analyzed by fluorescence of ethidium bromide under UV light in the GelDoc system (Bio-Rad).

Table 2.16 TAE buffer (1x)

Component	Concentration
Tris-acetate, pH 7.5 (Roth)	40 mM
Sodium acetate (Roth)	20 mM
EDTA (Duchefa)	1 mM

2.9 Purification of DNA fragments

Target DNA fragments from PCR amplification or restriction digest, were purified by innuPREP DOUBLEpure Kit (Analytic Jena). There were two cases: First, there was only a single DNA fragment (e.g. PCR amplification), so only the PCR buffer was to exchange against the elution buffer; second, there were more than one DNA fragments and only one of them was the desired, and a separation by agarose gel electrophoresis was necessary.

For purification of a PCR product with only one specific fragment, 45 µl of PCR product was mixed with 500 µl Binding buffer and transferred to the spin filter. After centrifugation at 10 000 x g for 2 min, the spin filter with DNA was placed into an elution tube, and added with 20 – 50 µl elution buffer. After incubation for 1 min, the PCR product was recovered by centrifugation at 6 000 x g for 1 min.

For purification of restriction digest products or PCR products with more than one fragment, the products were firstly separated by agarose gel electrophoresis, and the desired DNA band

visualized by UV was cut and transferred to 2 ml tube. The agarose gel slice with DNA was lysed by adding 650 µl of gel solubilizer and incubation at 50 °C for 10 min. After adding of 50 µl binding optimizer, the DNA solution was transferred to a spin filter and centrifuged at 10 000 x g for 1 min. The DNA in spin filter was washed twice with washing solution, subsequently centrifugated to remove residual ethanol. Finally the DNA was eluted in 20 – 50 µl of elution buffer.

2.10 Construction of vectors

The Gateway® Technology is a universal cloning method that provides a rapid and highly efficient way to transfer gene of interest into multiple vector systems. Two simple steps to generate expression vectors: first, construct an entry clone by moving blunt-end PCR fragment into a pENTR vector; second, LR recombination reaction between an entry clone and destination vector to generate an expression construct.

2.10.1 Entry vectors

The blunt-end fragments were produced by high fidelity PCR using Phusion DNA polymerase (New England Biolabs), gene specific primers and Arabidopsis genomic DNA and cDNA clone. The cDNA clones of *CDS1* (BX813816), *CDS2* (pda06248), and *CDS3* (BX826782) were obtained from the RIKEN BioResource Center (Seki *et al.*, 2002, 2003; Sakurai *et al.*, 2005) and Genoscope / Life Technologies (INRA, The French National Resources Center for Plant Genomics, Castelli *et al.*, 2004). The qualified PCR products were cloned into pENTR /SD/D-TOPO vector (Invitrogen) to generate entry vectors pENTR_*CDS*. The TOPO cloning reaction mixture was set up in order (Table 2.17).

Table 2.17 Set up TOPO cloning reaction mixture

Component	**Volume**
PCR product*	0.5 to 2 µl
Dilute Salt solution** (1:4)	0.5 µl
Sterile water	Add to 2.5 µl
pENTR /SD/D-TOPO vector	0.5 µl
Total	3 µl

*0.5:1 to 2:1 molar rate of product:TOPO vector

**Salt solution: 1.2 M NaCl, 0.06 M $MgCl_2$.

After gently mixing, the reaction mixture was incubated at 23 °C for 5 min and subsequently transformed into electrocompetent *E. coli* cells (see section 2.5.1). The kanamycin resistant colonies were checked by colony PCR to ensure that the gene of interest was cloned into the vector, and avoid false positive colonies which contained empty vectors. After purification from a 5 ml pre-culture, the putative vectors were digested by suitable restriction endonucleases which cut both the gene of interest and the vector sequence. If the restriction analysis showed a correct size and direction of insertion, sequencing was performed using primer M13F and M13R. When the inserted sequence was proved, the entry vector was ready for performing the LR recombination reaction.

2.10.2 Expression vectors

The Gateway® LR recombination reaction (Invitrogen) was carried out for moving gene of interest into destination vectors. The LR (attL x attR) reaction is catalyzed by Gateway LR Clonase™ II enzyme mix, as shown in Fig. 2.1. The recombination between the entry clone pENTR_*CDS* containing attL flanked *CDS* gene and the destination vector generates the expression clone pDEST_*CDS* containing the *CDS* gene flanked by attB sequences, and a by-product pDONR. As demonstrated in Fig. 2.1, the pDEST_*CDS* contains an antibiotic resistance gene (e.g. AmpR) which is different from kanamycin resistance gene (KanR) in the entry clone, allowing a selection for transformation after LR reaction. In contrast, both of the destination vector (pDEST vector) and the by-product pDONR have a F plasmid-encoded gene *ccdB* that inhibits the growth of *E. coli* (Bernard and Countuier, 1992), and kills the transformed *E. coli*. Except antibiotic resistance gene for bacteria, the destination vector may also contain other selection markers which will function in the transformed organisms, such as yeast and plants.

The LR reaction was done by following procedures. First, the reaction mixture was set up as below. The molar rate of entry clone:destination vetor is as close to 1:1 as possible.

Component	Volume
Entry clone pENTR_*CDS*	1 - 3.5 µl
Destination vector pDEST	0.5 µl
TE buffer, pH 8.0	to 4 µl

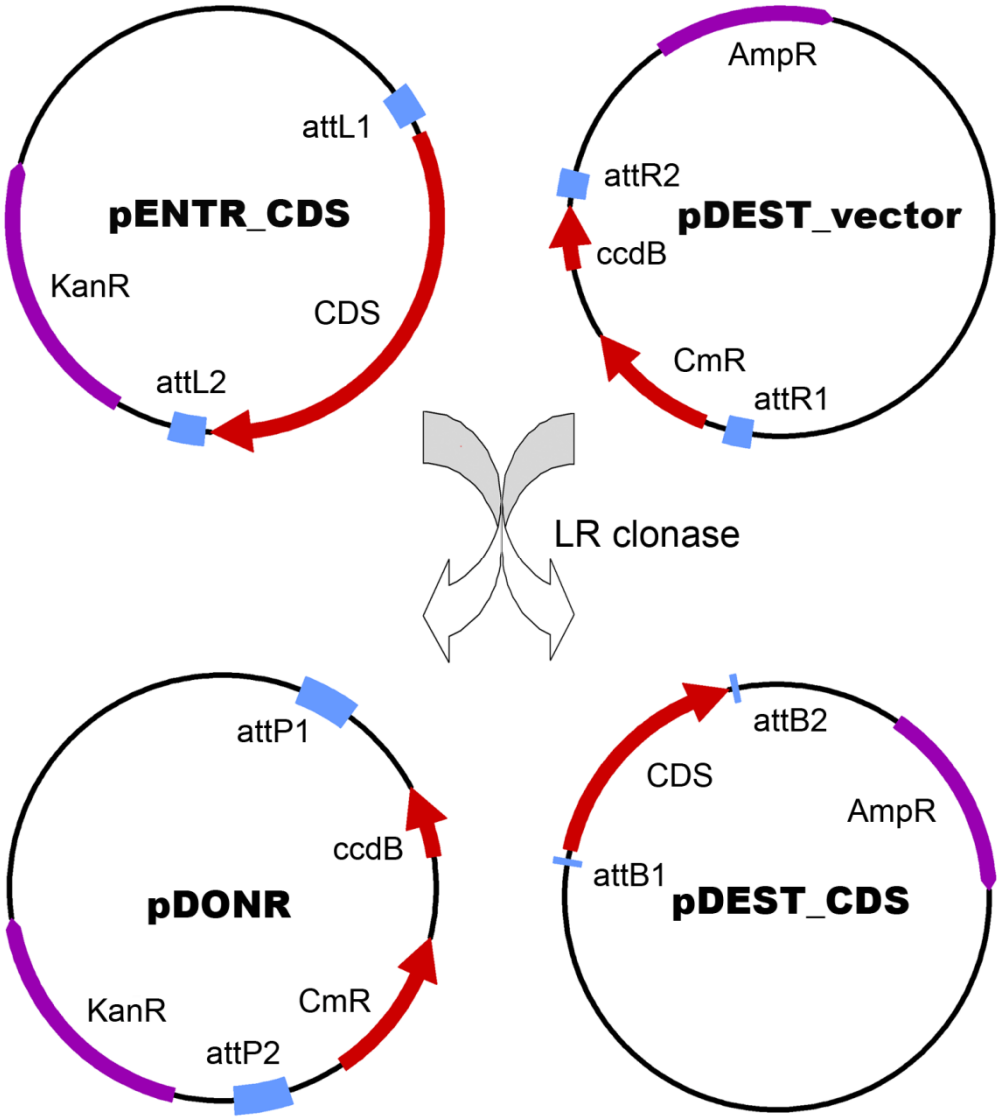

Figure 2.1 LR attL x attR reaction mediated by Gateway LR clonase II enzyme mix. pENTR_CDS, the entry vector that contains gene of interest to be moved; pDEST_vector, the destination vector to receive the gene of interest; pDEST_CDS, the expression clone that contains gene of interest; pDONR, the by-product of LR reaction. attL, attR, attB, and attP, bacteriophage λ-derived DNA recombinant sequence that allow recombinational cloning of gene of interest by Gateway clonase. KanR, kanamycin resistance gene; AmpR, ampicillin resistance gene; CmR, chloramphenicol resistance gene; ccdB, F plasmid-encoded gene that inhibites growth of *E. coli*. The size of features is propositional to the vector they locate.

The LR Clonase II enzyme mix was added and the reaction was carried out at 25 °C for 1 hour. To terminate the reaction, 1 µl of Proteinase K solution was added and the mixture was incubated at 37 °C for 10 min. Electocompetent E. coli DH5α cells were transformed with LR reaction products by adding 1 µl of mixture to 40 µl and following the electrotransformation protocol described in section 2.5. Transformants were selected on LB plates with suitable

antibiotics. The plasmids of expression clones were purified and restriction analyzed before transforming into destination organisms.

With Gateway technology, expression constructs were generated. For subcellular localization, cDNAs were transferred into destination vector pK7FWG2.0 (Karimi *et al.*, 2002, 2007), in which the whole cDNAs without stop code or N-terminal part of cDNAs were fused to N-terminal of eGFP gene. For heterozygous functional studies in yeast, cDNAs were transferred into galactose-inducible vector pYES-DEST52 (Invitrogen). For complementation assays in Arabidopsis, cDNAs were transferred into pMDC7 and pH7WG2, in the former expression of gene was highly induced by β-estradiol (Zuo *et al.*, 2000; Curtis *et al.*, 2003). For RNA interference, the gene-specific sequence tag of At4g22340 and the whole cDNA sequence without stop codon of *CDS2* was transferred into the pWatergate vector.

2.11 Plasmid isolation

The plasmids were prepared from *E. coli*, *A. tumefaciens*, and *S. cerevisiae* using different strategies based on the copy number and the downstream usage.

Because of the high copy number, plasmids from *E. coli* like DH5α are usually purified and used for the following cloning purposes. Lots of commercial kits have been developed and satisfy this requirement. The innuPREP Plasmid Mini Kit was used in this work and briefly described below. Before the isolation, E. coli cells with desired plasmids were cultivated in a small volume (usually 5 ml) of LB medium overnight. The cells were harvested by centrifugation at 12 000 rpm for 1 min. After removing the supernatant, bacterial cells were resuspended in 250 µl resuspension buffer, and lysed by adding 250 µl of lysis buffer containing NaOH and SDS, inverting the tube 5 times, and incubating no more than 5 min. The mixture was neutralized by adding 350 µl of neutralization buffer and thoroughly shaking. The cellular debris, chromosomal DNA and proteins were spun down at 12 000 rpm for 10 min. The plasmid in the supernatant was transferred to a spin filter that was placed into a receiver tube, and centrifuged at 12 000 rpm for 1 min. After discarding the filtrate, the plasmid was washed with 500 µl washing solution and subsequently washed with 700 µl of washing solution B. The residual ethanol from washing

solution B was completely removed by another centrifugation. The plasmids were recovered by adding 50 µl of elution buffer. 5 ml of overnight culture yielded more than 5 µg of plasmid DNA, which should be sufficient for downstream cloning.

Plasmids transformed into agrobacteria should be isolated and verified before starting the transformation of plants. Plasmids in agrobacterial cells were prepared with a protocol that is similar to that of E. coli. But because of the low copy of plasmids in agrobacteria, the purified plasmids from small volume culture were not enough for verification, such as restriction analysis, sequencing. To this end, the plasmids were retransformed and propagated in *E. coli*, like DH5α, Top10.

The plasmid isolation from yeast cells was performed using a colony plasmid rescue method which was modified from method of Hoffman and Winston (1987). Half of a colony of yeast (about 2 mm in diameter) was picked up and resuspended in 20 µl of plasmid rescue buffer (Table 2.18) in a 2 ml tube. A small volume of glass beads (0.5 mm diameter, Roth) and 20 µl of Phenol:Chloroform:Isoamylalcohol (PCI, 25:24:1, Roth) were added. The cells were homogenized by vortexing for 5 min. The phases were separated by centrifugation at 14 000 rpm for 5 min, and the upper phase contained the DNA, including plasmid DNA. The upper phase (not more than 10 µl) was transferred to a new tube, and avoided transferring the lower phase. 1 to 4 µl of the upper phase was used for transforming electrocompetent E. coli and verifying the plasmid.

Table 2.18 Plasmid rescue buffer

Component	Concentration
Triton X-100 (Merck)	2 %
SDS (Duchefa)	1 %
NaCl (Roth)	100 mM
Tris-HCl, pH8.0 (Roth)	10 mM
EDTA, pH 8.0 (Duchefa)	1 mM

2.12 DNA sequence analysis

A restriction enzyme (or restriction endonuclease) recognizes and cuts within or near a specific nucleotide sequence (Roberts and Murray, 1976), giving rise to specific end and size of DNA

fragments and being a useful tool for cloning. DNA fragments or plasmids were cut by a single enzyme or two enzymes (double digest, Thermo Scientific) into more than two specific fragments, giving the information of the size and insertion direction of gene of interest. For digestion of a purified PCR product or a plasmid, the following mixture (Table 2.19) was added and incubated at 37 °C for 1 hour.

Table 2.19 Restriction digestion mixture

Component	Volume
ddH_2O	16 µl
10X buffer	2 µl
DNA fragment or plasmid	1 µl
Restriction enzyme*	1 µl
Total	20 µl

*For double digestion, 1 µl of each enzyme was added, and recommended buffer was added.

Fragment or plasmid samples mixed with corresponding primer, were determined on an ABI PRISM® 3730 genetic analyzer in Fraunhofer IME. Base-pair errors were avoided by comparing sequencing results with the sequences in TAIR (www.arabidopsis.org). The insertion sites of T-DNA insertion, the DNA fragments were amplified by high fidelity PCR, using gene-specific primer LP/RP and T-DNA left border primer LBb1.3 (Table A1). After purification, the fragments were sequenced. The cDNA in pENTR entry clone were sequenced using M13F and M13R before moving into destination vectors by the LR recombination reaction.

2.13 Preparation of yeast mitochondrial membranes

The yeast YBR029c (*cds1*) cells containing pYES-DEST52_*CDSs* were obtained from Haselier *et al.* (2010). The yeast cells were cultivated and mitochondrial fractions were isolated from the cultures according to Zinser and Daum (1995) as described before (Haselier *et al.*, 2010). Before the day of purification, 2 flasks of 200 ml minimal medium (SC-U) were inoculated with yeast pre-culture to a initial OD_{600}≈0.02 and shaken at 140 rpm at 28 °C, overnight. The cells were harvested in falcon tubes by centrifugation at 2400 rpm x 20 °C x 4 min (also for the following centrifugation steps without mention). Each pellet was resuspended in 20 ml of ice-cold ddH_2O and centrifuged again. After removing the supernatant, the cell wet weight was determined and

the pellets were washed once with 20 ml Buffer A (Table 2.20). The washed cell pellets were resuspended in a certain volume of Buffer A (1 ml per g cell wet weight), and added with dithiothreitol (DTT, Roth) to a final concentration of 10 mM. The cells were shaken at 30 °C for 10 min and centrifuged. After removing the supernatant, the pellets were washed with 20 ml of Buffer B (Table 2.20) once, and resuspended in a certain volume of Buffer B (5.7 ml per g cell wet weight). At this point, a control of Zymolyase digestion was prepared by diluting 10 µl of suspension in 1 ml ddH_2O and stored on ice. For digestion of yeast cell walls, a certain volume of Zymolyase 20T (MP biomedicals) stock solution was added (2 mg Zymolyase per cell wet weight) and the suspension was gently shaken at 30 °C for 45 min. For checking the Zymolyase digestion, 5 µl of suspension was diluted in 5 ml ddH_2O, mixed by vortexing, and compared with the control: the digested sample should be clear unlike the milky control, because without cell wall the cells were destroyed osmotically. After the test, the spheroplasts were harvested by centrifugation at 2400 rpm x 4 °C x 4 min (also for the following centrifuge unless mention). The following steps should be done at 4 °C or ice-cold as possible. The pellets were washed once with 20 ml ice-cold Buffer B, and subsequently with 20 ml of ice-cold Buffer C (Table 2.20). After discarding the supernatant, the following 3 steps 3 times were repeated: the pellet was resuspended in Buffer C (2 ml per g cell wet weight); the spheroplasts were broken with Dounce homogenizer, 20 relapse; after centrifugation, the supernatant was collected in a fresh Falcon tube on ice. The collected supernatant was centrifuged at 10000 xg x 4 °C x 30 min. For preparing the mitochondrial fraction, the pellets were resuspended in Buffer C and centrifuged at 4000 rpm x 4 °C x 10 min to remove the spheroplast impurities. The supernatant was transferred to a new centrifuge tube and centrifuged at 10000 xg x 4 °C x 10 min. After washing with 20 ml ice-cold Buffer C again, the pellet should be a crude mitochondrial fraction which was resuspended in an appropriate volume of 10 mM Tris-H_2SO_4 buffer (pH 7.4). The suspension was divided into aliquots, quick frozen in liquid nitrogen and stored at – 80 °C.

Table 2.20 Buffers and solution for mitochondrial fraction preparation

Buffer or Solution	Component	Concentration
Buffer A	Tris-HCl, pH 9.4	100 mM
Buffer B	Sorbitol (Roth)	1.2 M
	Kalium phosphate, pH 7.4	20 mM
Buffer C	Mannitol (Roth)	0.6 M

	Tris-H_2SO_4, pH 7.4	10 mM
Zymolyase stock solution	Sorbitol (Roth)	1.2 M
	Zymolyase 20T (MP biomedicals)	10 mg/ml

2.14 Enzymatic assay

Before the assay, the protein concentration of yeast mitochondrial membranes was measured by the Bradford method (Bradford, 1976) using bovine serum albumin (Roth) as calibration standards. The quantified total protein concentration was used for the following activity calculation. CDS activity in mitochondrial membrane was determined in 50 µl reaction mixture containing 5 µg proteins according to Andre et al. (2000, Table 2.21). The reaction was started by adding CTP, incubated at 30 °C for 20 min, and the catalysis was stopped and lipids were extracted by adding 500 µl methanol:chloroform (1:1, v/v) and centrifugation at 1000 rpm for 3 min. The amount of reaction products was quantified by scintillation counting (LS 6500, Beckman).

Table 2.21 Enzymatic assay mixture

Component	**Concentration**
Bis-Tri-Propane-HCl, pH 8.0 (BTP, Roth)	50 mM
$MgCl_2$ (Merck)	5 mM
Triton X-100 (Merck)	0.5 %
PA (18:1/18:1) (Sigma)	0.2 mM
CTP (Sigma) with [5-^{3}H]CTP (Perkin-Elmer)	1.2 mM, $3x10^5$ dpm
Proteins	5 µg
H2O	to 50 µl

2.15 Microscopic analysis

For studying subcellular localization of fusion proteins, a rapid transient expression method was used according to Sparkes *et al.* (2006), described above in the section of tobacco transformation. For the colocalization, agrobacteria GV3101::pMP90RK containing the construct of pTRAkc-rbcs1-cTP or pTRAkc-ERH (Maclean *et al.*, 2007), which show the chloroplast and ER localization, respectively, were introduced into leaf epidermal cells together with

GV3101::pMP90RK containing *CDS* constructs. For visualization of mitochondrial, infiltrated areas of leaves were cut out after 48 hours incubation and incubated in 500 nM Mito Tracker Red (Invitrogen) solution with 0.04 % silwet L-77. The infiltrated areas of leaves were cut out and observed using a confocal laser microscope (Leica).

To determine the starch in seedlings, Arabidopsis were germinated and grown on MSG plates, and harvested at day 3, 4, 5 and 7. Seedlings were harvested at hour 4 in 8-hour photoperiod, decolorized in 80 % (v/v) ethanol at 80 °C for 5 min, stained with Lugol solution (Sigma) for 2 min, and briefly destained with distilled water twice. The transmission images of starch-stained seedlings were taken with a Keyence microscope. To analyze the cells of cotyledons and roots, the slides were prepared by A. Weth as described before (Haselier at al., 2010), and observed with a Keyence microscope.

To analyze the red fluorescence of chlorophyll, cotyledons from 5-day-old seedlings were harvested at hour 4 in 8-hour photoperiod and observed with a Leica fluorescence microscope. The fluorescence was excited at 450 - 490 nm and detected at 515 nm.

The ultrastructure of cotyledons and roots from WT and *cds1cds2* seedlings were analyzed by transmission electron microscopy using a Zeiss EM10 electron microscope. The EM slide preparation and microscopy were performed in cooperation with Agnes Weth and Professor Werner Baumgartner in Biology II, RWTH, as described before (Haselier at al., 2010).

2.16 Phospholipid analysis

***In vivo* phospholipid labeling of seedlings and lipid extraction** About 40 mg 5-day-old seedlings of WT (≈ 80 plants) and *cds1cds2* (≈ 200 plants) were harvested from MSG plates and incubated in 2 ml 1/2 MSG medium (Table 2.22) containing 2 µl [^{33}P] phosphoric acid(Hartmann-Analytic, FF-1, 370MBq (10mCi)/ml), under light overnight (18 hours). Phospholipids were extracted according to Babiychuk *et al.* (2003). The supernatant was carefully removed, and the seedlings were washed 5 times with 1 ml NaCl/EDTA solution. After washing, 2 ml NaCl/EDTA solution was added and the seedlings were boiled in a water bath for 10 min to inactivate lipases (under a hood, and open lids of tubes). After cooling and brief spin,

the solution was removed and the lipids were extracted by adding 3 ml chloroform/methanol (1:2, v/v), and incubating for 15 min at RT (gently shaked several times during incubation). 3 ml chloroform was added (chloroform:methanol = 2:1, v/v) and extraction was incubated for another 15 min. After mixing with 1.5 ml 1X salt solution (Table 2.22), the organic phase was separated from aqueous phase by centrifugation at 1000 rpm at RT for 3 min. The lower phase (organic phase) was transferred and filtrated with glass wool, and harvested in a new falcon tube. The solvent was evaporated by nitrogen stream under the hood and the residue was dissolved in 500 µl chloroform.

Separation of phospholipids by thin layer chromatography Before the separation, the radioactivity of phospholipids was measured: 5 µl of lipid extraction were mixed with 5 ml scintillation cocktail (Optiphase Hisafe 2, Perkin-Elmer) and measured in a scintillation counter (LS 6500, Beckman). Lipid extraction with 10000 dpm radioactivity was evaporated and dissolved in 40 µl chloroform and applied to thin layer chromatography on a silica gel 60 plate (0.25 mm layer thickness, Merck). The plate was placed vertically in a glass tank containing 100 ml of chloroform/methanol/glacial acetic acid (65:25:8, v/v) and incubated for 1 hour and 15 min to separate phospholipids. For separating phosphatidylserine (PS) and phosphatidylinositol (PI), phospholipids were applied on 1.8 % boric acid treated TLC plates with chloroform/triethylamine/ethanol/water (30:35:35:7, v/v).

Table 2.22 Medium and solution for phospholipid labeling and extraction

Medium or solution	Component	Concentration
1/2 MSG medium	MSG (Duchefa)	2.2 g/l
	Sucrose	10 g/l
	pH with KOH to 5.8	
NaCl/EDTA solution	NaCl (Roth)	0.45 %
	EDTA (Duchefa)	20 mM
1X salt solution	KCl	1 M
	H_3PO_4	0.2 M

Visualization and analysis of phospholipid labeling After drying under the hood, the plate with separated lipids was placed in an image cassette and covered with a imaging plate (BSA-MS 2025, Fuji Photo Film) overnight. The migrations of phospholipids were visualized in

a bioimage (FLA3000, FujiFilm). To quantify each phospholipid, the bands of lipids were scraped from the TLC plate, mixed in 5 ml scintillation cocktail and applied to scintillation counting.

Phospholipid analysis of calluses was performed similar to that of seedlings, except several extraction steps. Calluses were grown on agar-solidified callus inducing medium (CIM) as described above. For *in vivo* labeling, about 200 mg of Arabidopsis calluses were cut and separated into two portions, one was grown on CIM with 10 µM β-estradiol and the other on CIM without 10 µM β-estradiol, and incubated for one week. Calluses were transferred to falcon tubes and incubated in 1 ml CIM with or without 10 µM β-estradiol, containing 2 µl of [^{33}P] phosphoric acid, at room temperature without light overnight. After removing the medium, the callus was washed 5 times with 1 ml NaCl/EDTA solution. 3 ml of NaCl/EDTA was added and the callus was boiled in a water bath for 10 min. The lipids were extracted by adding 3 ml of chloroform/methanol (1:2, v/v) and vortexed for 30 min. 3 ml of chloroform was added and the tubes were vortexed for another 30 min. The following steps for extraction and analysis were similar to that of seedling described above.

2.17 Lipid profiling

Lipid extraction from the following materials was carried out according to Roughan *et al.* (1978).

About 50 mg seedlings were harvested in glass tubes with screw caps and weighted. 3 ml of boiling water was added into glass tubes and incubated in 100 °C water bath for 10 min to destroy all lipase activity. After water was removed completely, lipids were extracted firstly with 3 ml chloroform/methanol (1:2, v/v) for 5 min, with gently shake. The organic lipid extract was transferred to a new glass tube, the leaves were extracted with 3 ml of chloroform/methanol (2:1, v/v). On this point, the leaves should be pale white. Organic extracts were collected and combined and 3 ml of chloroform and 2.25 ml of 300 mM NH_4OAc solution were added and mixed by vortexing. Phase separation was done by centrifuge, and the lower phase containing

lipids was collected, avoiding taking the aqueous phase. The solvent of lipid extract was evaporated by nitrogen stream. Lipid residue was dissolved in Q-TOF solvent for LC/MS.

Calluses of Arabidopsis were cut and separated into two portions and incubated on callus inducing medium with or without 10 µM of β-estradiol. About 100 mg of callus was harvested for extraction of lipids. The protocol used was similar to seedlings, except the two steps for extraction: for callus, after adding 3 ml of chloroform/methanol (1:2 or 2:1, v/v), lipid extraction was carried out by vortexing for 30 min.

Leaves were harvested from 1-month-old Arabidopsis plants grown in potting soil for 1 month, and used for extraction of lipids for LC/MS. Similar protocol as to seedlings was employed (see above).

Steady state membrane lipid composition of Arabidopsis leaves, seedlings and callused were analyzed by nanospray ionization tandem mass spectrometry (nanospray-MS/MS) in cooperation with Helga Peisker and Professor Peter Doermann at the Institute of Molecular Physiology and Biotechnology of Plants, University of Bonn. For glycerolipid quantification, an aliquot of the lipid sample was diluted in methanol:chloroform:300 mM ammonium acetate (665:300:35, v/v, Welti *et al.* , 2002). Two internal phospholipid standards each were added for PC, PE, PG, PA and PS (Avanti Polar Lipids) to the samples according to Welti *et al.* (2002). The lipid standards MGDG, DGDG, SQDG and PI (Larodan) were hydrogenated prior to addition to the sample according to Buseman *et al.* (2006). The samples were supplied to a Q-TOF (quadrupole time-of-flight) mass spectrometer (Q-TOF 6530; Agilent) in chloroform/methanol/ 300 mM ammonium acetate (300:665:35, v/v) at a flow rate of 0.5 µl min^{-1} with a nanospray ion source (HPLC Chip/MS 1200 with infusion chip; Agilent). After ionization in the positive mode with a fragmentor voltage of 270 V, ammonium or proton adducts were selected in the quadrupole and fragmented in the collision cell (Welti *et al.*, 2002). After correction of isotopic overlap, lipid molecular species were quantified according to Devaiah *et al.* (2006).

2.18 Positional analysis of glycerolipids

The glycerolipids isolated from Arabidopsis seedlings were dissolved in chloroform and purified using silica columns (Strata 100 mg Silica columns, Phenomenex). After washing the columns with chloroform, the galactolipids were eluted with acetone/isopropanol (1:1) and the phospholipids with methanol. The glycerolipids were dried and dissolved in ethanol. An aliquot of the glycerolipid fractions was mixed with digestion buffer (40 mM Tris-HCl, 50 mM Na-borate, pH 7.2) and Rhizopus arrhizus lipase and incubated for 1 h at room temperature (Fischer *et al.*, 1973; Williams *et al.*, 1995). After extraction with chloroform/methanol (1:1) the lyso-glycerolipids (lyso-MGDG, lyso-DGDG, lyso-PC, lyso-PE and lyso-PG) were measured by Q-TOF mass spectrometry (see above). The amounts of lyso-glycerolipids were obtained following electronic neutral loss or precursor ion scanning of the MS/MS experiments according to Devaiah *et al.* (2006) except for lyso-MGDG, lyso-DGDG and lyso-PG which were measured as ammonium adducts in the positive mode. Data were corrected for isotopic overlap, and after background subtraction, the percentages of the molecular species within each lyso-glycerolipid class were calculated.

3 RESULTS AND DISCUSSION

3.1 Bioinformation analysis of plant cytidinediphosphate diacylglycerol synthases (CDS) sequences

3.1.1 Conserved domains of cytidinediphosphate diacylglycerol synthases

Cytidinediphosphate diacylglycerol synthase (CDS), also known as phosphatidate cytidylyltransferase, transfers a cytidyl group of cytidine triphosphate to phosphatidic acid, generating cytidinediphosphate diacylglycerol (CDP-DAG), an important intermediate in glycerolipids biosynthesis. It is known that CDS is a universal enzyme that is found in both prokaryotes (Icho *et al.*, 1985; Martin *et al.*, 2000; Sato *et al.*, 2000) and eukaryotes (Wu *et al.*, 1995; Shen *et al.*, 1996; Kopka *et al.*, 1997; Weeks *et al.*, 1997; Volta *et al.*, 1999; Inglis-Broadgate *et al.*, 2005). In Arabidopsis, there is a small *CDS* family consisting of 5 genes, named *CDS1* to *CDS5*, of which *CDS4* and *CDS5* were shown to encode the plastidial isoforms catalyzing formation of CDP-DAG essential for prokaryotic PG biosynthesis in plastids (Haserlier *et al.*, 2010). *CDS1* to *CDS3* of Arabidopsis were heterologously expressed in yeast *cds1* null mutant and functionally rescued the nonviable phenotype of the haploid mutant strain (Haselier *et al.*, 2010). In addition, based on sequence similarity CDS1 of Arabidopsis was claimed to be a eukaryotic enzyme (Kopka *et al.*, 1997).

A BLAST search (NCBI/BLAST/blastp) was carried out using AtCDS1 amino acid sequence as query sequence. CDS amino acid sequences from typical organisms, including *E. coli*, *S. cerevisiae*, *A. thaliana*, *D. melanogaster*, and *H. sapiens*, were selected and applied to the multiple sequence alignment with Clustal X2 (Larkin *et al.*, 2007). The alignment was shaded by Genedoc (Nicholas et al., 1997), and shown in Fig. 3.1. Firstly, a conserved domain of phosphatidate cytidylyltransferase (PLN02594, underlined sequences) was found in all CDSs from both prokaryotes and eukaryotes. Secondly, the CDS sequences were separated into two classes based on similarity: CDS1, CDS2 and CDS3 from Arabidopsis were similar to those from eukaryotes, such as *S. cerevisiae*, *D. melanogaster* and *H. sapiens*; in contrast, AtCDS4 and AtCDS5 were closely related to the prokaryotic isoform like *E. coli*.

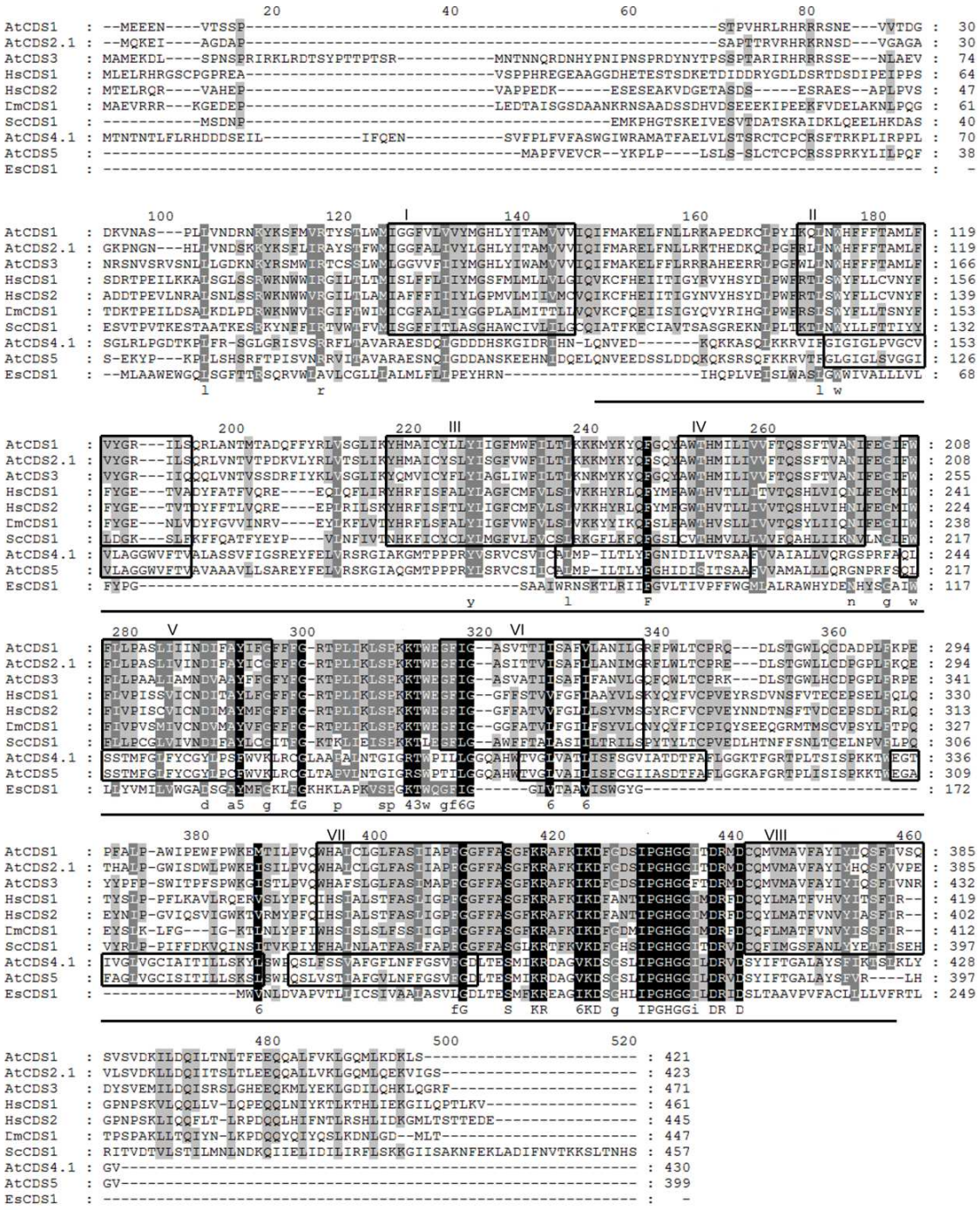

Figure 3.1 Multiple sequence alignment of cytidinediphosphate diacylglycerol synthase (CDS) proteins. The amino acid sequences of CDS in *Arabidopsis thaliana* (AtCDS1, NP_176433.2; AtCDS2.1, NP_193965.1; AtCDS3, NP_194407.5; AtCDS4.1, NP_566035.2; AtCDS5, NP_191621.1) were compared with CDS of *E. coli* (EcCDS1, YP_006137261.1), *S. cerevisiae* (ScCDS1, NP_009585.1), *D. melanogaster* (DmCDS1, NP_524661.1), *H. sapiens* (HsCDS1, NP_001254.2; HsCDS2, NP_003809.1). Alignment was performed with Clustal X2 using a multiple alignment model. The alignment results were shaded by Genedoc using a conservation model. Dashes represent gaps to maximize similarity of sequences. The conserved amino acid residues in all sequences are shaded in black and gray, and indicated by letters below the alignment. The different shading levels represent distinct of sequence conservation. The conserved domain of phosphatidate cytidylyltransferase (PLN02594) is underlined. Predictive transmembrane domains were shown as boxes.

Except EcCDS1 which is a membrane-associated enzyme, all the other CDS enzymes shown in the alignment are integral membrane proteins. Furthermore, the number and pattern of transmembrane domains differ between prokaryotic and eukaryotic proteins. Moreover, two highly conserved regions were found in all enzymes aligned: one is between box V and VI, the other between VII and VIII. These domains were believed to be the catalytic regions (Fig. 3.1).

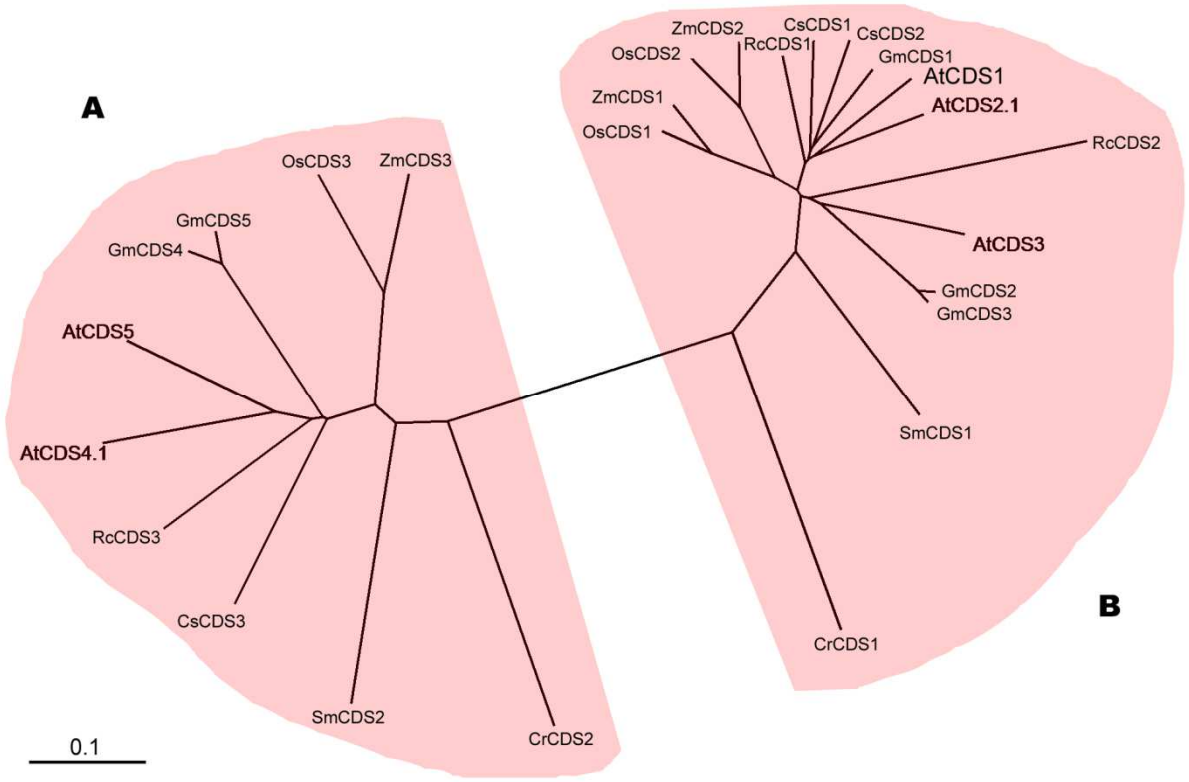

Figure 3.2 Phylogenetic tree of putative cytidinediphosphate diacylglycerol synthases from eukaryotic photosynthetic active organisms. Parts of the matched proteins from a BLAST search in plants using AtCDS1 as quary sequence are shown in this figure, including AtCDS1 (Accession number NP_176433.2), AtCDS2.1 (NP_193965.1), AtCDS3 (NP_194407.5), AtCDS4.1 (NP_566035.2) and AtCDS5 (NP_191621.1) from *Arabidopsis thaliana*, CrCDS1 (XP_001691838.1) and CrCDS2 (XP_001691107.1) from Chlamydomonas reinhardtii, CsCDS1 (XP_004134792.1), CsCDS2 (XP_004167856.1) and CsCDS3 (XP_004140488.1) from *Cucumis sativus*, GmCDS1 (XP_003556374.1), GmCDS2 (XP_003518535.1), GmCDS3 (XP_003545113.1), GmCDS4 (XP_003538330.1) and GmCDS5 (XP_003551170.1) from *Glycine max*, OsCDS1 (NP_001044302.1), OsCDS2 (NP_001064355.1) and OsCDS3 (NP_001045756.2) from *Oryza sativa Japonica Group*, RcCDS1 (XP_002518397.1), RcCDS2 (XP_002531200.1) and RcCDS3 (XP_002511659.1) from *Ricinus communis*, SmCDS1 (XP_002980195.1) and SmCDS2 (XP_002974179.1) from *Selaginella moellendorffii*, ZmCDS1 (NP_001132909.1), ZmCDS2 (NP_001151263.1) and ZmCDS3 (NP_001150623.1) from *Zea mays*. The phylogenetic tree was constructed by the neighbor-joining method with Clustal X2 program and viewed by treeview program. The scale indicates branch lengths.

3.1.2 Two types of CDS appear to exist in plants

To gain an evolutionary view of CDS in plants, a protein BLAST using AtCDS1 as a query sequence was performed. Beside *Arabidopsis thaliana*, amino acid sequence from three dicot species (*Cucumis sativus*, *Glycine max* and *Ricinus communis*), two monocot plants (*Oryza sativa Japonica Group* and *Zea mays*), a lycophyte (*Selaginella moellendorffii*), and an algae (*Chlamydomonas reinhardtii*) were selected for comparison. These eukaryotic photosynthetic active organisms were found to possess at least two CDS candidate sequences. However, no similar CDS sequence was found in gymnosperm, likely because candidate proteins haven't been analyzed so far.

An unrooted phylogenetic tree of proteins from selected plants was constructed using the NJ (Neighbor-joining) method proposed by Saitou and Nei (1987). As shown in Fig. 3.2, the phylogenetic analysis clearly demonstrated a distinct classification of these amino acid sequences into two groups. The plastidial isoforms of AtCDS4 and AtCDS5 belong to group A, while the putative extraplastidial isoforms AtCDS1, AtCDS2 and AtCDS3 is classified into group B. Furthermore, subgroups of dicot and monocot proteins were easily distinguished in both group A and group B. In addition, AtCDS3 together with GmCDS2, GmCDS3 and RcCDS2 is separated from the dicot protein group including AtCDS1 and AtCDS2. Based on these analyses, CDS are ubiquitous proteins in plants. Moreover, the division of CDS proteins into plastidial and extraplastidial isoforms is typical in plants. The study of CDS in Arabidopsis will help us to understand CDS roles and functions in plants.

3.1.3 Expression level of putative extraplastidial *CDSs* in Arabidopsis

The expression pattern of extraplastidial *CDSs* in Arabidopsis were analyzed, using the data from Arabidopsis eFP Browser-BAR (website: bar.utoronto.ca, Winter *et al.*, 2007). As shown in Fig. 3.3, *CDS1* and *CDS2* are constitutively expressed in all of the given tissues and developmental stages of Arabidopsis. *CDS1* has the highest expression level in almost all samples, indicating that it should be the main contribution of the extraplastidial CDS activities. *CDS2* has lower transcription level than *CDS1*. Unlike *CDS1* and *CDS2*, *CDS3* is specifically expressed in stamens at flower stage 12 and mature pollens. *CDS3* is also expressed in seeds from embryogenesis to germination in relatively low levels, and becomes very hardly detectable

when the vegetative stage starts. These data indicate that *CDS1* and *CDS2* should have indispensible role in Arabidopsis growth and development, and *CDS3* may act as complementary activity in specific organs, like mature pollens and stamens.

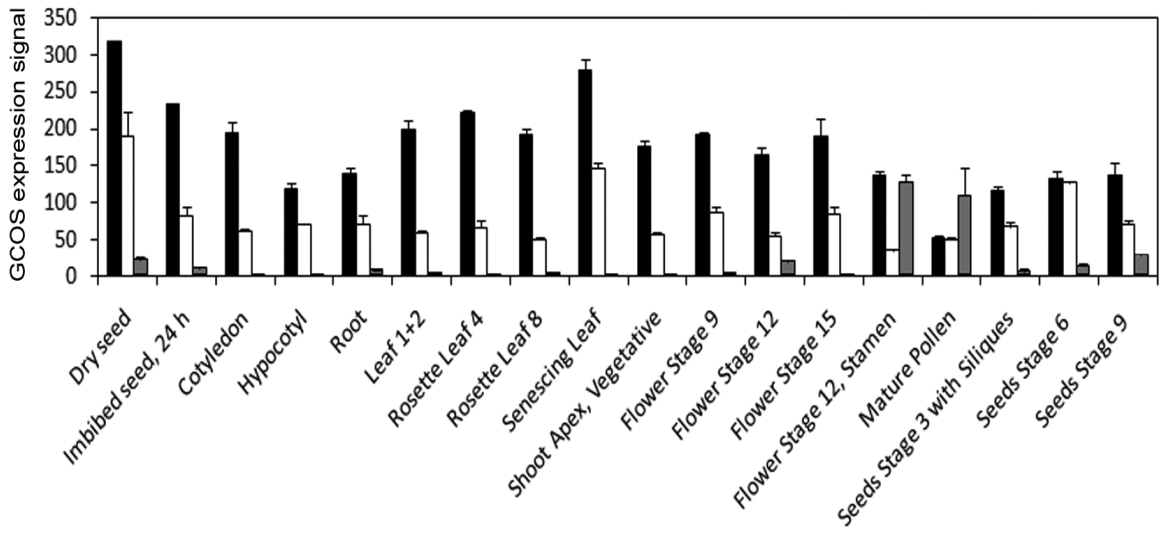

Figure 3.3 Expression levels of *CDS1* (black), *CDS2* (white) and *CDS3* (gray) in the given structures in Arabidopsis. Data are from Arabidopsis eFP Browser-BAR (bar.utoronto.ca, Winter et al., 2007), in which data are normalized by the GCOS (Gene Chip Operating Software) method , and a target signal (TGT) = 100 and a background value (Bkg) = 20 for array scanning were used. The average values and standard deviations were given.

3.2 Enzymatic properties of CDS1, CDS2 and CDS3

To determine the enzymatic properties of extraplastidial isoforms CDS1, CDS2 and CDS3, the *in vitro* enzyme assays were performed using mitochondrial membranes from yeast cells heterologously expressing *CDS1*, *CDS2* or *CDS3*. Since CDS catalyzes the reaction of PA and CTP, and produces CDP-DAG and pyrophosphate, we used radioactively ^{14}C labeled phosphatidic acid (PA) or ^{3}H labeled CTP as substrate to measure the enzymatic performance. As shown in Fig. 3.4, CDP-DAG was only formed in the present of CDS enzyme (CDS3 in this assay). When the CDS3 concentration in the reaction increased, the content of labeled PA decreased accompanied by an increasing concentration of the product CDP-DAG (Fig. 3.4A). In other assay with unlabeled PA and ^{3}H labeled CTP, a good linear relationship between CDS content and reaction rate was shown in the range of substrate and protein content tested (Fig. 3.4B). The data demonstrated that the conversion from PA to CDP-DAG in the reaction is the

result of CDS catalysis and, in the given range of substrate and enzyme concentration, is linear with the activity of CDS, which could be influenced by pH, metal ions, detergents and PA species.

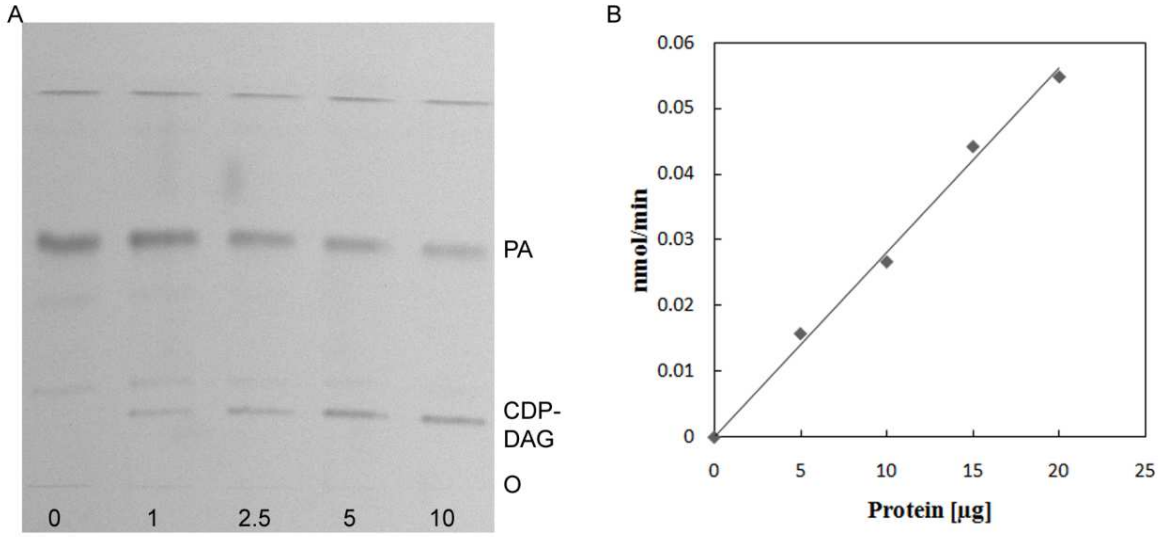

Figure 3.4 Relationship between protein concentration and CDS activity demonstrated by a CDS3 fraction.
A. Image of TLC-separated PA and CDP-DAG, after incubating the reaction mixture containing ^{14}C labeled PA and unlabeled CTP as substrate and mitochondrial membrane from yeast *cds1* null mutant expressing AtCDS3 as enzyme source. PA, phosphatidic acid; CDP-DAG, cytidinediphosphate diacylglycerol; O, migration origin; the numbers under the origin represent the protein content (µg) in reaction mixture.
B. CDS3 activity as a function of the protein content in the assay gave a linear graph of protein-reaction rate.

The extraplastidial CDS isoforms CDS1, CDS2 and CDS3 heterologously expressed in *cds1* null mutant yeast mitochondrial membrane showed broad but different optimum pH (Fig. 3.5): CDS1 and CDS2 were most active at pH 8 while CDS3 had a pH optimum at about 7.5 similar to the plastidial CDS enzymes. CDS isoforms of Arabidopsis were found to require Mg^{2+} for activity. The extraplastidial enzymes reached highest activity at 2 to 5 mM Mg^{2+}, unlike the plastidial enzymes, which were most active with 20 mM Mg^{2+} (Andrews and Mudd, 1985; Haselier *et al.*, 2010). Different from CDS of pea (*Pisum sativum*) chloroplast envelopes, which were almost completely inhibited by Triton X-100 (Kleppinger-Sparace and Moore, 1985), the activity of CDS enzymes from Arabidopsis expressed in yeast membrane was 4 to 12 fold stimulated by Triton X-100 at 0.6 %. In addition, activities of the extraplastidial isoforms as a function of the substrate concentrations reached the highest activities at 2 mM CTP which is more than ten-fold lower concentration than that of CDS4 and CDS5 (30 mM CTP; Haselier *et al.*, 2010). Except

the absolute value of activities, all three extraplastidial proteins functionally expressed in yeast mitochondrial membranes displayed enzymatic properties very similar to each other.

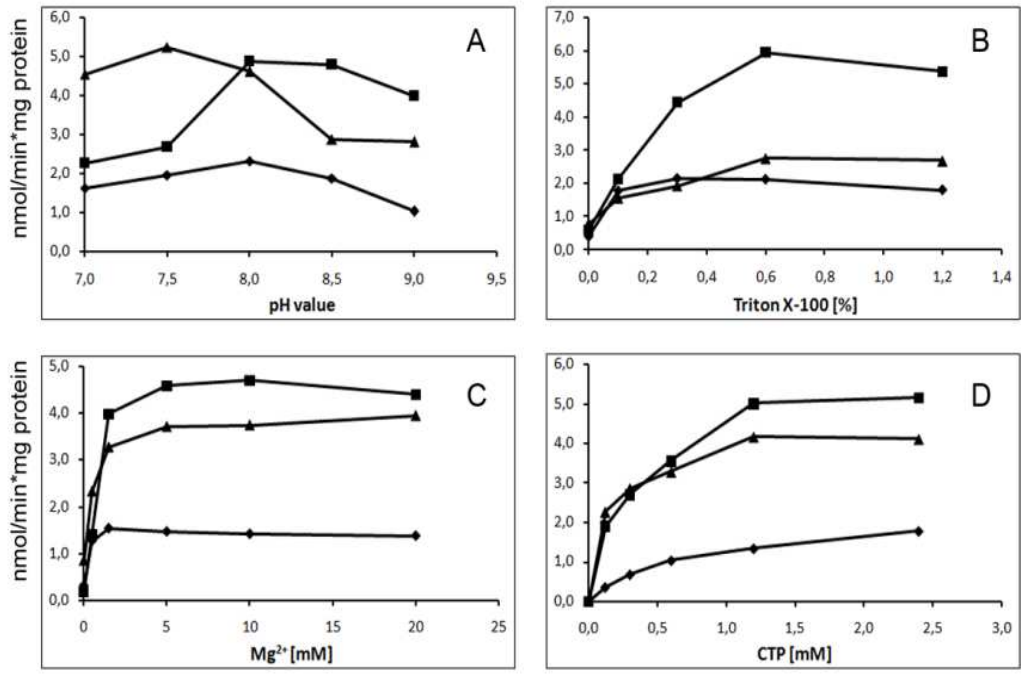

Figure 3.5 CDS1, CDS2 and CDS3 activity as a function of (A) pH value of the reaction mixture, (B) Triton X-100 concentration, (C) Mg^{2+} concentration and (D) CTP concentration. CDS1, diamonds; CDS2, squares; CDS3, triangles.

The preference for PA species of the extraplastidial proteins was studied using dioleoyl, dipalmitoyl and 1-palmitoyl-2-oleoyl species. Similar to CDS4 and CDS5, the extraplastidial isoforms were most active with the 18:1/18:1 species of PA and their activities decreased in the order of 16:0/18:1 PA to 16:0/16:0 PA (Fig. 3.6). On the other hand, the extraplastidial isoforms had lower K_m for PA, and reached the reaction saturation at 0.2 – 0.4 mM which is much lower than that of plastidial isoforms (2 mM for CDS4 and CDS5; Haselier *et al.*, 2010). The preference of unsaturated PA species reflects a requirement of CDS enzymes from Arabidopsis for a fluid physical state under the *in vitro* assay conditions. In summary, the various isoforms encoded by the five Arabidopsis genes have similar properties except that the extraplastidial enzymes reached substrate saturation at considerably lower concentrations than the plastidial isoforms.

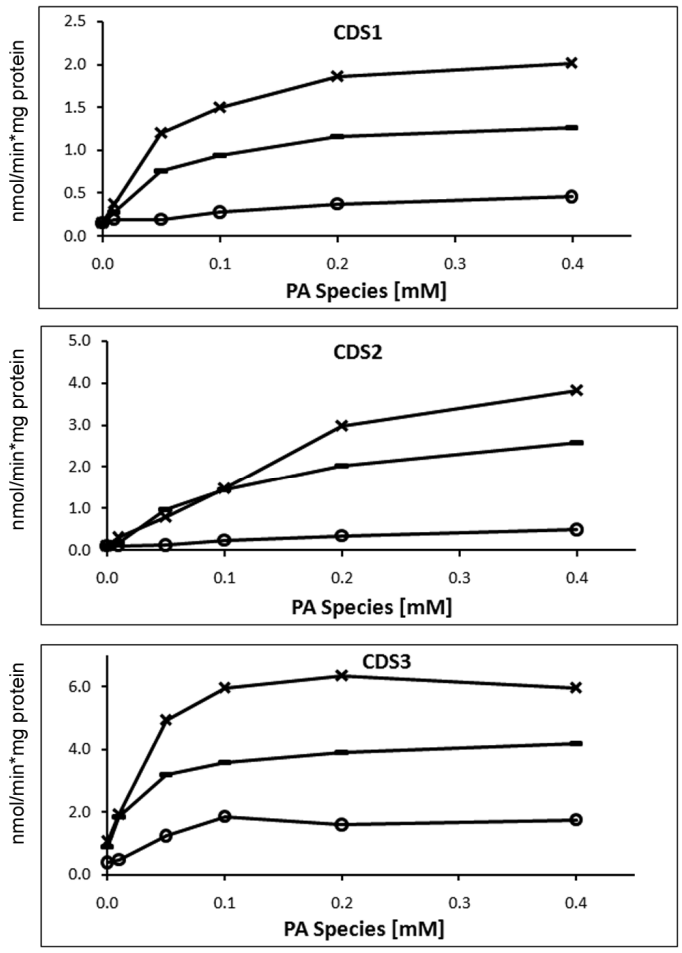

Figure 3.6 Activity of CDS1, CDS2 and CDS3 enzymes as a function of the PA species: 18:1/18:1, crosses; 16:0/18:1, bars; 16:0/16:0, circles.
PA, phosphatidic acid.

3.3 Subcellular localization of CDS from Arabidopsis

To gain insight into the subcellular localization of the extraplastidial CDS proteins from Arabidopsis, firstly, predictions performed by several predictor programs were collected and compared to get some hints for our experiments. As reported before, CDS1, CDS2 and CDS3 of Arabidopsis lack typical N-terminal targeting sequences so that different prediction programs for subcellular localization give inconsistent results, ranging from plasma membrane to most organelles (Heazlewood *et al.*, 2005, 2007; Haselier *et al.*, 2010). In contrast, CDS4 and CDS5 are predicted to be the plastidial isoforms by most programs, in accordance with experimental results in tobacco BY2 cells (Haselier *et al.*, 2010). So it is necessary to launch experiments for the subcellular localization of the extraplastidial CDS isoforms. This test was achieved by transient expression of GFP fusion proteins in plant cells in this work. Firstly, parts or whole sequence of the open reading frames of the *CDS* genes were cloned (Fig. 3.7) and fused to the 5' end of enhanced green fluorescent protein (eGFP) sequence and transiently expressed under the control of cauliflower mosaic virus 35S promoter in BY2 cells and tobacco leaf epidermal cells,

respectively. The tobacco leaf epidermal cells were found to be better suited for the expression of CDS fusion proteins than the previously used BY2 cells (Haselier *et al.*, 2010), as leaf epidermal cells showed higher transformation rate, stronger GFP signals, were easier to handle, and less time consuming.

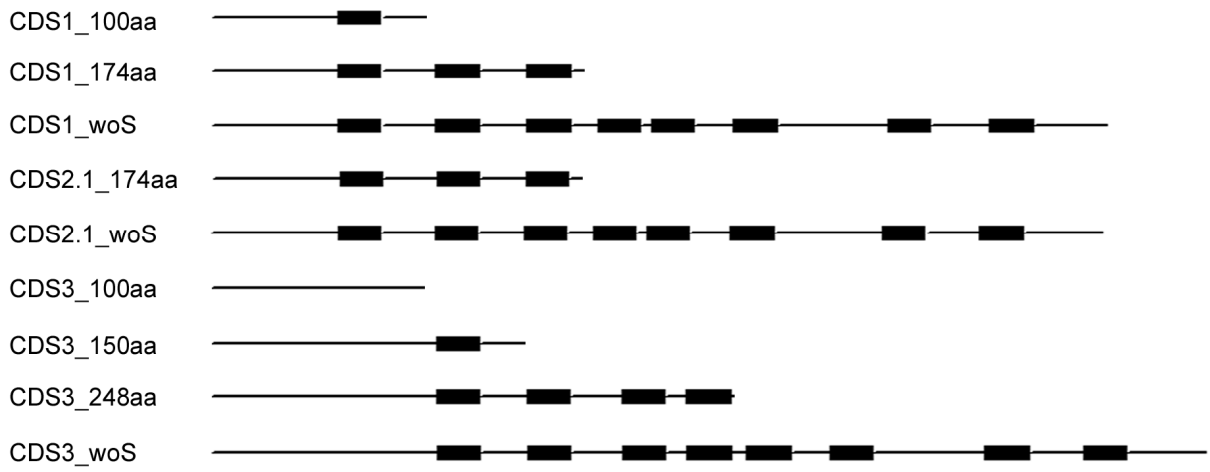

Figure 3.7 Schematic diagram of full-length and N-terminal regions of extraplastidial CDS amino acid sequences for the development of fusion proteins. Black boxes and lines represent transmembrane domains (TMD) and non-TMD, respectively. CDS1_woS, CDS2_woS and CDS3_woS are full-length sequences (woS, without stop codon), and the other are deletion constructs are named by the length of sequences (aa, amino acid).

For colocalization experiments in tobacco leaf epidermal cells, agrobacteria containing certain GFP and RFP constructs were mixed and infiltrated into mesophylar air space of tobacco leaves. As demonstrated in Fig. 3.8 A and B, both CDS1-GFP and CDS2.1-GFP exhibited colocalization with SEKDEL-RFP, an ER marker in tobacco leaves (Maclean *et al.*, 2007). The N-terminal peptide fusions CDS1_174-GFP and CDS2.1_174-GFP, in which five of the eight transmembrane domains were removed, showed colocalization with the ER marker as well (Fig. 3.8 E and F). On the other hand, none of the GFP fusion proteins gave signal pattern typical of chloroplast or mitochondria (Fig. 3.8 C and D). Moreover, CDS3 had results similar to CDS1 and CDS2 but weaker fluorescent signals (Fig. 3.8 G and H). This also holds true with regard to the other fusion proteins containing different N-terminal region, however, of which the GFP signals were very weak.

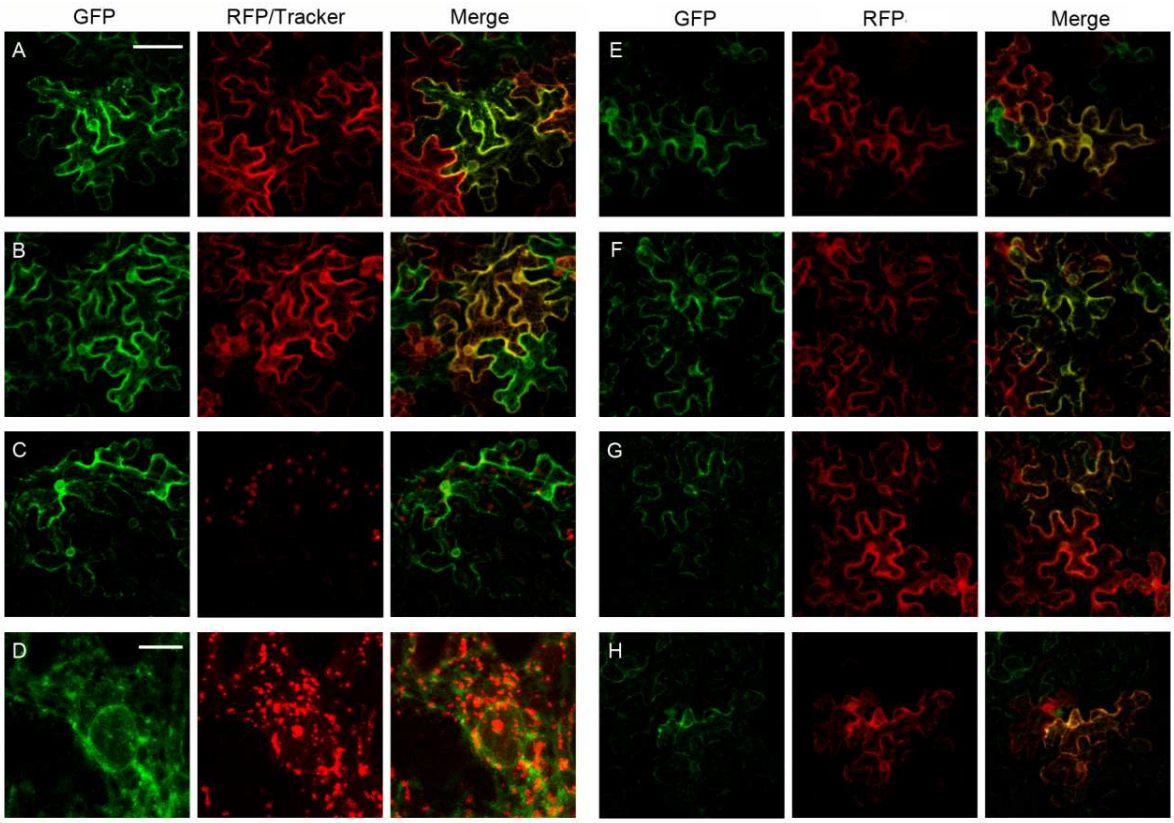

Figure 3.8 Subcellular localization of AtCDS1, AtCDS2 and AtCDS3 transiently expressed as GFP fusion proteins in tobacco leaf epidermal cells. First column, GFP signal; second column, RFP and mito tracker signal, respectively; third column, merge of first and second column.
(A) expression of CDS1_GFP and the ER marker SEKDEL_RFP; (B) CDS2_GFP and EKDEL_RFP;
(C) CDS1_GFP and chloroplast marker cTP_RFP; (D) CDS2_GFP counter stained with Mito Tracker Red.;
(E) the N' region (residues 1-174) of CDS1 fused to GFP and ER marker SEKDEL_RFP;
(F) the N' region (residues 1_174) of CDS2_GFP and SEKDEL_RFP;
(G) CDS3_GFP and SEKDEL_RFP; (H) the N' region (residues 1-150) of CDS3_GFP and SEKDEL_RFP.
Bar for A, B, C, and E to H is equal to 50 µm, in D to 10 µm. (cTP, chloroplast-transit peptide sequence of a Rubisco small-subunit gene from *Solanum tuberosum*).

Based on these data, it is likely that the extraplastidial CDS enzymes represent ER membrane proteins and the N-terminal regions covering at least the first transmembrane domains of the proteins can serve as signal peptides which direct CDS1, CDS2.1 and CDS3 to ER membrane. This is in line with the results obtained with CDS3 constructs: CDS3_100-GFP, without any TMD (Fig. 3.7) showed a nucleic localization, while the longer CDS3 fusion proteins were localized in ER (Fig. 3.7 and 3.8). We, however, cannot exclude the possibility that the proteins are located not only in ER but also in mitochondrial membranes at least to a certain extent and mitochondrial GFP signals escape detection because they are for instance rather week or located next to ER structures. The different subcellular localization of CDS1, CDS2 and CDS3 on the

one hand and CDS4 and CDS5 on the other hand is in line with the division into two groups in phylogenetic analysis (Fig. 3.1 and 3.2) and their different roles and functions in phospholipid biosynthesis.

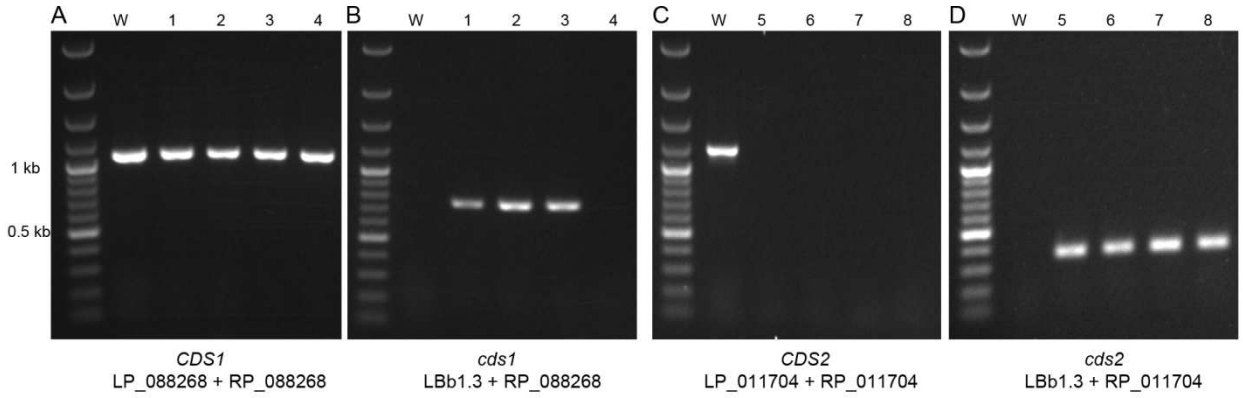

Figure 3.9 Isolation of heterozygous and homozygous *cds1* and *cds2* mutants. With the combination of primer pairs, PCR was performed to check whether the T-DNA insertion existed in the gene of interest. The PCR products were loaded and separated on 1 % agarose gel, stained by ethidium bromide and visualized by UV. The DNA markers (100 bp Plus, Fermentas) were co-migrated to indicate the size of products. W represents wild type plants, and the numbers represent plants of interest. A, PCR products obtained from the combination of two genomic specific primers LP_088268 and RP_088268; B, PCR products from the combination of a genomic specific primer RP_088268 and a T-DNA specific primer LBb1.3; C, PCR product from the combination of two genomic specific primers LP_011704 and RP_011704; D, PCR products from the combination of a genomic specific primer RP_011704 and a T-DNA specific primer LBb1.3.

3.4 Identification and characterization of *cds1* and *cds2* single mutants

To study the biological function of genes, several ways to create loss-of-function mutations have been developed, and one powerful way is via T-DNA insertional mutagenesis, which occurred within particular genetic elements, including 5' and 3' untranslated regions (UTRs), exons, introns, and predicted promoter regions (Alonso *et al.*, 2003). Several T-DNA insertion mutants obtained from the Nottingham Arabidopsis Stock Centre (NASC) were analyzed in our study. Homozygous mutant lines were identified by PCR using gene-specific primers LP and RP, as well as a T-DNA left border (LB) primer. As shown in Fig. 3.9, the combination of LP and RP primers gave rise to PCR products in WT but not in the homozygous mutant, because the elongation time is suitable for WT fragments (usually about 1 kb), but is too short for fragments containing a T-DNA insertion. In contrast, the primer pair of LB and RP led to PCR products in

the homozygous mutants but not in WT, as the LB primer sequence exists in the T-DNA mutant only. The heterozygous mutant that contains a T-DNA in one of the alleles had PCR products from both primer pairs.

The positions of the insertion sites were analyzed by sequencing the PCR amplification products. These studies showed that the T-DNA in *cds1* (SALK_088268) is situated in the 5' untranslated region of At1g62430, 25 bp upstream of the start codon. The *cds2* mutant (SALK_011704) contains a T-DNA in the intron of the 5' untranslated regions at position minus 69. In addition, a region of 40 bp before the insertion site is missing. The *cds3* mutant (SALK_002579), however, harbors a T-DNA in the region of the probable promoter at position minus 539 bp, about 30 bp upstream of 5' untranslated region, and losses 5 bp fragment (Fig. 3.10).

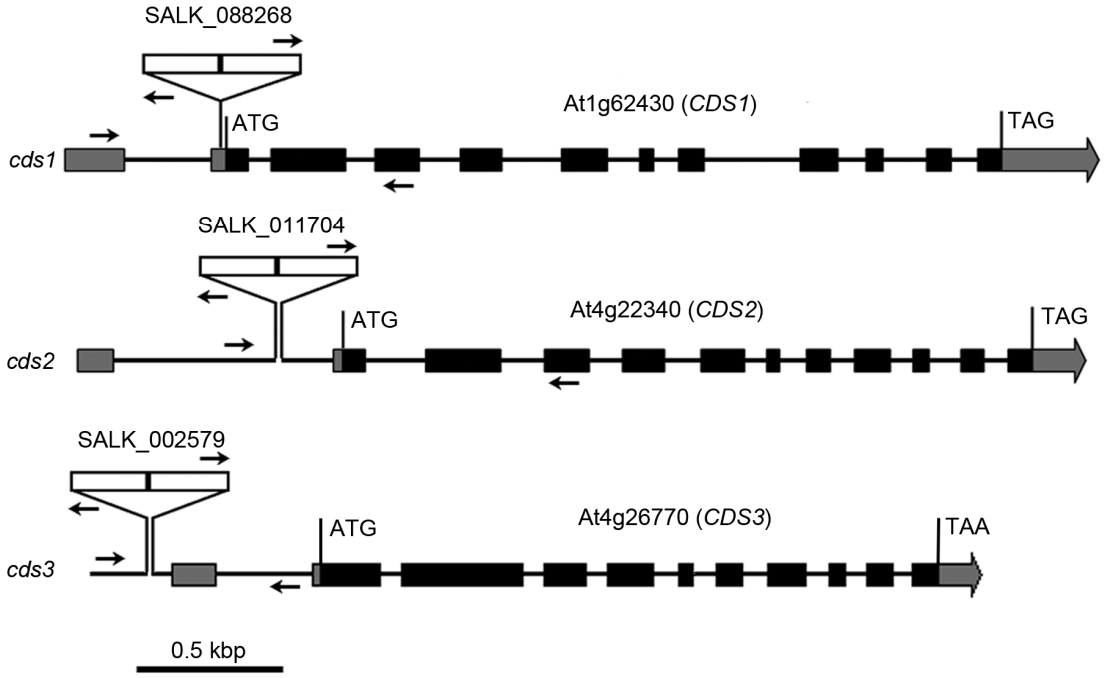

Figure 3.10 Schematic diagram of T-DNA insertions in the *cds1* (SALK_088268), *cds2* (SALK_011704) and *cds3* (SALK_002579) lines. The alleles of At1g62430 (*CDS1*), At4g22340 (*CDS2*) and At4g26770 (*CDS3*) were shown in exon-intron structure. The black bars represent exons, black lines represent introns and promoter region, and gray bars and arrows represent the 5' and 3' untranslated regions, respectively. Small arrows indicate the probably positions of primers for genotyping and sequencing, but the size does not fit to scale.

Based on the microarray data (Winter et at., 2007), *CDS1* and *CDS2* are constitutively expressed in Arabidopsis, while *CDS3* is only expressed in certain plant structures like stamens and mature

pollens (Fig. 3.3). To study the biological functions of the extraplastidial CDS isoforms during the vegetative growth phase of Arabidopsis, we have thus focused on *CDS1* and *CDS2*. Analysis of RT-PCR products of WT, *cds1* (SALK_088268) and *cds2* (SALK_011704) mutant leaves showed that *CDS1* transcripts in the *cds1* mutant and *CDS2* transcripts in the *cds2* mutant were undetectable, while the expression levels of the other *AtCDS*s were very similar to WT: *CDS4* and *CDS5* was not altered by the know-out of *CDS1* or *CDS2*, while *CDS3* was undetectable in neither WT nor single mutants. That is in line with microarray data, *CDS3* transcripts were undetectable in leaf tissue (Fig. 3.11).

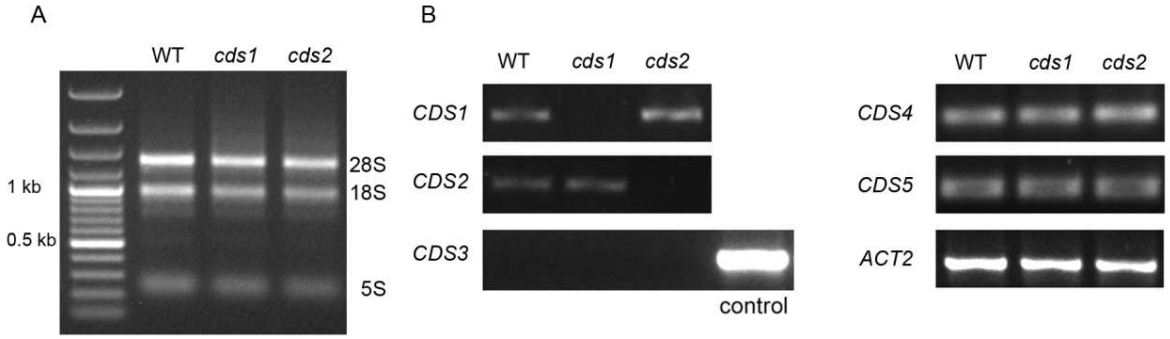

Figure 3.11 Total RNA isolation and RT-PCR analysis of CDS transcription in Arabidopsis WT, *cds1* and *cds2* rosette leaves. A, agarose gel electrophoresis of total RNA. Total RNA was purified from 6-week-old rosette leaves, quantified by a spectrophotometer (Nanodrop 2000c, Thermo Scientific). 0.5 µg of total RNA were separated by 1 % agarose gel. The bands of 28S, 18S and 5S rRNA were indicated. DNA ladder were used to show the relative migration and amount of RNA. B, The total RNA was used to synthesize cDNA for transcript analysis. Transcript levels of CDS1 to CDS5 in WT, *cds1* and *cds2* were determined by semi-quantitative RT-PCR. The PCR products synthesized from cDNA were loaded and separated on 1 % agarose gel, stained by ethidium bromide and visualized by UV. Transcript level of *actin2* demonstrates the RNA concentration and quality in the samples. For *CDS3*, the pENTR_CDS3 plasmid was used as a control.

As depicted in Fig. 3.12, homozygous mutants of both *cds*1 and *cds*2 showed no obvious phenotype with regard to growth and development. They were able to germinate on soil or MS medium with or without sucrose and grow as rapidly as the wild type. Mutant plants also developed flowers, siliques and seeds like the WT. In addition, lipid analysis of rosette leaves gave no indication that the lipid metabolism of the single *cds* mutants was altered. Hence, single mutations in *CDS* genes have no obvious effect on plant physiology, suggesting that a defect in *CDS1* can largely be compensated by *CDS2* and vice versa, as has been reported for *CDS4* and *CDS5* (Haselier *et al.*, 2010).

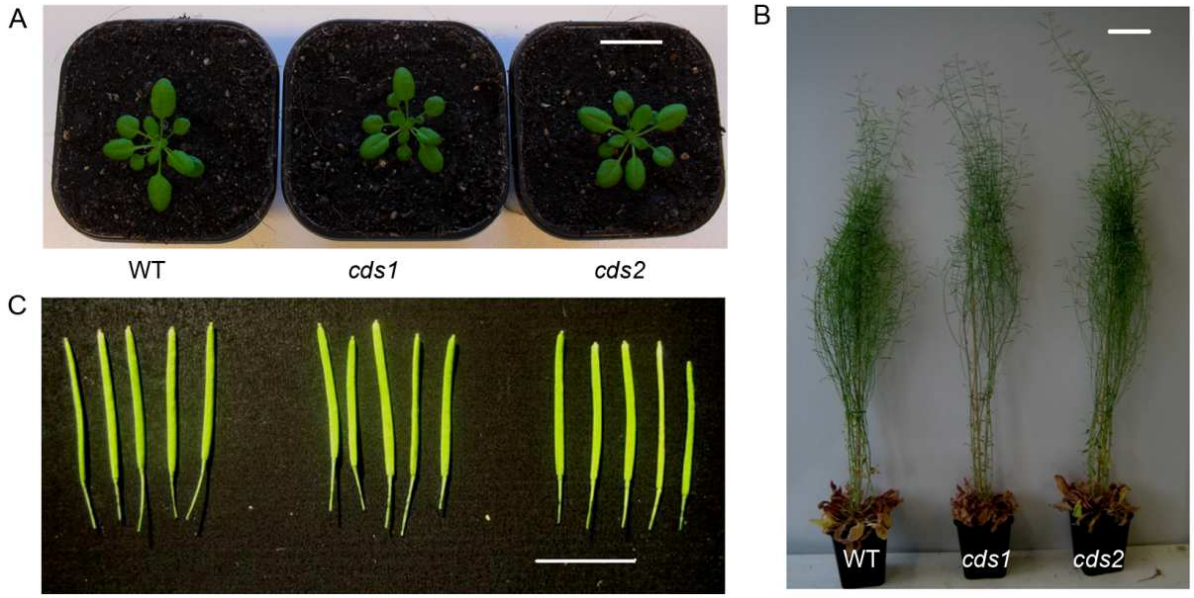

Figure 3.12 Phenotype of *cds1* and *cds2* in comparison with WT. A, Plants of WT, *cds1* and *cds2* grown on MSG plates for three weeks and transferred to soil for another two weeks, under short day conditions (8-h-light/16-h-dark, 22 °C). B, plants of WT, *cds1* and *cds2* with silique. C, siliques of WT, *cds1* and *cds2*. Bar is 2 cm in A, 5 cm in B, and 1 cm in C.

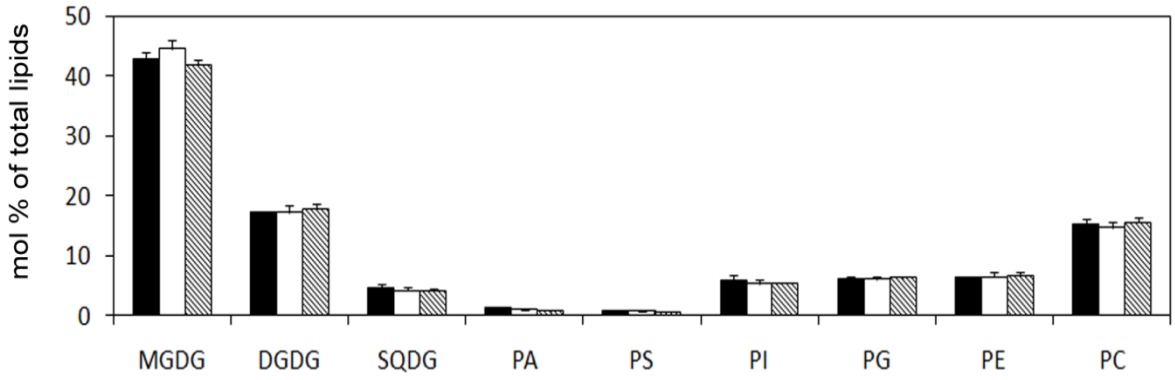

Figure 3.13 Glycerolipid composition of WT, *cds1* and *cds2* rosette leaves.
Lipids from WT (black bars), *cds1* (white bars) and *cds2* (diagonal bars) rosette leaves were extracted and analyzed. Data were obtained from 4 biological replicates and given in average mole percentage and standard deviation. (monogalactosyldiacylglycerol (MGDG), digalactosyldiacylglycerol (DGDG), sulfoquinovosyldiacylglycerol (SQDG), phosphatidic acid (PA), phosphatidylcholine (PC), phosphatidylethanolamine (PE), phosphatidylglycerol (PG), phosphatidylinositol (PI) and phosphatidylserine (PS)).

3.5 Identification and characterization of double mutant

3.5.1 Development of double mutants by crossing and RNA interfering constructs

To directly demonstrate that *CDS1* and *CDS2* have redundant functions, double mutants were created by crossing homozygous *cds1* and *cds2* mutant plants. The F1 progeny were genotyped by PCR and mutant plants heterozygous for the two *CDS* genes were self-pollinated. In the F2 progeny some seedlings developed distinctly slower than the others. To investigate whether these tiny seedlings represent homozygous double mutants, mutant plants of the F2 generation, which possessed one functional *CDS* gene only, were identified and self-pollinated. Abnormal tiny seedlings were also discovered among the F3 progeny. Moreover, the statistical analysis exhibited a segregation, the ratio of abnormal and normal seedlings is a good fit to the 1:3 (χ_c^2=0.644, P>0.05 (Table 3.1). Genotype analysis based on PCR revealed that all of the abnormal seedlings represented homozygous *cds1cds2* double mutants and normal seedlings were heterozygous double mutants (Fig. 3.14).

Table 3.1 Segregation of phenotype from a heterozygous double mutant *cds1*+/-*cds2*-/-. *$\chi_c^2=\Sigma\frac{(|A-T|-0.5)^2}{T}$

Phenotype	Actual number (A)	Theoretical number (T)	A-T	χ_c^2*
Normal	334	326.25	7.75	0.161
Abnormal	101	108.75	-7.75	0.483
Total	435	435	0	0.644
df=1, $\chi^2_{0.05(1)}$=3.84				
$\chi_c^2<\chi^2_{0.05(1)}$, P>0.05				

The *cds1cds2* double mutants germinated on MSG plates with or without sucrose, but grew slowly, had green but smaller cotyledons, shorter hypocotyls and radicles than WT seedlings (Fig. 3.14 and 3.15). More critically, *cds1cds2* mutants failed to develop true leaves and died about 3 weeks after germination, no matter whether they were fed with sucrose or not. The different phenotype of the single and double mutants indicates that *CDS1* and *CDS2* have redundant functions, similar to the plastidial isoforms, *CDS4* and *CDS5*. The phenotype of *cds1cds2* homozygous double mutants, however, is distinctly different from that of *cds4cds5*: (1) the size of seedlings of *cds1cds2* is smaller to *cds4cds5*; (2) *cds1cds2* has small but green cotyledons, while *cds4cds5* has normal size but yellowish cotyledons; (3) *cds1cds2* is seedling

lethal no matter whether they were fed with sucrose or not, while *cds4cds5* can finish the whole life cycle when fed with sucrose. It is known that *cds4cds5* lacks the plastidial PG and shows a phenotype similar to the *pgp1* mutants (Hagio *et al.*, 2002; Xu *et al.*, 2002, 2006; Babiychuk *et al.*, 2003; Haselier *et al.*, 2010). These data indicate that CDS1 and CDS2 have different biological functions in lipid biosynthesis and physiology in Arabidopsis from that of CDS4 and CDS5, though all of them are involved in the biosynthesis of CDP-DAG.

The knock-out double mutant *cds1cds2* led to seedling lethal phenotype that prevented further studies on the biological role of CDS1 and CDS2 in Arabidopsis growth and development. We also tried to construct RNAi lines using *cds1* (SALK_088268) was used as parent plant, and transformed with RNAi constructs of *CDS2*. The constructs including pAgrikola_4g22340GST (GST, gene-specific sequence tags; Hilson *et al.*, 2004; Appendix Fig. A2) and pWatergate_ 3'UTR4G22340 in which the 35S promoter of pHELLSGATE is replaced with the Arabidopsis RbcS promoter (Wesley *et al.*, 2001; Appendix Fig. A6) were transformed into *cds1cds2* via floral dip method (Clough and Bent, 1998). More than 8 000 seeds were sown on MSG plates, but no abnormal seedlings could be selected although several seedlings showed reduced *CDS2* transcript level, perhaps much more seeds need be screened in further work.

3.5.2 Rescue double mutant by *CDS1* and *CDS2*

To confirm that growth defect and seedling lethal phenotype of *cds1cds2* double mutants is result from losing both CDS1 and CDS2 functions, complementation assays were carried out. To this end, heterozygous double mutants (*CDS1+/-cds2*), which were homozygous for *cds2* and heterozygous for *cds1*, were transformed with *CDS1* or *CDS2* cDNA under the control of XVE-Olex-46 promoter system, under which gene expression is strongly induced by β-estradiol. Heterozygous double mutants *CDS1+/-cds2* containing *XVE::CDS1* or *XVE::CDS2* were selected by antibiotics and genotyped from the F1 progeny, of which the seeds were harvested and analyzed. As depicted in Fig. 3.15, homozygous double mutants expressing a chimeric *CDS1* or *CDS2* gene developed and grew like WT plants while the seedlings of *cds1cds2* without complementation construct stopped growing, became yellowish and died. Hence, the seedling lethal phenotype of *cds1cds2* double mutants was rescued by inducing the expression of a

functional *CDS1* or *CDS2* gene. These data demonstrate that the growth defect of double mutants is caused by deficiency of both genes.

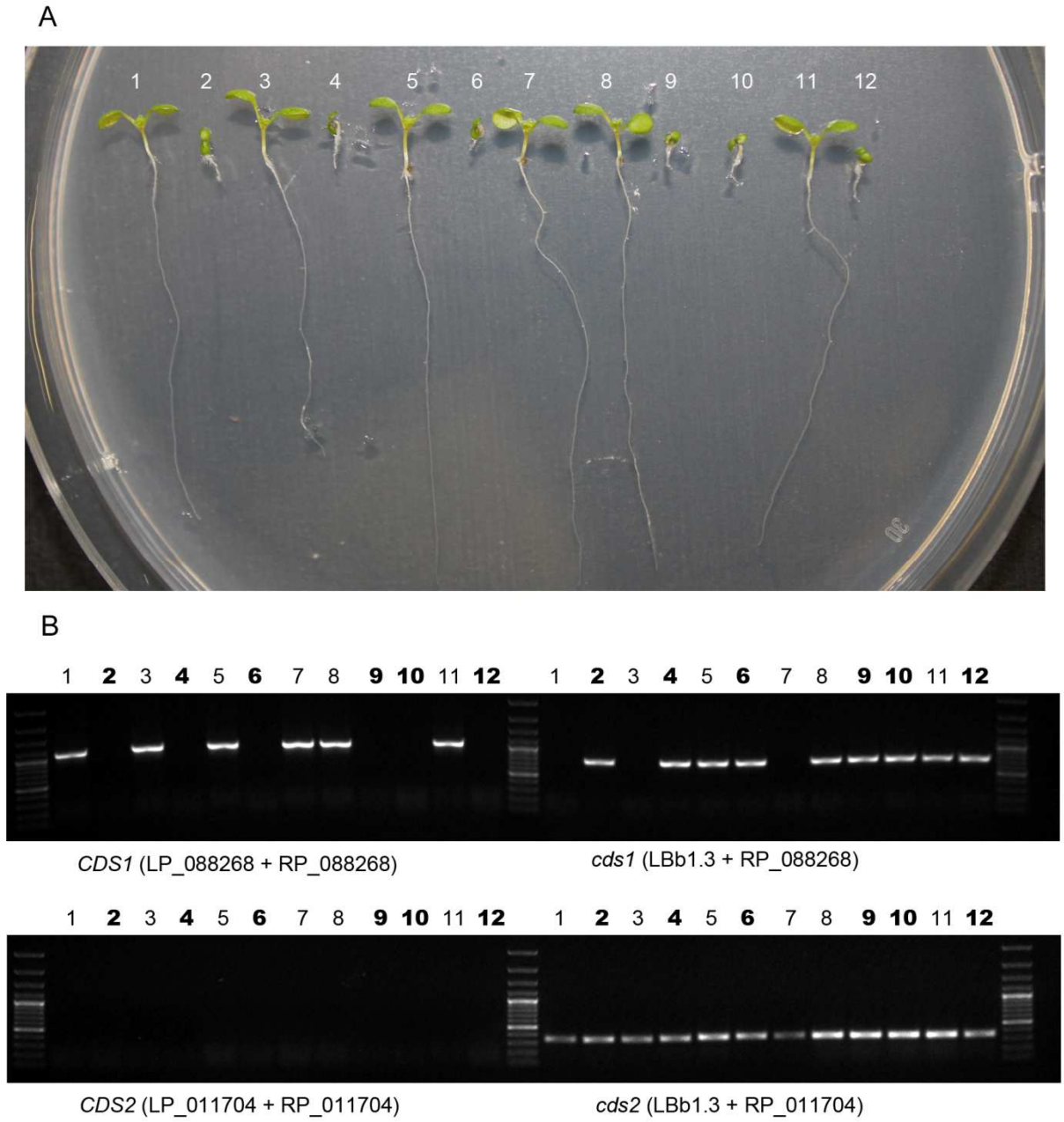

Figure 3.14 Phenotype and genotype of *cds1cds2* double mutants. A. Seeds from heterozygous double mutant that contains one functional CDS1 were harvested and sown on MSG plates. After 2 days stratification in the dark at 4 °C, seeds were cultivated for 10 day under short day condition (8 hour light / 16 hour dark, at 22 °C). Seeds on plates were cultivated vertically to facilitate comparison of the length of hypocotyls and radicles. B. 10-day-old seedlings shown in A were used for DNA isolation and PCR. The primer pairs are given under the electrophoresis image. The double mutants were indicated in black.

Estradiol is sensitive to light and air in media, therefore the inducing plants must be wet with medium containing 10 µM estradiol every day to keep normal growth. This procedure, however, is prone to infections, so that it was hard to finish a whole plant life cycle. To overcome this problem, *CDS1* and *CDS2* cDNA under the control of 35S promoter were transformed into heterozygous double mutants that were homozygous for *cds2* and heterozygous for *cds1*. Double mutants containing a chimeric *CDS1* or *CDS2* gene grew normally on MSG plates or in soil like WT, but failed to develop normal flowers and seeds. This may be because expression level controlled by the 35S promoter cannot satisfy the requirement of extraplastidial CDS like the native promoter does.

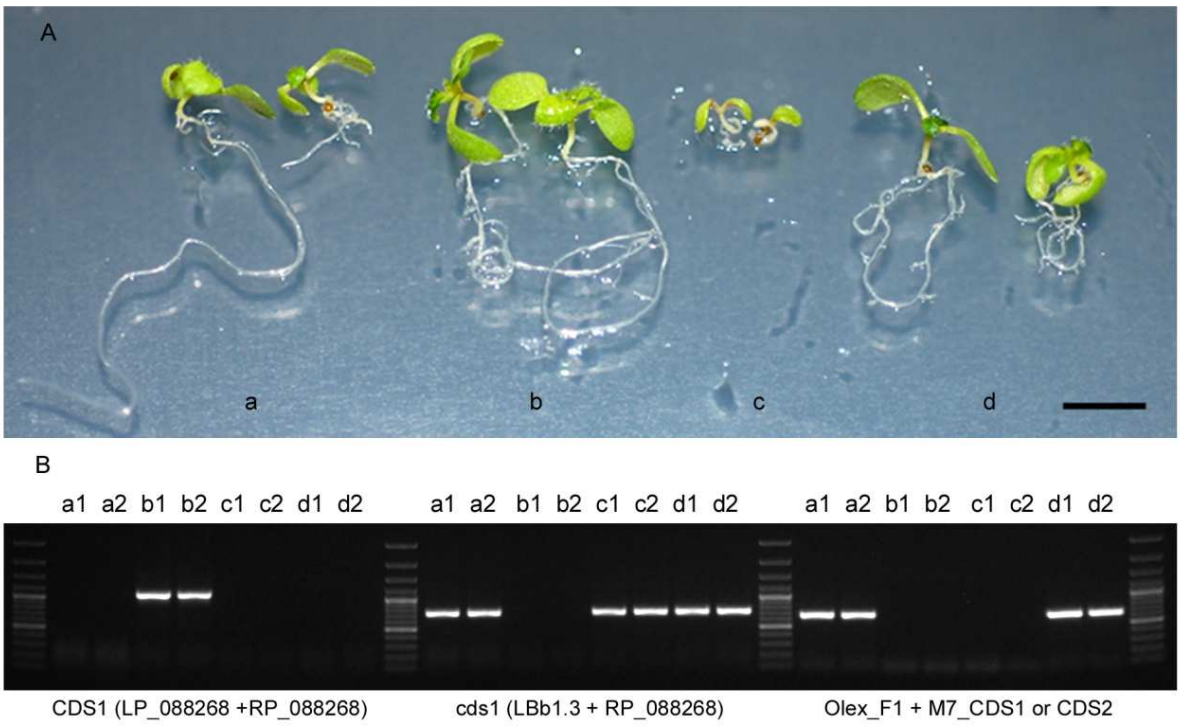

Figure 3.15 Complementation assay of *cds1cds2* by *CDS1* or *CDS2* cDNA.
A, seedlings were grown on MSG plates containing 2 % sucrose and 10 µM β-estradiol and wet by MSG containing 10 µM β-estradiol every day for 2 weeks; a, *cds1cds2* containing an estradiol inducible *CDS2* gene (*cds1cds2+XVE::CDS2*); b, WT; c, *cds1cds2* double mutant; d, *cds1cds2+XVE::CDS1*. Bar = 5 mm.
B, genotyping of the seedlings shown in A. Because double mutant were derived from heterozygous containing one functional CDS1, the genotyping for CDS2 was omitted. The primer pairs for PCR were given under the electrophoresis image. For checking the inducible promoter and CDS1 and CDS2 cDNA, primers of Olex_F1 and M7_CDS1 were used for plant a, b and c, primers of Olex_F1 and M7_CDS2 were used for plant d1 and d2.

3.5.3 Characterization of the *cds1cds2* double mutants

Although *cds1cds2* double mutants showed growth deficiency, but developing seeds and embryos had no obviously difference in seed phenotype between homozygous and heterozygous mutants. So we focused on seedling development. Firstly, the transcription of extraplastidial *CDS* was analyzed. RT-PCR showed that both of *CDS1* and *CDS2* were disrupted in *cds1cds2* seedlings, while *CDS3* was not upregulated, since non transcript was detected as in WT and *cds4cds5*.

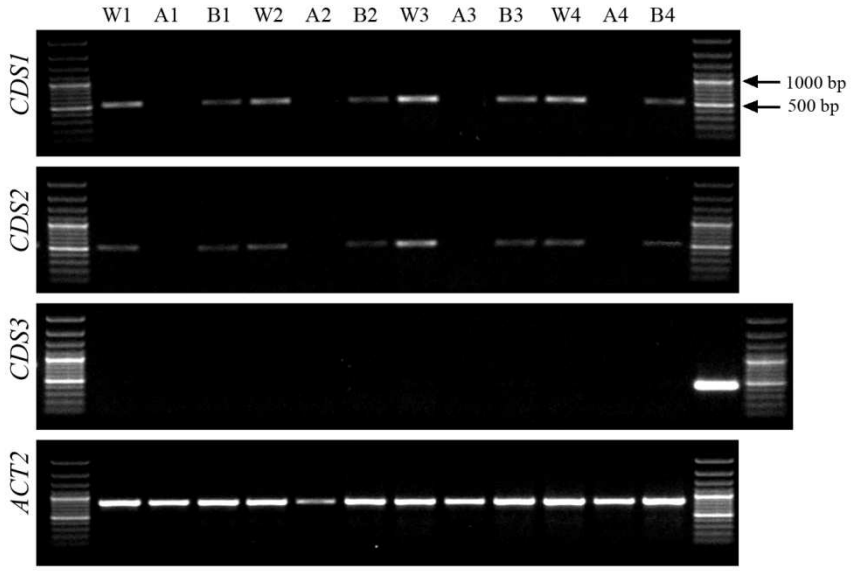

Figure 3.16 Transcription of *CDS1*, *CDS2* and *CDS3* in 5-day-old seedlings of *cds1cds2* was detected.
Transcript levels of *CDS1*, *CDS2* and *CDS3* in 5-day-old seedlings of WT (W1-W4), *cds1cds2* (A1-A4) and *cds4cds5* (B1-B4) were determined by RT-PCR. The PCR products synthesized from cDNA were loaded and separated on 1 % agarose gel, stained by ethidium bromide and visualized by UV. Transcript level of *actin2* demonstrates the RNA concentration and quality in the samples. For *CDS3*, the pENTR_CDS3 plasmid was used as a control.

The seeds of mutants and WT were sown on agar-solidified MSG medium, stratified in the dark at 4 °C for 2 days, and cultivated in short day condition (8-hour-light/16-hour-dark, 22 °C). Seedlings of different cultivation time were harvested, decolorized, and stained by Lugol solution. As shown in Fig. 3.17, double mutants are compared with WT from 3 days to 7 days, because it is possible to distinguish the homozygous double mutant seedlings from heterozygous ones based on the size 3 days after the cotyledons and root break the seed coat. Unlike WT seedlings, which expanded cotyledons, elongated hypocotyls and radicles, the double mutant

plants reached a small size and stopped growing. More interestingly, the content of starch visualized by staining of Lugol solution was kept in a high level in double mutants, while dramatically decreased in WT. These data indicate that double mutants can synthesize carbohydrates but failed to utilize them for growth, unlike the *cds4cds5* mutant deficient in which the starch was effectively consumed.

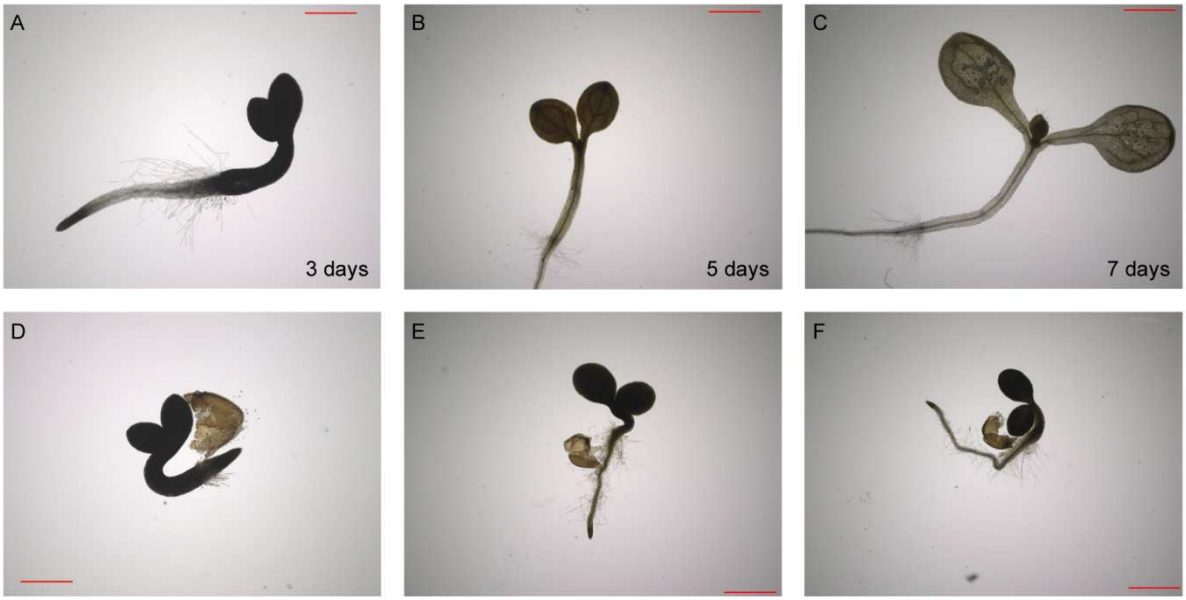

Figure 3.17 Starch staining of WT and *cds1cds2* with Lugol solution. A, B and C, WT; D, E and F, *cds1cds2*. A and D, 3-day-old seedling; B and E, 5-day-old seedling; C and F, 7-day-old seedling. Bar for A and D is equal to 500 µm, and bar for B, C, E, and F is equal to 1000 µm.

To determine whether the growth defect of the *cds1cds2* double mutant is caused by dysfunction in photosynthesis, the chlorophyll auto-fluorescence of cotyledons from *cds1cds2* double mutants was studied by fluorescence microscopy. As shown in Fig 3.18, *cds1cds2* double mutant mesophyll cells emit signal as strong as WT. In that way, the *cds1cds2* mutant differs from the thylakoid defective *cds4cds5* mutant (Haselier *et al.*, 2010), which had a rather weak auto-fluorescence signal. In addition, *cds4cds5* needed externally added sucrose for growth while *cds1cds2* cannot be rescued by feeding with sucrose. These data combined with the green color of cotyledons indicated that the thylakoid membranes of *cds1cds2* double mutant may be intact. As described below, this conclusion was supported by ultrastructural analyses (Fig. 3.20).

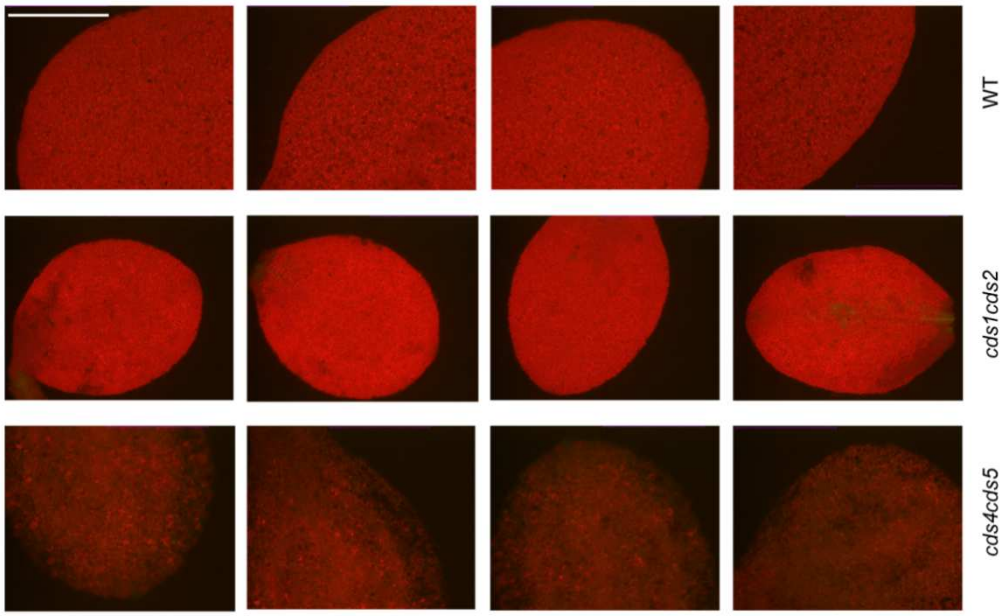

Figure 3.18 Auto-fluorescence of cotyledons from WT (first row), *cds1cds2* (second row) and *cds4cds5* mutants (third row).
Signals were obtained from cotyledons of 7-day-old seedlings, grown on MSG medium under short day conditions (8 h light/16 h dark) at 22 °C. Bar = 500 µm.

Another evidence for the growth defect of *cds1cds2* mutants was found when the leaf sections of *cds1cds2* were compared with that of WT and *cds4cds5*. Light microscopy showed that *cds1cds2* had smaller epidermal and mesophyll cells. The average radius of mesophyll cells in *cds1cds2* is about 2/3 of that of WT. In addition, it is easy to see that the blade of *cds1cds2* was thinner than that of WT and *cds4cds5* (Fig. 3.19).

Ultrastructural comparison of mesophyll cells from cotyledons, shown in Fig. 3.20, demonstrated that mesophyll cells of the double mutant had a smaller cell size than that of WT, consisting with light microscopy analysis (Fig. 3.19). In addition, vacuoles in the double mutant cells were relatively small so that cytoplasm with organelles took up more space of mutant cells than of WT cells. This finding points to a defect in cell expansion of the double mutant resulting in strong suppression of growth (Fig. 3.14 and 3.17).

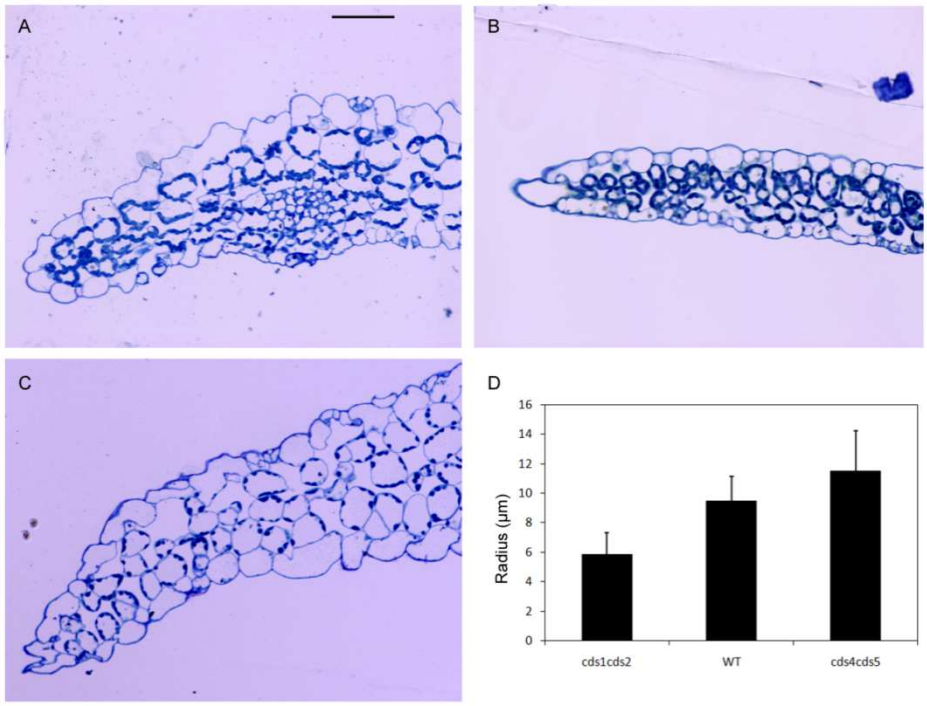

Figure 3.19 *cds1cds2* double mutants had smaller cells than WT and *cds4cds5*. Microscopic analysis of WT (A), *cds1cds2* (B) and *cds4cds5* (C) were performed with toluidine blue stained semithin sections (1µl) of cotyledons. Bar for A, B and C is 50 µm. D, comparison of average radius of mesophyll cells from WT, *cds1cds2* and *cds4cds5*. The radius was measured from more than 40 mesophyll cells, and the average radius and standard deviation were given.

The size of chloroplasts in the double mutant was slightly smaller than that of WT organelles. Moreover, chloroplasts in double mutants accumulated much more starch than WT chloroplasts. This result was in accordance with the starch staining experiment in Fig. 3.17. The *cds1cds2* double mutants appeared to have a typical thylakoid structure, but due to the starch grains accumulating in the organelles, thylakoid membranes were compressed (Fig. 3.20C-F). With regard to mitochondria and ER, we observed no obvious difference in structure between double mutant and WT (Fig. 3.20E-H). Microscopic analyses demonstrated the disruption of *CDS1* and *CDS2* genes in *cds1cds2* double mutants led to defect in cell expansion which could be one of the reasons causing suppression of growth. The auto-fluorescence and accumulation of starch indicates there is not defect in photosynthesis function which is damaged by disruption of the plastidial isoforms CDS4 and CDS5.

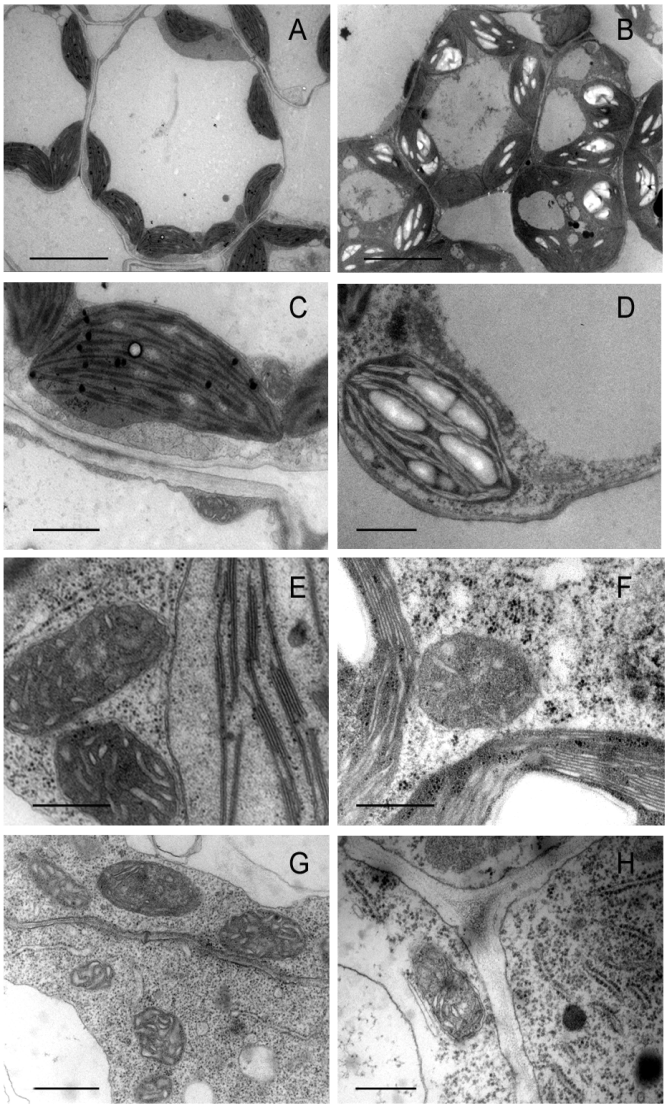

Figure 3.20 Ultrastructure of WT and *cds1cds2* mutant cells of cotyledons and radicles was analyzed by electron microscope in Bio II, RWTH, performed by Agnes Weth and Prof. Dr. Werner Baumgartner.
Transmission electron microscopy images of mesophyll cells from cotyledons (A - F) and cortex cells from radicles (G, H) from WT (A, C, E and G) and *cds1cds2* seedlings (B, D, F and H) grown on MSG plates containing 2 % sucrose for 5 days.
(A and B) survey of mesophyll cells, (C and D) typical structure of chloroplasts, (E and F) mitochondria and part of chloroplasts, (G and H) mitochondria and ER membranes, Bar = 5 µm in A and B, Bar = 1 µm in C and D, Bar = 0.5 µm in D – H.

To study the viability of cells, calluses were induced using different tissues as starting materials (Fig. 3.21). In contrast to WT and *cds4cds5* mutant tissues, which were easily induced to form calluses, *cds1cds2* double mutant failed to develop callus regardless whether cotyledons, hypocotyls or radicles were transferred on callus inducing medium. Merely *cds1cds2* containing a functional *CDS1* or *CDS2* gene was able to form callus when *CDS* gene expression was induced by estradiol in the medium. If such a callus was cut into two pieces and transferred to callus inducing medium with or without estradiol, it only survived on media with estradiol while in the absence of estradiol callus stopped growing and died unlike WT calluses (Fig. 3.22). These data provide strong evidence that CDS1 or CDS2 functions are indispensible for callus formation and growth.

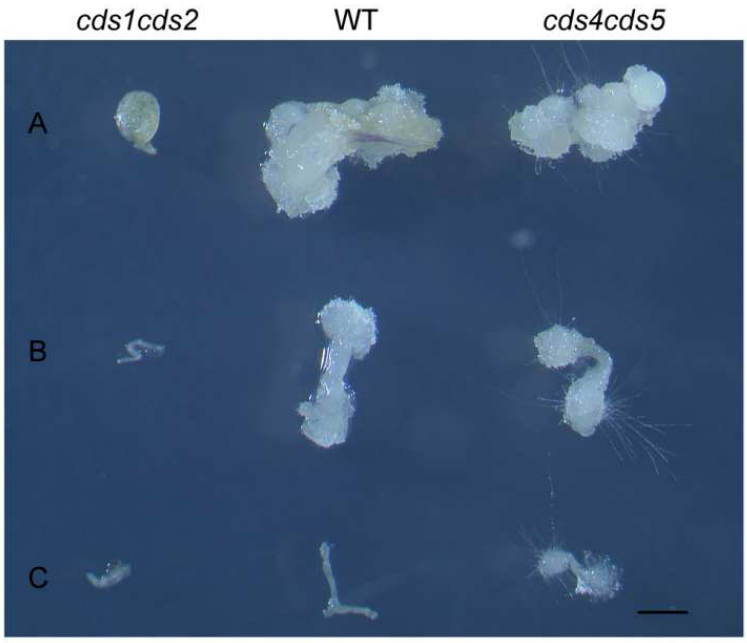

Figure 3.21 Callus derived from Arabidopsis seedlings.
Cotyledons (A), hypocotyls (B) and radicles (C) of 5-day-old *cds1cds2*, WT and *cds4cds5* seedlings were transferred onto callus inducing medium and incubated 12 days at 26 °C in the dark. Bar = 1 mm.

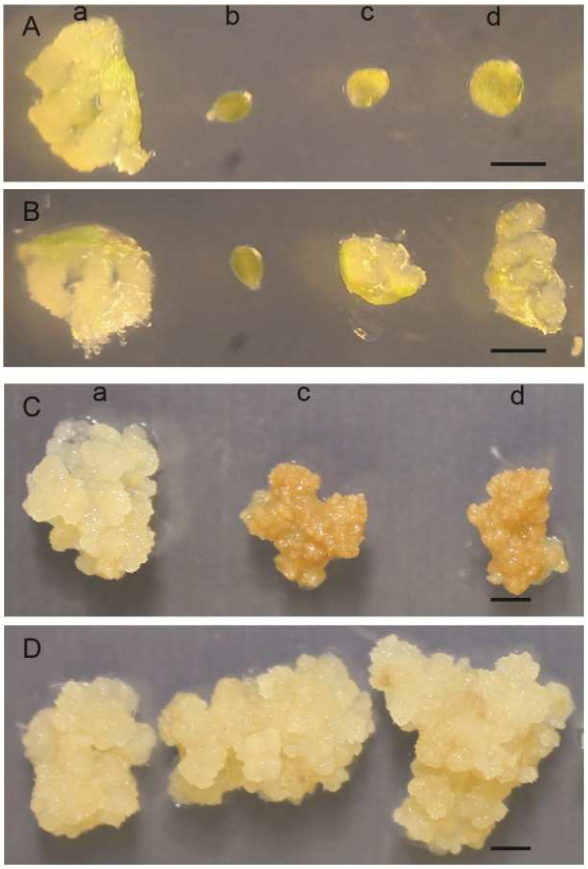

Figure 3.22 Callus development and growth require a functional *CDS1* or *CDS2* gene.
A and B: cotyledons of WT (a), *cds1cds2* (b), *cds1cds2+XVE::CDS1* (c) and *cds1cds2+XVE::CDS2* (d) were transferred onto callus inducing medium without (A) and with 10µM β-estradiol (B), respectively, and incubated at 26 °C in dark for 2 weeks. Bar = 1 mm.
C and D: callus of WT (a), *cds1cds2+XVE::CDS1* (c) and *cds1cds2+XVE::CDS2* (d) were cut and transferred onto callus inducing medium without (C) and with 10 µM β-estradiol (D), respectively, and incubated at 26 °C in dark for 3 weeks. Bar = 2 mm.

3.6 *In vivo* phospholipid labeling experiments with *cds1cds2* seedlings and calluses

The biosynthesis of phospholipids in Arabidopsis seedlings was studied using *in vivo* [^{33}P] phosphoric acid labeling. As shown in Fig. 3.23, firstly and remarkably, the labeling of PI and PG, the products of CDS-catalyzed reactions, were dramatically decreased in double mutant seedlings. PI labeling in *cds1cds2* was about one third of that of wild type and PG was less than 50 % compared to WT seedlings. However, the labeling of CL, the downstream biosynthesis product of mitochondrial PG, was maintained at low levels very similar to WT.

Labeling of PC, the major phospholipid of eukaryotes, was increased from 28 % in WT to 46 % in double mutant tissue. On the other hand, the percentage of PE in double mutant seedlings was almost equal to that in WT seedlings, although Arabidopsis predominantly produced PE by an aminoalcohol phosphotransferase activity as well (Fig. 3.23; Nerlich *et al.*, 2007).

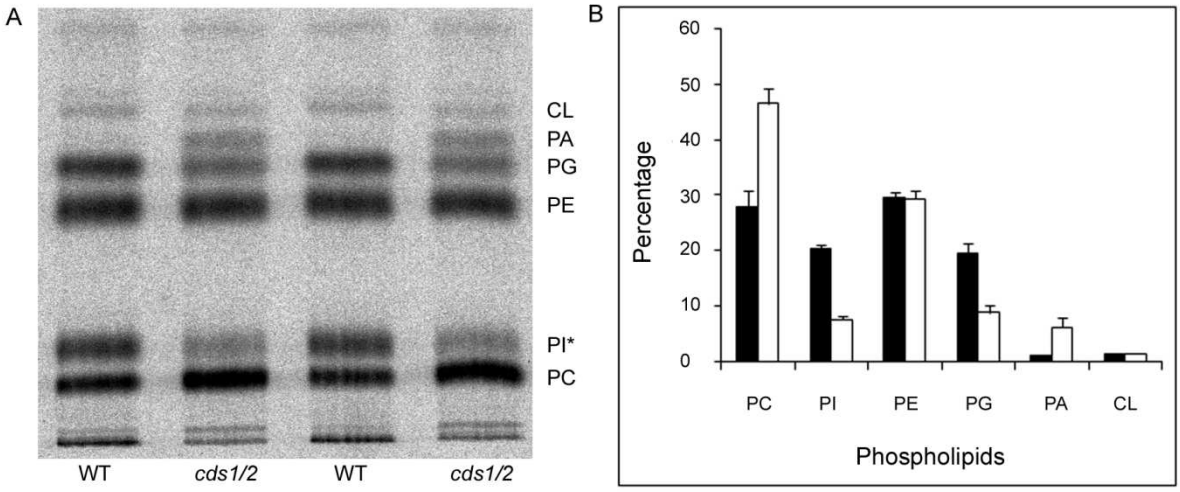

Figure 3.23 Phospholipid labeling pattern of *cds1cds2* seedlings differs from that of WT seedlings.
(A) Lipids extracted from [^{33}P] phosphate-treated seedlings of WT and *cds1cds2* were separated by thin layer chromatography, labeled phospholipids were visualized by a Bioimager, identified by cochromatography with authentic phospholipids and quantified by scintillation counting (phosphatidic acid (PA), phosphatidylcholine (PC), phosphatidylethanolamine (PE), phosphatidylglycerol (PG), phosphatidylinositol (PI), cardiolipin (CL)). * Separation of PI and phosphatidylserine (PS) in chloroform/triethylamine/ethanol/water (30:35:30:7) on 1.8 % boric acid-treated TLC plates verified that labeled PI was not contaminated with labeled PS.
(B) Labeling of the given phospholipids from WT (black bars) and *cds1cds2* seedlings (white bars) were scintillation counted and calculated in % of total labeling. Data were calculated from five biological replicates and standard deviations are given.

PA, the lipophilic substrate of the CDS reaction, accumulated in the double mutant while it was hardly detectable in WT seedlings. These results indicate that the PA pool in phospholipid biosynthesis is regulated by extraplastidial CDS, the disruption of which will increase the biosynthesis of PC and PE and decrease that of PI and PG. These results are in line with the identification of CDS1 and CDS2 as integral membrane enzymes of the ER and underline the importance of CDS activity for regulation of phospholipid metabolism.

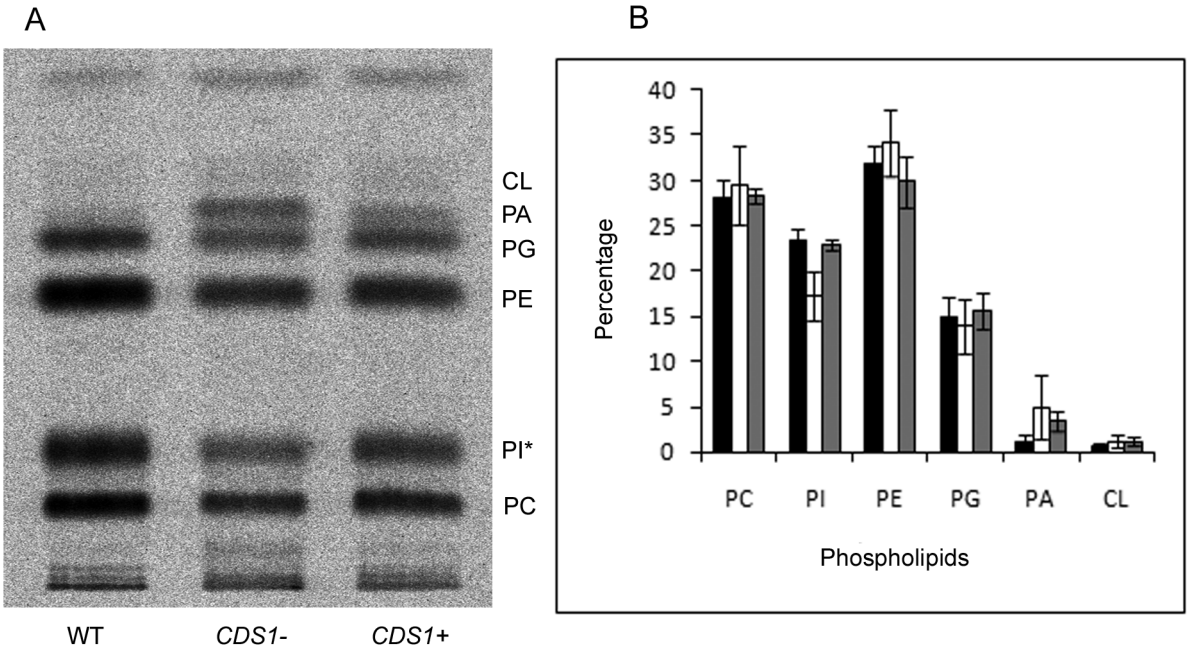

Figure 3.24 Phospholipid labeling pattern of WT and *cds1cds2+VXE::CDS1* mutant calluses.
A. Calluses were cultivated on medium without (*CDS1-*) and with (*CDS1+*) β-estradiol. After [^{33}P] phosphate treatment for 18 hours, lipids were extracted from the calluses, separated by thin layer chromatography and labeled phospholipids were visualized by Bioimaging (phosphatidic acid (PA), phosphatidylcholine (PC), phosphatidyl-ethanolamine (PE), phosphatidylglycerol (PG), phosphatidylinositol (PI), cardiolipin (CL)).
* Separation of PI and phosphatidylserine (PS) on 1.8 % boric acid-treated TLC plates in chloroform/triethylamine/ethanol/water (30:35:30:7) verified that labeled PI was not contaminated with labeled PS.
B. Labeling of the given phospholipids from WT (black bars), *cds1cds2+VXE::CDS1* without inducing (white bars) and with inducing (gray bars) were scintillation counted and calculated in % of total labeling. Data were calculated from four biological replicates and standard deviations are given.

The phospholipid biosynthesis in callus was also investigated. Because *cds1cds2* cannot form callus, we firstly induced and cultivated callus of *cds1cds2+VXE::CDS1* which were induced to growth by estradiol (Fig. 3.22). The callus of *cds1cds2+VXE::CDS1* were transferred and

incubated on callus inducing medium without estradiol for one week and used as partly disruption of extraplastidial CDS, following by labeling experiments. The analysis of ^{33}P labeling experiments of calluses revealed similar changes in phospholipid biosynthesis compared with seedling experiment (Fig. 3.24). Without induced expression of *CDS1*, *cds1cds2+ VXE::CDS1* callus accumulated more PA which was hard to detect in WT, and produced less PI and PG. These alternations in phospholipid biosynthesis were drawn back close to WT level by the inducing expression of *CDS1*. The differences in labeling patterns of WT and double mutant calluses, however, were less pronounced than that from double mutant and WT seedlings, likely because the calluses still maintained some extraplastidial CDS activity induced from some residual estradiol after transfer from estradiol containing to inductor free medium.

3.7 Steady state lipid compositions of double mutants and WT

3.7.1 Lipid composition of leaves, seedlings and calluses of WT

The steady state membrane lipid composition was determined by nanospray ionization tandem mass spectrometry (nanospray-MS/MS). Firstly, the data for rosette leaves, seedlings and calluses of WT were analyzed to determine the membrane lipid patterns of these WT structures. As shown in Fig. 3.25, the typical thylakoid membrane lipids monogalactosyldiacylglycerol (MGDG) and digalactosyldiacylglycerol (DGDG) consisted of more than 60 % in membrane lipids in leaves but less than 15 % in calluses, in line with calluses lacking thylakoid membranes. In contrast to the galactolipids, the level of the major eukaryotic lipids phosphatidylethanolamine (PE), phosphatidylcholine (PC) and phosphatidylinositol (PI) was highest in callus, lower in seedlings and lowest in leaves. These data indicate that the extraplastidial membranes predominated in callus. Phosphatidylserine (PS) is a very low abundant anionic membrane lipid (Fig. 3.25) that is formed by a base-exchange mechanism in Arabidopsis (Yamaoka *et al.*, 2011). It comprised about 1% in leaves, but higher levels in non-photosynthetic active tissues, as reported before (Yamaoka *et al.*, 2011). Like PI and PS, phosphatidylglycerol (PG) belongs to the group of anionic membrane lipids. In contrast to PI and PS, the percentage of PG decreased in order of leaves, seedlings and calluses as the content of thylakoid membranes did because PG

is the only phospholipid in thylakoids and about 85% of leaf PG is located in the inner chloroplast membranes (Browse *et al.* 1986).

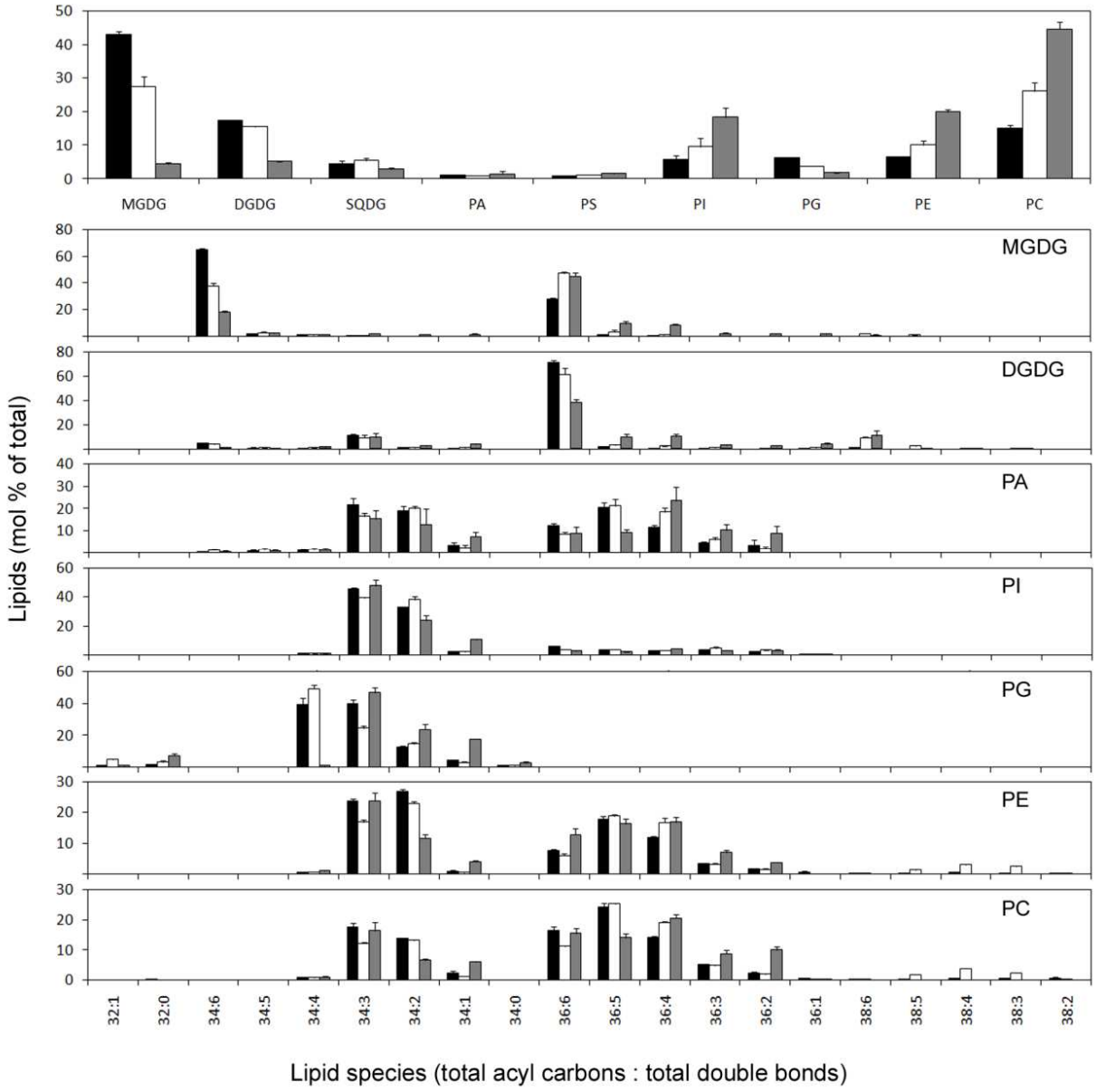

Figure 3.25 Glycerolipid composition and molecular species composition of WT rosette leaves, seedlings and calluses.

Lipids from rosette leaves of 6-week-old plants (black bars), 5-day-old seedlings (white bars) and calluses (gray bars) of WT were extracted and analyzed. Data are given in mole percentage and molecular species in total acyl carbons: total double bonds (monogalactosyldiacylglycerol (MGDG), digalactosyldiacylglycerol (DGDG), sulfoquinovosyldiacylglycerol (SQDG), phosphatidic acid (PA), phosphatidylserine (PS), phosphatidylinositol (PI), phosphatidylglycerol (PG), phosphatidylethanolamine (PE) and phosphatidylcholine (PC)). Mean values and standard deviations of four independent analyses are depicted.

Analysis of molecular species patterns of various glycerolipids gave further information about the lipid structures and their subcellular origins. The main species of MGDG are the prokaryotic 34:6 (18:3/16:3) carrying a 18:3 acyl group at the *sn*-1 and a 16:3 acyl group at the *sn*-2 glycerol position, and the eukaryotic 36:6 (18:3/18:3) species. Because of the different fatty acid specificities of the *sn*-2 acyltransferases catalyzing the second acylation step in the course of *de novo* glycerolipid biosynthesis in plastids and microsomal membranes, prokaryotic lipid species are formed in plastids while the biosynthesis of eukaryotic species occurs at the ER. As given in Fig. 3.25, the decrease in total MGDG content from leaves to calluses was caused by a marked decrease in its prokaryotic species. Unlike leaves and seedlings, calluses were found to contain eukaryotic MGDG and DGDG 36:X species with less than six double bounds. This altered pattern of eukaryotic galactolipid species indicates that the desaturase activities of calluses, especially the 18:2 desaturase activities, are depressed. Moreover, calluses failed to form the typical plastidial 34:4 PG species ($18:3/16:1^{\Delta 3t}$) because the plastidial desaturase FAD4 that converts the 16:0 acyl groups at the *sn*-2 position of PG into the $16:1^{\Delta 3t}$ acyl groups is expressed in photosynthetic active tissue only (Browse *et al.* 1985; Gao *et al.*, 2009).

3.7.2 Membrane lipid composition of *cds* double mutants

To study the effect on membrane lipid compositions by disruption of *CDS1* and *CDS2* genes of Arabidopsis, lipids extracted from *cds1cds2* double mutant seedlings were analyzed in comparison to WT and the *cds4cds5* double mutant. These data showed considerable differences in the patterns of lipid classes present in double mutant and WT seedlings (Fig. 3.26). Galactolipids amounted to 27 % MGDG and 15 % DGDG in WT seedlings, but to distinctly lower levels in the total glycerolipids of both mutant seedlings whereas the level of the anionic glycolipid sulfoquinovosyldiacylglycerol (SQDG) was only slightly changed in the mutants. The defect in thylakoid development of the *cds4cds5* mutant was reflected in a drastic reduction in the levels of galactolipids, as reported before (Haselier *et al.*, 2010). Seedlings of the *cds1cds2* mutant showed similar, though less pronounced reductions, in the amount of these plastidial membrane lipids (Fig. 3.26). Ultrastructure analysis of the *cds1cds2* mutant seedlings, however, provided no evidence for defects in thylakoid development. Therefore it is likely that overall chloroplast physiology is affected in *cds1cds2*. The numerous starch grains accumulating in the double mutant seedlings support this assumption (Fig. 3.17, Fig. 3.20).

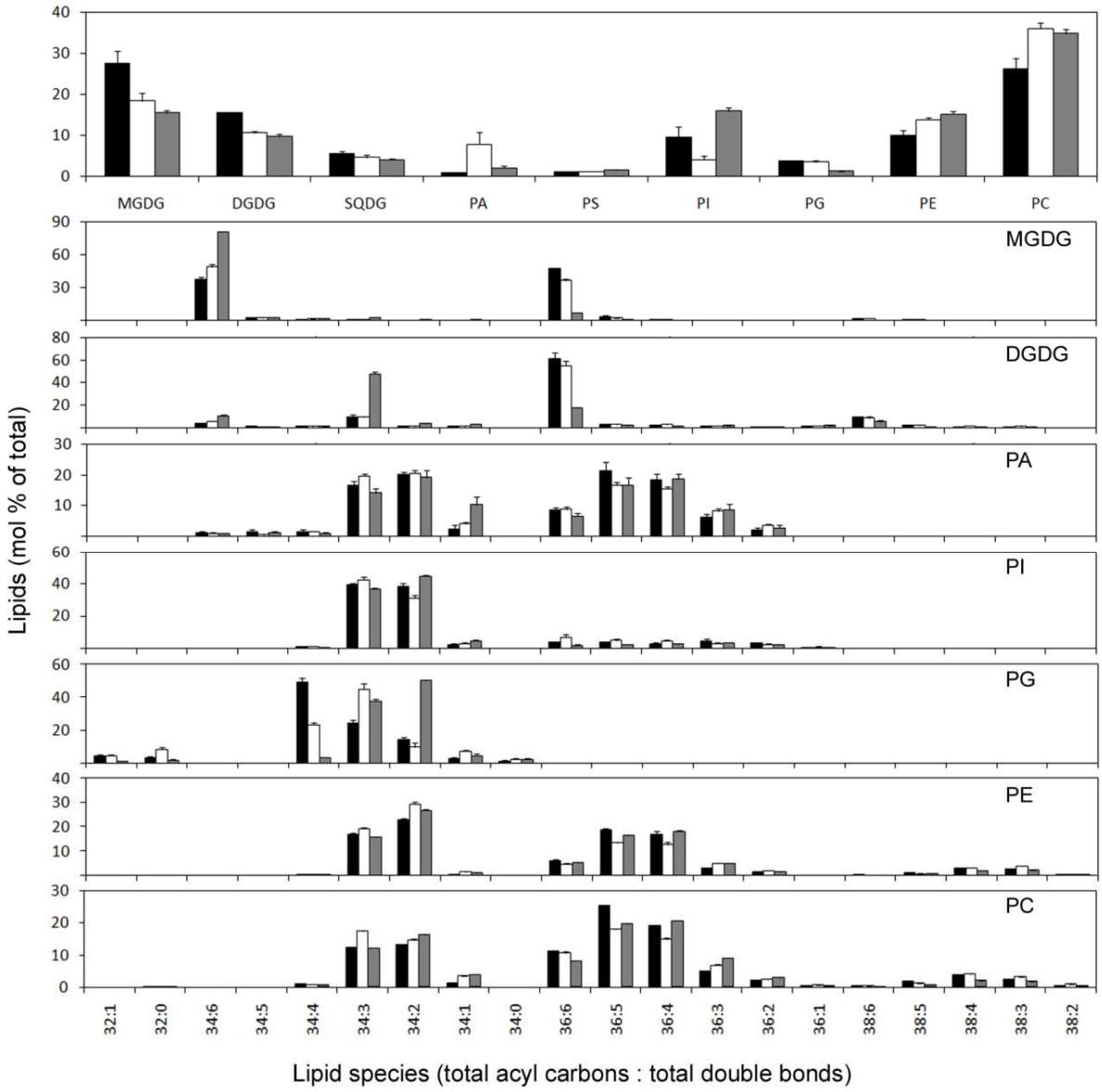

Figure 3.26 Glycerolipid composition and molecular species composition of WT, *cds1cds2* and *cds4cds5* seedlings. Lipid extracts of 5-day-old seedlings of WT (black bars), *cds1cds2* (white bars) and *cds4cds5* (gray bars) were analyzed and data are given as mean values of at least three independent replicates and SDS in mole percentage and molecular species in total acyl carbons: total double bonds (monogalactosyldiacylglycerol (MGDG), digalactosyl-diacylglycerol (DGDG), sulfoquinovosyldiacylglycerol (SQDG), phosphatidic acid (PA), phosphatidylserine (PS), phosphatidylinositol (PI), phosphatidylglycerol (PG), phosphatidylethanolamine (PE) and phosphatidylcholine (PC)).

Interestingly, the two different mutants had similar alterations in their galactolipid species composition, namely an increased level of the prokaryotic 34:6 (MGDG) and 34:3 (DGDG) species formed in plastids and a decreased level of the eukaryotic 36:6 species derived from the ER (Fig. 3.26). In the *cds4cds5* mutant this can be explained by redirecting prokaryotic PA from

PG to galactolipids, especially to MGD. This was supported by positional analysis shown in Fig. 3.27. The level of C_{16} acyl groups at the *sn*-2 position of galactolipids increased and that of C_{18} groups decreased in *cds4cds5* mutant so that the mutant possessed extremely high proportions of prokaryotic galactolipids (ca. 90% MGDG and ca. 80% DGDG).

These altered species compositions were less pronounced in plastids of the *cds1cds2* mutant. Their prokaryotic MGDG increased from the WT level of 44% to about 56% whereas their proportion of prokaryotic DGDG was hardly affected (Fig. 3.26). Increased levels of prokaryotic galactolipids in the *cds1cds2* mutants cannot be explained by redirecting prokaryotic PA to MGDG, but mechanisms different to those in *cds4cds5* plastids have to be considered, for instance the postulated affected overall chloroplast physiology of the *cds1cds2* mutant causing reduced lipid transport from the ER to plastids.

Unlike galactolipids, the levels of the sum of PC and PE of eukaryotic cells rose from 36 % in WT to about 50 % in the *cds1cds2* and *cds4cds5* mutant. The molecular species composition of PC and PE, but also the alterations in species composition between WT and mutants were very similar, namely a slight increase in 34:X and a decrease in 36:X species. Because PC and PE are largely synthesized at the ER, both 34:X and 36:X should be eukaryotic species lacking C_{16} acyl groups at the *sn*-2 position. This was supported by positional analyses, in which the *sn*-2 fatty acid mixture consisted of C_{18} acyl groups (98 %) in the WT as well as in the *cds* double mutant extracts (Fig. 3.27).

PA, the central intermediate of glycerolipid biosynthesis, amounted to less than 1 % of total glycerolipids of WT and *cds4cds5* mutant. This level was 8-fold higher in the *cds1cds2* mutant (Fig. 3.26), in accordance with the accumulation of PA in radioactive labeling experiments (Fig. 3.23). In addition, PA showed a lipid species composition very similar to those of PC and PE, in particular with regard to the 34:X and 36:X species (Fig. 3.26). These data are consistent with PA originating from the eukaryotic pathway at the ER, like PE and PC.

The anionic membrane lipid PS comprised about 1 % in the total glycerolipids of WT and mutant seedlings (Fig. 3.26) and was undetectable in phosphate labeling experiments (Fig. 3.23). Unlike PS, the anionic phospholipids PI and PG are synthesized in CDP-diacylglycerol dependent reactions and both phospholipids showed reduced labeling patterns in *cds1cds2*

mutant seedlings (Fig. 3.23). The level of PI in total glycerolipid extracts was clearly reduced in *cds1cds2* but increased in *cds4cds5* seedlings while its molecular species composition showed slight alterations only. On the other hand, the steady state PG level of the *cds1cds2* mutant was hardly affected (Fig. 3.26) while phosphate labeling experiments revealed a defect in microsomal PG synthesis (Fig. 3.23) These different results are presumably due to the relative low levels of extraplastidial PG (Browse *et al*., 1986) and the different sensitivities of the methods utilized.

Surprisingly, both double mutants showed considerably altered PG species compositions. The level of the typical plastidial 34:4 PG species carrying the $16:1^{\Delta 3t}$ at position 2 was strongly reduced, while the level of 34:3 PG was increased in both mutants. In *cds1cds2* seedlings 34:3 PG likely represents the prokaryotic 18:3/16:0 or 18:2/16:1 species (Devaiah *et al.*, 2006) because the major proportion of leaf PG is located in plastids (Browse *et al.*, 1986). In the *cds4cds5* mutant, however, 34:3 PG should be of eukaryotic (16:0/18:3) origin like 34:2(16:0/18:2) the level of which markedly increased in the *cds4cds5* mutant (Fig. 3.26).

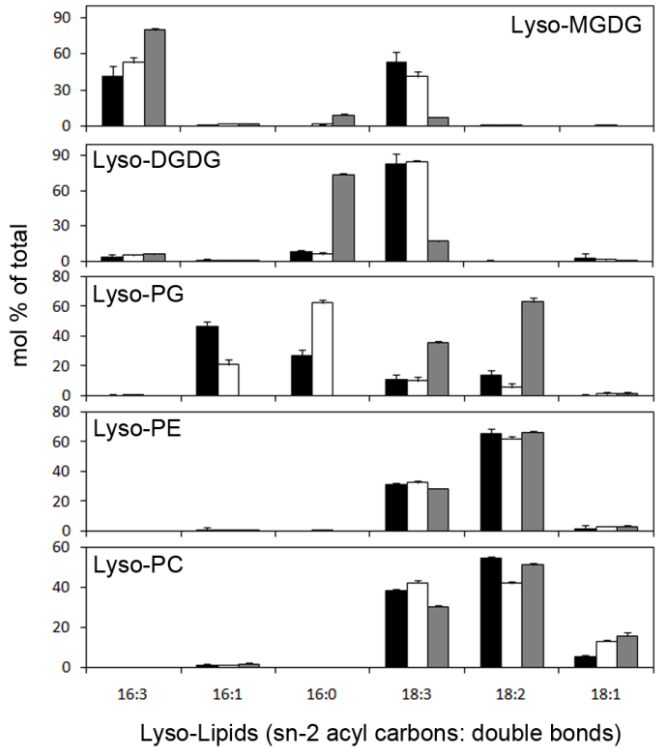

Figure 3.27 Fatty acid composition at the sn-2 position of the given glycerolipids. Lipids extracted from 5-day-old seedlings of WT (black bars), *cds1cds2* (white bars) and *cds4cds5* (gray bars), were digested with *Rhizopus arrhizus* lipase to remove the fatty acid esterified at sn-1 position, and the resulting lysolipids were analyzed by Q-TOF MS/MS to get the *sn*-2 fatty acid mixture. Data of at least three independent replicates are given as mean values and SDS in mole percentage of acyl groups esterified at the *sn*-2 position (monogalactosyldiacylglycerol (MGDG), di-galactosyldiacylglycerol (DGDG), phosphatidyl-glycerol (PG), phosphatidylethanolamine (PE) and phosphatidylcholine (PC)).
Lyso glycerolipid: glycerolipid carry only one acyl group at the glycerol backbone.

Analysis of the *sn*-2 fatty composition of PG revealed that the *cds4cds5* mutant in fact possesses eukaryotic but no prokaryotic PG as expected from mutant lacking plastidial CDS activity. On the other hand, the *cds1cds2* mutant contained prokaryotic PG species in levels very similar to WT level (WT 75%, mutant 83%), but the C_{16} fatty acid pattern at the *sn*-2 position varied

considerably between WT and *cds1cds2* mutant. As shown in Fig 3.27, mutant PG contained lower amounts of $16:1^{\Delta 3t}$ but substantial higher amounts of 16:0 than WT PG. Hence, the alterations in PG species in the *cds1cds2* mutant can be explained by reduced desaturase activity encoded by the *FAD4* gene that convert 18:X/16:0 PG into $18:X/16:1^{\Delta 3t}$ PG (Gao *et al.* 2009).

Determination of membrane lipids from the *cds1cds2+VXE::CDS1* calluses grown without and with estradiol in comparison to WT calluses gave the results summarized in Fig. 3.28. Mutant calluses cultivated with inductor showed a glycerolipid pattern typical of undifferentiated tissue, like WT calluses, in which phospholipids predominate. In callus without estradiol, the levels of the phospholipids PC, PE and PA were slightly increased whereas the level of PI and PG were decreased. Hence, *cds1cds2+VXE::CDS1* calluses gave results similar to those of phospholipid labeling experiment (Fig. 3.23) and to the steady state phospholipid pattern of *cds1cds2* seedlings (Fig.3.26).

As observed by the labeling experiments, changes in the lipid composition were less pronounced in calluses than in seedling. PI, unlike PG, is exclusively synthesized at the ER (Löfke *et al.*, 2008). Both phosphate labeling experiments and glycerolipid analysis of the *cds1cds2* seedlings (Fig. 3.23 and 3.26) and calluses (Fig. 3.24 and 3.27) detected substantially reduced PI level. PI does not only serve as a membrane lipid but its phosphorylated derivates also play a pivotal role in nearly all cellular processes by serving as signaling molecules which mediate temporal and spatial information to downstream effectors (Xue *et al.*, 2009; Graham and Burd, 2011; Gillaspy, 2011). Therefore it is like that the defect in PI biosynthesis is decisive in causing the seedling lethal phenotype of the *cds1cds2* mutant. In addition, the increase in PA might contribute to the observed phenotype of the mutant (Fig. 3.23 and 3.26) since it serves not only as a central intermediate in glycerolipid biosynthesis but also as second messenger in plants (Xu *et al.*, 2005).

According to our data, neither CDS1 nor CDS2 appears to provide mitochondria with CDP-diacylglycerol for CL biosynthesis and, based on the transcript pattern of *CDS3* given in Fig. 3.3, this enzyme cannot play an role in CL biosynthesis among vegetative growth. Further experiments are required to elucidate via which mechanism CL is formed.

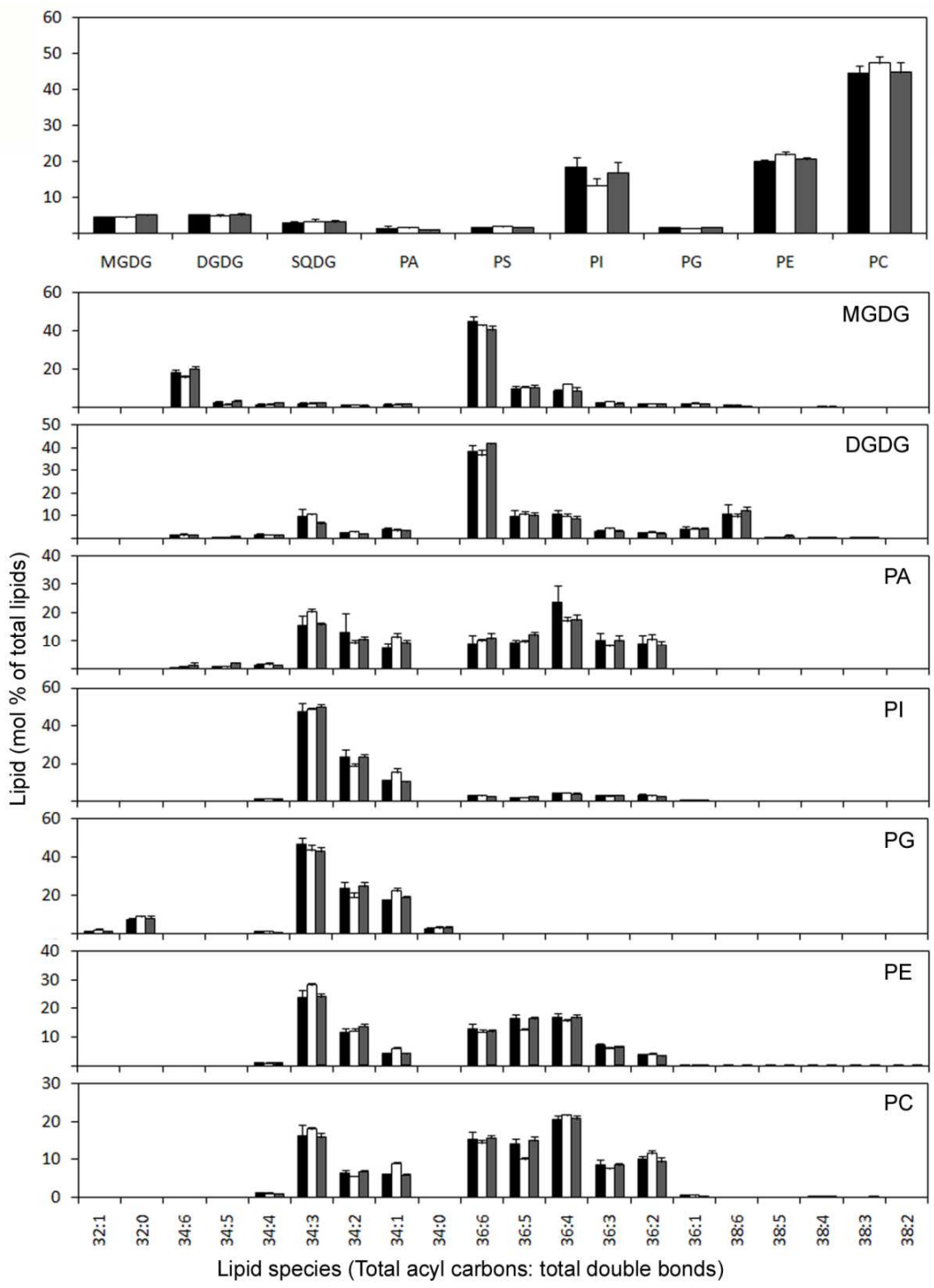

Figure 3.28 Glycerolipid composition and molecular species composition of Arabidopsis WT and *cds1cds2+VXE::CDS1* mutant calluses.

Lipids extracts were analyzed from calluses of WT (black bars) and of *cds1cds2+VXE::CDS1* mutant cultivated for one week in the absence (white bars) or the presence of β-estradiol (grey bars). Data are given as mean values of five independent replicates and SDS in mole% and molecular species in total acyl carbons: total double bonds. (Abbreviation see Fig. 3.26).

3.8 Conclusion and outlook

In Arabidopsis, there is a small gene family encoding CDP-DAG synthases (CDS), termed *CDS1* to *CDS5*. Bioinformational analyses show that they can be divided into two groups, the prokaryotic isoforms and the eukaryotic isoforms. In consistence with the division, CDS4 and CDS5 have been demonstrated to be the plastidial enzymes in the former work, while CDS1, CDS2 and CDS3 are shown to be extraplastidial CDS, localized in the ER membrane in this work. In addition, our data show that the N-terminal including at least one transmembrane domain of extraplastidial CDS is essential for the properly targeting of the enzymes. The enzymatic properties of both plastidial and extraplastidial enzymes, however, are very similar: except that the extraplastidial isoforms reach substrate saturation at considerably lower concentration than the plastidial isoforms, all of these enzymes have similar optimal pH, need Mg^{2+} for activity, and prefer PA species with dioleoyl.

In order to learn the biological functions of genes, several T-DNA insertion mutants have been identified and analyzed. The transcription analysis clearly shows that *CDS1* in *cds1* mutant and *CDS2* in *cds2* mutant are undetectable, while the expression of the other *CDSs* is similar to WT: *CDS3* is undetectable, *CDS4* and *CDS5* is not altered. The *cds1* and *cds2* single mutants, however, show no obvious alteration in phenotype, nor in lipid composition, suggesting a redundant function of *CDS1* and *CDS2* in Arabidopsis.

Homozygous double mutant *cds1cds2* has been created and show a remarkable phenotype comparing with WT and heterozygous mutants. The *cds1cds2* mutants can germinate and develop seedlings, but they have smaller cotyledons, shorter hypocotyls and radicles. More severely, *cds1cds2* are failed to develop true leaves and die after 3 weeks no matter they are fed with sucrose or not. In that way, *cds1cds2* is different from *cds4cds5*, which are deficient in autotrophic growth but can finish life cycle by feeding sucrose. The lethal phenotype of *cds1cds2* can be complemented by functional expression of either *CDS1* or *CDS2* cDNA. These data confirm that *CDS1* and *CDS2* have redundant activity. Microscopic analyses show that *cds1cds2* accumulates substantial starch grains in chloroplasts and has a defect in cell expansion. Furthermore, the callus formation experiment demonstrates the cell division of *cds1cds2* is arrested.

The *in vivo* phospholipid labeling shows the biosynthesis of PI and PG decreases in *cds1cds2* comparing with WT. In contrast, *cds1cds2* accumulates more PC and remarkable PA. These alternations of phospholipids are confirmed and clarified by steady state lipid composition analysis. Disruption of extraplastidial *CDS* leads to deficiency of PI biosynthesis and accumulation of the substrate, PA, which is channeled to PE and PC biosynthesis. In addition, the galactolipids (MGDG and DGDG) and the sulfolipid (SQDG) decrease in *cds1cds2* mutant. Unlike *cds4cds5* which is deficiency in the plastidial PG biosynthesis and lack prokaryotic PG, *cds1cds2* shows only a slight decrease in PG content. Base on the altered glycerolipid composition of the double mutant in comparison to wild type seedlings, it is likely that the drastic decrease in the level of PI and the increase in PA cause defects in cell division and expansion.

Considering the data in this work and former ones, a profile of biological functions of *CDS* genes in Arabidopsis appears: CDS1 and CDS2 producing extraplastidial CDP-DAG are involving in the biosynthesis of PI, while CDS4 and CDS5 channel PA into CDP-DAG for the plastidial PG biosynthesis. But there are still many open questions need to be explored: For instance, what is the biological function of *CDS3* which is specifically expressed in mature pollen? Cause the accumulation of PA or the decrease of PI or both lipid alterations, what are the signal transduction mechanisms involved? In which way mitochondria are provided with CDP-DAG for the biosynthesis of CL in the inner mitochondria? Do Arabidopsis possesses further *CDS* genes unrelated to known CDS sequences or lipid transfer mechanisms from plastidials to mitochondria to enable CL biosynthesis? Further research may help us to answer these questions.

REFERENCES

Alonso, J.M., Stepanova, A.N., Leisse, T.J., Kim, C.J., Chen, H., Shinn, P., Stevenson, D.K., Zimmerman, J., Barajas, P. and Cheuk, R. (2003a) Genome-wide insertional mutagenesis of Arabidopsis thaliana. *Science Signalling*, **301**, 653.

Alonso, J.M., Stepanova, A.N., Leisse, T.J., Kim, C.J., Chen, H., Shinn, P., Stevenson, D.K., Zimmerman, J., Barajas, P., Cheuk, R., Gadrinab, C., Heller, C., Jeske, A., Koesema, E., Meyers, C.C., Parker, H., Prednis, L., Ansari, Y., Choy, N., Deen, H., Geralt, M., Hazari, N., Hom, E., Karnes, M., Mulholland, C., Ndubaku, R., Schmidt, I., Guzman, P., Aguilar-Henonin, L., Schmid, M., Weigel, D., Carter, D.E., Marchand, T., Risseeuw, E., Brogden, D., Zeko, A., Crosby, W.L., Berry, C.C. and Ecker, J.R. (2003b) Genome-Wide Insertional Mutagenesis of Arabidopsis thaliana. *Science*, **301**, 653-657.

Andrews, J. and Mudd, J.B. (1985b) Phosphatidylglycerol synthesis in pea chloroplasts pathway and localization. *Plant Physiol.*, **79**, 259-265.

Aronsson, H. and Jarvis, P. (2002) A simple method for isolating import-competent Arabidopsis chloroplasts. *FEBS Lett.*, **529**, 215-220.

Awai, K., Maréchal, E., Block, M.A., Brun, D., Masuda, T., Shimada, H., Takamiya, K.-i., Ohta, H. and Joyard, J. (2001) Two types of MGDG synthase genes, found widely in both 16: 3 and 18: 3 plants, differentially mediate galactolipid syntheses in photosynthetic and nonphotosynthetic tissues in Arabidopsis thaliana. *P Natl. Acad. Sci. USA*, **98**, 10960-10965.

Babiychuk, E., Müller, F., Eubel, H., Braun, H.P., Frentzen, M. and Kushnir, S. (2003) Arabidopsis phosphatidylglycerophosphate synthase 1 is essential for chloroplast differentiation, but is dispensable for mitochondrial function. *Plant J.*, **33**, 899-909.

Beisson, F., Koo, A.J.K., Ruuska, S., Schwender, J., Pollard, M., Thelen, J.J., Paddock, T., Salas, J.J., Savage, L. and Milcamps, A. (2003) Arabidopsis genes involved in acyl lipid metabolism. A 2003 census of the candidates, a study of the distribution of expressed sequence tags in organs, and a web-based database. *Plant Physiol.*, **132**, 681-697.

Bell, R.M., Mavis, R.D., Osborn, M. and Roy Vagelos, P. (1971) Enzymes of phospholipid metabolism: Localization in the cytoplasmic and outer membrane of the cell envelope of Escherichia coli and Salmonella typhimurium. *BBA - Lipids Lipid Metab.*, **249**, 628-635.

Bernard, P. and Couturier, M. (1992) Cell killing by the F plasmid CcdB protein involves poisoning of DNA-topoisomerase II complexes. *J Mol. Biol.*, **226**, 735-745.

Bethesda-Research-Laboratories (1986) BRL pUC host: E. coli DH5α competent cells. *FOCUS* **8**, 9.

Block, M.A., Dorne, A.-J., Joyard, J. and Douce, R. (1983) The phosphatidic acid phosphatase of the chloroplast envelope is located on the inner envelope membrane. *FEBS Lett.*, **164**, 111-115.

Bourgis, F., Kader, J.-C., Barret, P., Renard, M., Robinson, D., Robinson, C., Delseny, M. and Roscoe, T.J. (1999) A plastidial lysophosphatidic acid acyltransferase from oilseed rape. *Plant Physiol.*, **120**, 913-922.

Bradford, M. (1976) A rapid and sensitive method for the quantitation of microgram quantities of protein utilizing the principle of protein-dye binding Anal Biochem 72: 248–254. *Find this article online*.

Browse, J., McCourt, P. and Somerville, C.R. (1985) A Mutant of Arabidopsis Lacking a Chloroplast-Specific Lipid. *Science*, **227**, 763-765.

Browse, J., Warwick, N., Somerville, C. and Slack, C. (1986) Fluxes through the prokaryotic and eukaryotic pathways of lipid synthesis in the '16: 3' plant Arabidopsis thaliana. *Biochem. J.*, **235**, 25.

Buseman, C.M., Tamura, P., Sparks, A.A., Baughman, E.J., Maatta, S., Zhao, J., Roth, M.R., Esch, S.W., Shah, J. and Williams, T.D. (2006) Wounding stimulates the accumulation of glycerolipids containing oxophytodienoic acid and dinor-oxophytodienoic acid in Arabidopsis leaves. *Plant Physiol.*, **142**, 28-39.

Carter, J.R. and Kennedy, E.P. (1966) Enzymatic synthesis of cytidine diphosphate diglyceride. *J. Lipid Res.*, **7**, 678.

Castelli, V., Aury, J.M., Jaillon, O., Wincker, P., Clepet, C., Menard, M., Cruaud, C., Quétier, F., Scarpelli, C. and Schächter, V. (2004) Whole genome sequence comparisons and "full-length" cDNA sequences: a combined approach to evaluate and improve Arabidopsis genome annotation. *Genome Res.*, **14**, 406-413.

Clough, S.J. and Bent, A.F. (1998) Floral dip: a simplified method for Agrobacterium-mediated transformation of Arabidopsis thaliana. *Plant J.*, **16**, 735-743.

Collin, S., Justin, A.M., Cantrel, C., Arondel, V. and Kader, J.C. (1999) Identification of AtPIS, a phosphatidylinositol synthase from Arabidopsis. *Eur. J. Biochem.*, **262**, 652-658.

Curtis, M.D. and Grossniklaus, U. (2003) A gateway cloning vector set for high-throughput functional analysis of genes in planta. *Plant Physiol.*, **133**, 462-469.

Delhaize, E., Hebb, D.M., Richards, K.D., Lin, J.-M., Ryan, P.R. and Gardner, R.C. (1999) Cloning and Expression of a Wheat (Triticum aestivumL.) Phosphatidylserine Synthase cDNA overexpression in plants alters the composition of phospholipids *J. Biol. Chem.*, **274**, 7082-7088.

Devaiah, S.P., Roth, M.R., Baughman, E., Li, M., Tamura, P., Jeannotte, R., Welti, R. and Wang, X. (2006) Quantitative profiling of polar glycerolipid species from organs of wild-type Arabidopsis and a PHOSPHOLIPASE Dα1 knockout mutant. *Phytochemistry*, **67**, 1907-1924.

Eastmond, P.J., Quettier, A.L., Kroon, J.T.M., Craddock, C., Adams, N. and Slabas, A.R. (2010) PHOSPHATIDIC ACID PHOSPHOHYDROLASE1 and 2 regulate phospholipid synthesis at the endoplasmic reticulum in Arabidopsis. *Plant Cell*, **22**, 2796-2811.

Fischer, W., Heinz, E. and Zeus, M. (1973) The suitability of lipase from Rhizopus arrhizus delemar for analysis of fatty acid distribution in dihexosyl diglycerides, phospholipids and plant sulfolipids. *Hoppe-Seyler's Zeitschrift für physiologische Chemie*, **354**, 1115-1123.

Frentzen, M. (2004) Phosphatidylglycerol and sulfoquinovosyldiacylglycerol: anionic membrane lipids and phosphate regulation. *Curr. Opin. Plant Biol.*, **7**, 270-276.

Frentzen, M., Heinz, E., McKeon, T.A. and Stumpf, P.K. (1983) Specificities and Selectivities of Glycerol-3-Phosphate Acyltransferase and Monoacylglycerol-3-Phosphate Acyltransferase from Pea and Spinach Chloroplasts. *Eur. J. Biochem.*, **129**, 629-636.

Frentzen, M., Neuburger, M., Joyard, J. and Douce, R. (1990) Intraorganelle localization and substrate specificities of the mitochondrial acyl-CoA: sn-glycerol-3-phosphate O-acyltransferase and acyl-CoA: 1-acyl-sn-glycerol-3-phosphate O-acyltransferase from potato tubers and pea leaves. *Eur. J. Biochem.*, **187**, 395-402.

Frentzen, M., Peterek, G. and Wolter, F.P. (1994) Properties and subcellular localization of a plastidial sn-glycerol-3-phosphate acyltransferase of Pisum sativum L. expressed in Escherichia coli. *Plant Sci.*, **96**, 45-53.

Frey, B. and Suppmann, B. (1995) Demonstration of the Expand PCR system's greater fidelity and higher yields with a lacI-based PCR fidelity assay. *Biochemica*, **2**, 8-9.

Froehlich, J.E., Benning, C. and Dörmann, P. (2001) The digalactosyldiacylglycerol (DGDG) synthase DGD1 is inserted into the outer envelope membrane of chloroplasts in a manner independent of the general import pathway and does not depend on direct interaction with monogalactosyldiacylglycerol synthase for DGDG biosynthesis. *J. Biol. Chem.*, **276**, 31806-31812.

Froehlich, J.E., Wilkerson, C.G., Ray, W.K., McAndrew, R.S., Osteryoung, K.W., Gage, D.A. and Phinney, B.S. (2003) Proteomic Study of the Arabidopsis t haliana Chloroplastic Envelope Membrane Utilizing Alternatives to Traditional Two-Dimensional Electrophoresis. *J. Proteome Res.*, **2**, 413-425.

Gao, J., Ajjawi, I., Manoli, A., Sawin, A., Xu, C., Froehlich, J.E., Last, R.L. and Benning, C. (2009) FATTY ACID DESATURASE4 of Arabidopsis encodes a protein distinct from characterized fatty acid desaturases. *Plant J.*, **60**, 832-839.

Ghosh, A.K., Chauhan, N., Rajakumari, S., Daum, G. and Rajasekharan, R. (2009) At4g24160, a soluble acyl-coenzyme A-dependent lysophosphatidic acid acyltransferase. *Plant Physiol.*, **151**, 869-881.

Gibellini, F. and Smith, T.K. (2010) The Kennedy pathway - De novo synthesis of phosphatidylethanolamine and phosphatidylcholine. *IUBMB Life*, **62**, 414-428.

Gillaspy, G.E. (2011) The cellular language of myo-inositol signaling. *New Phytol.*

Guo, J., Zhang, Z., Bi, Y., Yang, W., Xu, Y. and Zhang, L. (2005) Decreased stability of photosystem I in dgd1 mutant of Arabidopsis thaliana. *FEBS lett.*, **579**, 3619-3624.

Härtel, H., Dörmann, P. and Benning, C. (2000) DGD1-independent biosynthesis of extraplastidic galactolipids after phosphate deprivation in Arabidopsis. *P Natl. Acad. Sci. USA*, **97**, 10649-10654.

Härtel, H., Lokstein, H., Dormann, P., Grimm, B. and Benning, C. (1997) Changes in the composition of the photosynthetic apparatus in the galactolipid-deficient dgd1 mutant of Arabidopsis thaliana. *Plant Physiol.*, **115**, 1175-1184.

Hagio, M., Gombos, Z., Várkonyi, Z., Masamoto, K., Sato, N., Tsuzuki, M. and Wada, H. (2000) Direct evidence for requirement of phosphatidylglycerol in photosystem II of photosynthesis. *Plant Physiol.*, **124**, 795-804.

Hagio, M., Sakurai, I., Sato, S., Kato, T., Tabata, S. and Wada, H. (2002) Phosphatidylglycerol is essential for the development of thylakoid membranes in Arabidopsis thaliana. *Plant Cell Physiol.*, **43**, 1456-1464.

Halford, S., Dulai, K.S., Daw, S.C., Fitzgibbon, J. and Hunt, D.M. (1998) Isolation and chromosomal localization of two human CDP-diacylglycerol synthase (CDS) genes. *Genomics*, **54**, 140-144.

Hanenberg, A., Heim, S., Wissing, J.B. and Wagner, K.G. (1993) Characterization of cytidine triphosphate: phosphatidate cytidyltransferase from suspension cultured Catharanthus roseus cells. *Plant Sci.*, **88**, 13-18.

Haselier, A., Akbari, H., Weth, A., Baumgartner, W. and Frentzen, M. (2010) Two closely related genes of Arabidopsis encode plastidial cytidinediphosphate diacylglycerol synthases essential for photoautotrophic growth. *Plant Physiol.*, **153**, 1372-1384.

Heacock, A.M., Uhler, M.D. and Agranoff, B.W. (2002) Cloning of CDP-Diacylglycerol Synthase from a Human Neuronal Cell Line. *J. Neurochem.*, **67**, 2200-2203.

Heazlewood, J.L., Tonti-Filippini, J., Verboom, R.E. and Millar, A.H. (2005a) Combining experimental and predicted datasets for determination of the subcellular location of proteins in Arabidopsis. *Plant physiology*, **139**, 598-609.

Heazlewood, J.L., Tonti-Filippini, J., Verboom, R.E. and Millar, A.H. (2005b) Combining experimental and predicted datasets for determination of the subcellular location of proteins in Arabidopsis. *Plant Physiol.*, **139**, 598-609.

Heazlewood, J.L., Verboom, R.E., Tonti-Filippini, J., Small, I. and Millar, A.H. (2007) SUBA: the Arabidopsis subcellular database. *Nucleic Acids Res.*, **35**, D213-D218.

Hellens, R.P., Edwards, E.A., Leyland, N.R., Bean, S. and Mullineaux, P.M. (2000) pGreen: a versatile and flexible binary Ti vector for Agrobacterium-mediated plant transformation. *Plant Mol. Biol.*, **42**, 819-832.

Hilson, P., Allemeersch, J., Altmann, T., Aubourg, S., Avon, A., Beynon, J., Bhalerao, R.P., Bitton, F., Caboche, M. and Cannoot, B. (2004) Versatile gene-specific sequence tags for Arabidopsis functional genomics: transcript profiling and reverse genetics applications. *Genome Res.*, **14**, 2176-2189.

Houtkooper, R.H., Turkenburg, M., Karall, D., Pérez-Cerdá, C., Morrone, A., Malvagia, S., Wanders, R.J., Kulik, W. and Vaz, F.M. (2009) The enigmatic role of tafazzin in cardiolipin metabolism. *BBA - Mol. Cell Biol. Lipids*, **1788**, 2003-2014.

Icho, T., Sparrow, C. and Raetz, C. (1985) Molecular cloning and sequencing of the gene for CDP-diglyceride synthetase of Escherichia coli. *J. Biol. Chem.*, **260**, 12078-12083.

Inglis-Broadgate, S.L., Ocaka, L., Banerjee, R., Gaasenbeek, M., Chapple, J.P., Cheetham, M.E., Clark, B.J., Hunt, D.M. and Halford, S. (2005) Isolation and characterization of murine Cds (CDP-diacylglycerol synthase) 1 and 2. *Gene*, **356**, 19-31.

Ishizaki, O., Nishida, I., Agata, K., Eguchi, G. and Murata, N. (1988) Cloning and nucleotide sequence of cDNA for the plastid glycerol-3-phosphate acyltransferase from squash. *FEBS Lett.*, **238**, 424-430.

Jarvis, P., Dörmann, P., Peto, C.A., Lutes, J., Benning, C. and Chory, J. (2000) Galactolipid deficiency and abnormal chloroplast development in the Arabidopsis MGD synthase 1 mutant. *P. Natl. Acad. Sci. USA*, **97**, 8175-8179.

Jouhet, J., Maréchal, E. and Block, M.A. (2007) Glycerolipid transfer for the building of membranes in plant cells. *Prog. Lipid Res.*, **46**, 37-55.

Joyard, J. and Douce, R. (1977) Site of synthesis of phosphatidic acid and diacyglycerol in spinach chloroplasts. *BBA - Lipids Lipid Metab.*, **486**, 273-285.

Karimi, M., Depicker, A. and Hilson, P. (2007) Recombinational cloning with plant gateway vectors. *Plant Physiol.*, **145**, 1144-1154.

Karimi, M., Inzé, D. and Depicker, A. (2002) GATEWAY™ vectors for Agrobacterium-mediated plant transformation. *Trends Plant Sci.*, **7**, 193-195.

Kasajima, I., Ide, Y., Ohkama-Ohtsu, N., Hayashi, H., Yoneyama, T. and Fujiwara, T. (2004) A protocol for rapid DNA extraction fromArabidopsis thaliana for PCR analysis. *Plant Mol. Biol. Rep.*, **22**, 49-52.

Katayama, K., Sakurai, I. and Wada, H. (2004) Identification of an Arabidopsis thaliana gene for cardiolipin synthase located in mitochondria. *FEBS Lett.*, **577**, 193-198.

Kelley, M.J. and Carman, G.M. (1987) Purification and characterization of CDP-diacylglycerol synthase from Saccharomyces cerevisiae. *J. Biol. Chem.*, **262**, 14563-14570.

Kelly, A.A. and Dörmann, P. (2002) DGD2, an Arabidopsis gene encoding a UDP-galactose-dependent digalactosyldiacylglycerol synthase is expressed during growth under phosphate-limiting conditions. *J. Biol. Chem.*, **277**, 1166-1173.

Kelly, B.L. and Greenberg, M.L. (1990) Characterization and regulation of phosphatidylglycerolphosphate phosphatase in Saccharomyces cerevisiae. *BBA - Lipids Lipid Metab.*, **1046**, 144-150.

Kim, H.U. and Huang, A.H. (2004) Plastid lysophosphatidyl acyltransferase is essential for embryo development in Arabidopsis. *Plant Physiol.*, **134**, 1206-1216.

Kim, H.U., Li, Y. and Huang, A.H. (2005) Ubiquitous and endoplasmic reticulum–located lysophosphatidyl acyltransferase, LPAT2, is essential for female but not male gametophyte development in Arabidopsis. *Plant Cell*, **17**, 1073-1089.

Kleppinger-Sparace, K.F. and Moore Jr, T.S. (1985) Biosynthesis of cytidine 5'-diphosphate-diacylglycerol in endoplasmic reticulum and mitochondria of castor bean endosperm. *Plant Physiol.*, **77**, 12-15.

Kobayashi, K., Awai, K., Takamiya, K.-i. and Ohta, H. (2004) Arabidopsis type B monogalactosyldiacylglycerol synthase genes are expressed during pollen tube growth and induced by phosphate starvation. *Plant Physiol.*, **134**, 640-648.

Koncz, C. and Schell, J. (1986) The promoter of T L-DNA gene 5 controls the tissue-specific expression of chimaeric genes carried by a novel type of Agrobacterium binary vector. *Mol. Genet. Genomics*, **204**, 383-396.

Kopka, J., Ludewig, M. and Muller-Rober, B. (1997) Complementary DNAs Encoding Eukaryotic-Type Cytidine-5'-Diphosphate-Diacylglycerol Synthases of Two Plant Species. *Plant Physiol.*, **113**, 997-1002.

Kruse, O., Hankamer, B., Konczak, C., Gerle, C., Morris, E., Radunz, A., Schmid, G.H. and Barber, J. (2000) Phosphatidylglycerol is involved in the dimerization of photosystem II. *J. Biol. Chem.*, **275**, 6509-6514.

Kunst, L. and Somerville, C. (1988) Altered regulation of lipid biosynthesis in a mutant of Arabidopsis deficient in chloroplast glycerol-3-phosphate acyltransferase activity. *P Natl. Acad. Sci. USA*, **85**, 4143-4147.

Löfke, C., Ischebeck, T., Konig, S., Freitag, S. and Heilmann, I. (2008) Alternative metabolic fates of phosphatidylinositol produced by phosphatidylinositol synthase isoforms in Arabidopsis thaliana. *Biochem. J.* , **413**, 115-124.

Larkin, M., Blackshields, G., Brown, N., Chenna, R., McGettigan, P., McWilliam, H., Valentin, F., Wallace, I., Wilm, A. and Lopez, R. (2007) Clustal W and Clustal X version 2.0. *Bioinformatics*, **23**, 2947-2948.

Li, X.C., Zhu, J., Yang, J., Zhang, G.R., Xing, W.F., Zhang, S. and Yang, Z.N. (2012) Glycerol-3-phosphate acyltransferase 6 (GPAT6) is important for tapetum development in Arabidopsis and plays multiple roles in plant fertility. *Mol. Plant*, **5**, 131-142.

Lykidis, A. and Jackowski, S. (2000) Regulation of mammalian cell membrane biosynthesis. *Prog. Nucleic acid Re.*, **65**, 361-393.

Lykidis, A., Jackson, P.D., Rock, C.O. and Jackowski, S. (1997) The role of CDP-diacylglycerol synthetase and phosphatidylinositol synthase activity levels in the regulation of cellular phosphatidylinositol content. *J. Biol. Chem.*, **272**, 33402-33409.

Müller, F. and Frentzen, M. (2001) Phosphatidylglycerophosphate synthases from Arabidopsis thaliana. *FEBS Lett.*, **509**, 298-302.

Maclean, J., Koekemoer, M., Olivier, A., Stewart, D., Hitzeroth, I., Rademacher, T., Fischer, R., Williamson, A.L. and Rybicki, E. (2007) Optimization of human papillomavirus type 16 (HPV-16) L1 expression in plants: comparison of the suitability of different HPV-16 L1 gene variants and different cell-compartment localization. *J. Gen Virol.*, **88**, 1460-1469.

Malherbe, A., Block, M.A., Joyard, J. and Douce, R. (1992) Feedback inhibition of phosphatidate phosphatase from spinach chloroplast envelope membranes by diacylglycerol. *J. Biol. Chem.*, **267**, 23546-23553.

Maliga, P., Sz-Breznovits, Á. and Marton, L. (1973) Streptomycin-resistant plants from callus culture of haploid tobacco. *Nature*, **244**, 29-30.

Martin, C. and Smith, A.M. (1995) Starch biosynthesis. *Plant Cell*, **7**, 971.

Martin, D., Gannoun-Zaki, L., Bonnefoy, S., Eldin, P., Wengelnik, K. and Vial, H. (2000) Characterization of Plasmodium falciparum CDP-diacylglycerol synthase, a proteolytically cleaved enzyme. *Mol. Biochem. Parasit.*, **110**, 93-105.

McConn, M. and Browse, J. (1998) Polyunsaturated membranes are required for photosynthetic competence in a mutant ofArabidopsis. *Plant J.*, **15**, 521-530.

Moreau, P., Bessoule, J.J., Mongrand, S., Testet, E., Vincent, P. and Cassagne, C. (1998) Lipid trafficking in plant cells. *Prog. Lipid Res.*, **37**, 371-391.

Mullis, K., Faloona, F., Scharf, S., Saiki, R., Horn, G. and Erlich, H. (1986) Specific enzymatic amplification of DNA in vitro: the polymerase chain reaction. In *Cold Spring Harb Symp Quant Biol*, pp. 263-273.

Munnik, T. (2001) Phosphatidic acid: an emerging plant lipid second messenger. *Trends Plant Sci.*, **6**, 227-233.

Murata, N., Sato, N. and Takahashi, N. (1984) Very-long-chain saturated fatty acids in phosphatidylserine from higher plant tissues. *BBA - Lipids Lipid Metab.*, **795**, 147-150.

Murata, N. and Tasaka, Y. (1997) Glycerol-3-phosphate acyltransferase in plants. *BBA - Lipids Lipid Metab.*, **1348**, 10-16.

Nagata, T., Nemoto, Y. and Hasezawa, S. (1992) Tobacco BY-2 cell line as the "HeLa" cell in the cell biology of higher plants. *Int. Rev. Cytol*, **132**, 1-30.

Nakamura, Y., Awai, K., Masuda, T., Yoshioka, Y., Takamiya, K.-i. and Ohta, H. (2005) A novel phosphatidylcholine-hydrolyzing phospholipase C induced by phosphate starvation in Arabidopsis. *J. Biol. Chem.*, **280**, 7469-7476.

Nakamura, Y., Tsuchiya, M. and Ohta, H. (2007) Plastidic phosphatidic acid phosphatases identified in a distinct subfamily of lipid phosphate phosphatases with prokaryotic origin. *J. Biol. Chem.*, **282**, 29013-29021.

Nerlich, A., Von Orlow, M., Rontein, D., Hanson, A.D. and Dörmann, P. (2007) Deficiency in phosphatidylserine decarboxylase activity in the psd1 psd2 psd3 triple mutant of Arabidopsis affects phosphatidylethanolamine accumulation in mitochondria. *Plant Physiol.*, **144**, 904-914.

Nicholas, K.B., Nicholas, H. and Deerfield, D. (1997) GeneDoc: analysis and visualization of genetic variation. *Embnew. news*, **4**.

Nishida, I., Tasaka, Y., Shiraishi, H. and Murata, N. (1993) The gene and the RNA for the precursor to the plastid-located glycerol-3-phosphate acyltransferase of Arabidopsis thaliana. *Plant Mol. Biol.*, **21**, 267-277.

Nowicki, M., Müller, F. and Frentzen, M. (2005) Cardiolipin synthase of Arabidopsis thaliana. *FEBS Lett.*, **579**, 2161-2165.

Pan, W., Pham, V.N., Stratman, A.N., Castranova, D., Kamei, M., Kidd, K.R., Lo, B.D., Shaw, K.M., Torres-Vazquez, J., Mikelis, C.M., Gutkind, J.S., Davis, G.E. and Weinstein, B.M. (2012) CDP-diacylglycerol synthetase-controlled phosphoinositide availability limits VEGFA signaling and vascular morphogenesis. *Blood*, **120**, 489-498.

Qin, C. and Wang, X. (2002) The Arabidopsis phospholipase D family. Characterization of a calcium-independent and phosphatidylcholine-selective PLDζ1 with distinct regulatory domains. *Plant Physiol.*, **128**, 1057-1068.

Roberts, R.J. and Murray, K. (1976) Restriction Endonuclease. *Crit. Rev. Biochem. Mol. Biol.*, **4**, 123-164.

Roughan, P. and Slack, C. (1982) Cellular organization of glycerolipid metabolism. *Annu. Rev. Plant Physiol.*, **33**, 97-132.

Roughan, P., Slack, C. and Holland, R. (1978) Generation of phospholipid artefacts during extraction of developing soybean seeds with methanolic solvents. *Lipids*, **13**, 497-503.

Saitou, N. and Nei, M. (1987) The neighbor-joining method: a new method for reconstructing phylogenetic trees. *Mol. Biol. Evol.*, **4**, 406-425.

Sakurai, T., Satou, M., Akiyama, K., Iida, K., Seki, M., Kuromori, T., Ito, T., Konagaya, A., Toyoda, T. and Shinozaki, K. (2005) RARGE: a large-scale database of RIKEN Arabidopsis resources ranging from transcriptome to phenome. *Nucleic Acids Res.*, **33**, D647-D650.

Sato, N., Hagio, M., Wada, H. and Tsuzuki, M. (2000) Requirement of phosphatidylglycerol for photosynthetic function in thylakoid membranes. *P Natl. Acad. Sci. USA*, **97**, 10655-10660.

Schlame, M. and Greenberg, M.L. (1997) Cardiolipin synthase from yeast. *BBA - Lipids Lipid Metab.*, **1348**, 201-206.

Schlame, M. and Hostetler, K.Y. (1997) Cardiolipin synthase from mammalian mitochondria. *BBA - Lipids Lipid Metab.*, **1348**, 207-213.

Schlame, M., Ren, M., Xu, Y., Greenberg, M.L. and Haller, I. (2005) Molecular symmetry in mitochondrial cardiolipins. *Chem. Phys. Lipids*, **138**, 38-49.

Seki, M., Carninci, P., Nishiyama, Y., Hayashizaki, Y. and Shinozaki, K. (2003) High-efficiency cloning of Arabidopsis full-length cDNA by biotinylated CAP trapper. *Plant J.*, **15**, 707-720.

Seki, M., Narusaka, M., Kamiya, A., Ishida, J., Satou, M., Sakurai, T., Nakajima, M., Enju, A., Akiyama, K. and Oono, Y. (2002) Functional annotation of a full-length Arabidopsis cDNA collection. *Science*, **296**, 141-145.

Shen, H. and Dowhan, W. (1997) Regulation of phospholipid biosynthetic enzymes by the level of CDP-diacylglycerol synthase activity. *J. Biol. Chem.*, **272**, 11215-11220.

Shen, H., Heacock, P.N., Clancey, C.J. and Dowhan, W. (1996) The CDS1 gene encoding CDP-diacylglycerol synthase in Saccharomyces cerevisiae is essential for cell growth. *J. Biol. Chem.*, **271**, 789-795.

Somerville, C., Browse, J., Jaworski, J.G. and Ohlrogge, J. (2000) *Biochemistry and Molecular Biology of Plants: Chapter 10 Lipids.* Rockville, Maryland, USA.

Sparkes, I.A., Runions, J., Kearns, A. and Hawes, C. (2006) Rapid, transient expression of fluorescent fusion proteins in tobacco plants and generation of stably transformed plants. *Nat. Protoc.*, **1**, 2019-2025.

Sparrow, C.P. and Raetz, C. (1985) Purification and properties of the membrane-bound CDP-diglyceride synthetase from Escherichia coli. *J. Biol. Chem.*, **260**, 12084-12091.

Testerink, C. and Munnik, T. (2005) Phosphatidic acid: a multifunctional stress signaling lipid in plants. *Trends Plant Sci.*, **10**, 368-375.

Testerink, C. and Munnik, T. (2011) Molecular, cellular, and physiological responses to phosphatidic acid formation in plants. *J. Exp. Bot.*, **62**, 2349-2361.

Valianpour, F., Wanders, R.J., Barth, P.G., Overmars, H. and van Gennip, A.H. (2002) Quantitative and compositional study of cardiolipin in platelets by electrospray ionization mass spectrometry: application for the identification of Barth syndrome patients. *Clin. Chem.*, **48**, 1390-1397.

Van Schooten, B., Testerink, C. and Munnik, T. (2006) Signalling diacylglycerol pyrophosphate, a new phosphatidic acid metabolite. *BBA - Mol. Cell Biol. Lipids*, **1761**, 151-159.

Vaz, F.M., Houtkooper, R.H., Valianpour, F., Barth, P.G. and Wanders, R.J.A. (2003) Only one splice variant of the human TAZ gene encodes a functional protein with a role in cardiolipin metabolism. *J. Biol. Chem.*, **278**, 43089-43094.

Volta, M., Bulfone, A., Gattuso, C., Rossi, E., Mariani, M., Consalez, G., Zuffardi, O., Ballabio, A., Banfi, S. and Franco, B. (1999) Identification and Characterization of CDS2, a Mammalian Homolog of the Drosophila CDP-diacylglycerol Synthase Gene. *Genomics*, **55**, 68-77.

Weeks, R., DOWHAN, W., SHEN, H., BALANTAC, N., MEENGS, B., NUDELMAN, E. and LEUNG, D.W. (1997) Isolation and expression of an isoform of human CDP-diacylglycerol synthase cDNA. *DNA Cell Biol.*, **16**, 281-289.

Welti, R., Li, W., Li, M., Sang, Y., Biesiada, H., Zhou, H.E., Rajashekar, C., Williams, T.D. and Wang, X. (2002) Profiling membrane lipids in plant stress responses. *J. Biol. Chem.*, **277**, 31994-32002.

Wesley, S.V., Helliwell, C.A., Smith, N.A., Wang, M., Rouse, D.T., Liu, Q., Gooding, P.S., Singh, S.P., Abbott, D. and Stoutjesdijk, P.A. (2001) Construct design for efficient, effective and high-throughput gene silencing in plants. *Plant J.*, **27**, 581-590.

White, D.A., Albright, F.R., Lennarz, W. and Schnaitman, C.A. (1971) Distribution of phospholipid-synthesizing enzymes in the wall and membrane subfractions of the envelope of Escherichia coli. *BBA - Lipids Lipid Metab.*, **249**, 636-642.

Williams, J., Khan, M. and Wong, D. (1995) A simple technique for the analysis of positional distribution of fatty acids on di-and triacylglycerols using lipase and phospholipase A2. *J. Lipid Res.*, **36**, 1407-1412.

Winter, D., Vinegar, B., Nahal, H., Ammar, R., Wilson, G.V. and Provart, N.J. (2007) An "electronic fluorescent pictograph" browser for exploring and analyzing large-scale biological data sets. *PLOS One*, **2**, e718.

Wu, L., Niemeyer, B., Colley, N., Socolich, M. and Zuker, C.S. (1995) Regulation of PLC-mediated signalling in vivo by CDP-diacylglycerol synthase. *Nature*, **373**, 216-222.

Xu, C., Fan, J., Froehlich, J.E., Awai, K. and Benning, C. (2005) Mutation of the TGD1 chloroplast envelope protein affects phosphatidate metabolism in Arabidopsis. *Plant Cell*, **17**, 3094-3110.

Xu, C., Hartel, H., Wada, H., Hagio, M., Yu, B., Eakin, C. and Benning, C. (2002) The pgp1 mutant locus of Arabidopsis encodes a phosphatidylglycerolphosphate synthase with impaired activity. *Plant Physiol.*, **129**, 594-604.

Xu, C., Yu, B., Cornish, A.J., Froehlich, J.E. and Benning, C. (2006) Phosphatidylglycerol biosynthesis in chloroplasts of Arabidopsis mutants deficient in acyl-ACP glycerol-3-phosphate acyltransferase. *Plant J.*, **47**, 296-309.

Xue, H.W., Chen, X. and Mei, Y. (2009) Function and regulation of phospholipid signalling in plants. *Biochem. J.*, **421**, 145.

Xue, H.W., Hosaka, K., Plesch, G. and Mueller-Roeber, B. (2000) Cloning of Arabidopsis thaliana phosphatidylinositol synthase and functional expression in the yeast pis mutant. *Plant Mol. Biol.*, **42**, 757-764.

Yamaoka, Y., Yu, Y., Mizoi, J., Fujiki, Y., Saito, K., Nishijima, M., Lee, Y. and Nishida, I. (2011) Phosphatidylserine synthase1 is required for microspore development in Arabidopsis thaliana. *Plant J.*, **67**, 648-661.

Yu, B. and Benning, C. (2003) Anionic lipids are required for chloroplast structure and function in Arabidopsis. *Plant J.*, **36**, 762-770.

Yu, B., Wakao, S., Fan, J. and Benning, C. (2004) Loss of plastidic lysophosphatidic acid acyltransferase causes embryo-lethality in Arabidopsis. *Plant Cell Physiol.*, **45**, 503-510.

Zheng, Z., Xia, Q., Dauk, M., Shen, W., Selvaraj, G. and Zou, J. (2003) Arabidopsis AtGPAT1, a member of the membrane-bound glycerol-3-phosphate acyltransferase gene family, is essential for tapetum differentiation and male fertility. *Plant Cell*, **15**, 1872-1887.

Zinser, E. and Daum, G. (1995) Isolation and biochemical characterization of organelles from the yeast, Saccharomyces cerevisiae. *Yeast*, **11**, 493-536.

Zuo, J., Niu, Q.W. and Chua, N.H. (2000) An estrogen receptor‐based transactivator XVE mediates highly inducible gene expression in transgenic plants. *Plant J.*, **24**, 265-273.

APPENDIX

1. Primer list

Table A1 List of primers used in this work with indications of sequence, length, melting temperature and purpose. GST, gene-specific sequence tags, are cloned into RNAi vector pAgrikola. F or R at the end of primer indicates forward primer or reverse primer. For cloning cDNA into entry vector pENTR, forward primers are added with a "CACC" before the start code ATG. Rwo is used for amplifying the whole cDNA without stop code. Xaa indicates the number of amino acids amplified. Intron For and Rev are primers for checking the inserted sequences in RNAi vector pWatergate. LP and RP are the flanking sequence primers for T-DNA insertion. LB and RB refer to the left and right border primers of T-DNA insertion. Primers for KanMX4 cassette and YBR029c yeast mutant are used to check the yeast genotype of WT and *cds1* null mutant.

Name	**Sequence 5' → 3'**	**Length/bp**	**Tm/°C**	**Target/purpose**
Agri51	CAACCACGTCTTCAAAGCAA	20	55.3	GST in pAgrikola
Agri56	CTGGGGTACCGAATTCCTC	19	58.8	
Agri64	CTTGCGCTGCAGTTATCATC	20	57.3	
Agri69	AGGCGTCTCGCATATCTCAT	20	57.3	
4g22340GST_F	TAATCACAAGCCTGACATTGG	21	55.9	*CDS2* GST
4g22340GST_R	CATGTACCAGTACTATACAGAGGAA	25	59.7	
CDS1_F	CACCATGGAGGAAGAGAATGTTACTAG	27	63.4	CDS1
CDS1_R	CTATGAGAGCTTGTCCTTCAGCATT	25	61.3	
CDS1_Rwo	TGAGAGCTTGTCCTTCAGCATTTGT	25	61.3	
CDS1_100aa	TTTATCCTCAGGAGCTTTCCTCAGCAG	27	65.0	
CDS1_174aa	GTACATCTTCTTCTTTAATGTGAGAATGAAC	31	61.6	
CDS2.1_F	CACCATGCAGAAGGAAATTGCTGGTG	26	64.8	CDS2
CDS2.1_R	CTAAGATCCAATAACCTTTTCCTGCAACATTTGG	34	65.9	
CDS2.1_Rwo	AGATCCAATAACCTTTCCTGCAACATTTGG	30	64.0	
CDS2.1_174aa	GTACATCTTCTTTTTCAGCGTGAGAATAAAC	31	62.9	
CDS2.3_F	CACCATGCTAGATGTACTCAAGTTCAATTT	30	62.7	
CDS3_F	CACCATGGCAATGGAGAAAGATC	23	60.6	CDS3
CDS3_R	TTAAAACCTCCCTTGCAACTTATGTT	26	58.5	
CDS3_Rwo	AAACCTCCCTTGCAACTTATGTT	23	57.1	
CDS3_100aa	TGTCCTTATCCACATTGATCTGTACTTG	28	62.2	
CDS3_150aa	GGGTAAGCGACGTTCTTCATGAG	23	62.4	
CDS3_248aa	ATTGGCGACGGTGAAAGAAGATTGAGTAA	29	63.9	
CDS4_F	CACCATGGCGACTTTTGCTGAACTTG	26	64.8	CDS4
CDS4_R	TCAAACTCCGTAAAGTTTTAGGG	23	57.1	
CDS4_Rwo	AACTCCGTAAAGTTTTAGGGATG	23	57.1	
CDS5_F	CACCATGGCGCCTTTTGTTGAAGTC	25	64.6	CDS5
CDS5_R	TCAAACTCCATGAAGTCTTACGAACGAGTAG	31	65.5	
CDS5_Rwo	AACTCCATGAAGTCTTACGAACGAGTAG	28	63.7	

Name	Sequence 5’ → 3’	Length/bp	Tm/°C	Target/purpose
Intron For	TGCGCTGCAGTTATCATCATCATCATAGACAC	32	66.9	Intron in pWatergate
Intron Rev	TAATGCTAGTATATCATCTTACATGTTCGATC	32	61.8	
LBb1.3	ATTTTGCCGATTTCGGAAC	19	52.4	T-DNA (SALK)
LB4	CGTGTGCCAGGTGCCCACGGAATAGT	26	70.9	T-DNA (FLAG)
RB4	TCACGGGTTGGGGTTTCTACAGGAC	25	67.9	T-DNA (FLAG)
088268_LP	TGCTTGCTCTCTCTTCCAGAG	21	59.8	*cds1* (Salk_088268)
088268_RP	TGCAGAGGAAACCAAACAAAC	21	55.9	
LP_011704	TTTTTGTTTGGGTTGCTCAAC	21	54	*cds2* (Salk_011704)
RP_011704	CCATGTGGTATTTGATGAGGC	22	57.9	
LP_002579	AGGTGCCACAAGTGATTTCAC	21	57.9	*cds3* (Salk_002579)
RP_002579	GAGGAAATGAATTTGGGGTTG	21	55.9	
LP_115705	TTCTCTTCTGCCTTATCGTCG	21	57.9	*cds4* (Salk_115705)
RP_115705	AACCCATCCTCCAGCTAACAC	21	59.8	
LP_568C12	GTGCTCAAAAGTTGCTTGTCC	21	57.9	*cds5* (FLAG_568C12)
RP_568C12	CGAATCTTCTTCAACATTTTGC	22	54.7	
H1F1_T35S	TGCGGACTCTAGCATGG	17	55.2	35S promoter
H1R2_P35S	CCACTGACGTAAGGGATGAC	20	59.4	35S terminator
Olex_F1	ATATACAGCAGTCGAGGTAAG	21	55.9	XVE promoter
T3A_R1	ACCGATGATACGGACGAAAG	20	57.3	XVE terminator
H1F2_CDS1	GGCTAACCGTTGACTAAGG	19	56.7	CDS1 cDNA
H1R1_CDS1	GGATTCATCGGAGCCTCTG	19	58.8	
M7_CDS2_R1	AGTGTTGACTAGCCGTTGAC	20	57.3	CDS2 cDNA
M7_CDS2_F1	ACATGGGAGGGTTTCATTGG	20	57.3	
Oligo$(dT)_{18}$	TTTTTTTTTTTTTTTTT	18	33.2	RT-PCR
At2gqPF	GCTGCTCCTGCGCTTAACACT	21	61.8	qPCR CDS4
At2gqPR	CTGTCGCAATTACACCGCTGAA	22	60.3	
At3gqP_F	TCGTTGTCCTGGCCTCAATC	20	59.4	qPCR CDS5
At3gqP_R	TGAGTGAGCCGGAGTCTTTGA	21	59.8	
Actin2_F1	CATGGTTGGGATGAACCAGAAG	22	60.3	qPCR actin
Actin2_R1	TGCTCATACGGTCAGCGATAC	21	59.8	
M13F	GTAAAACGACGGCCAGT	17	52.8	sequencing
M13R	GGAAACAGCTATGACCATG	19	54.5	
kanB	CTGCAGCGAGGAGCCGTAAT	20	61.4	KanMX4-cassette
kanC	TGATTTTGATGACGAGCGTAAT	22	54.7	
029c_Aconf	AAACGCCCATGTAAATAACTATCAA	25	56.4	YBR029c yeast mutant
029c_Bconf	CCCTTTCTTAAACTACAAACGAACA	25	58.1	
029c_Cconf	CTTATACTTACTTGACGTGCCCTGT	25	61.3	
029c_Dconf	TGAGAAAATCATCCTAATTACTGCC	25	58.1	

2. Vectors used in this work

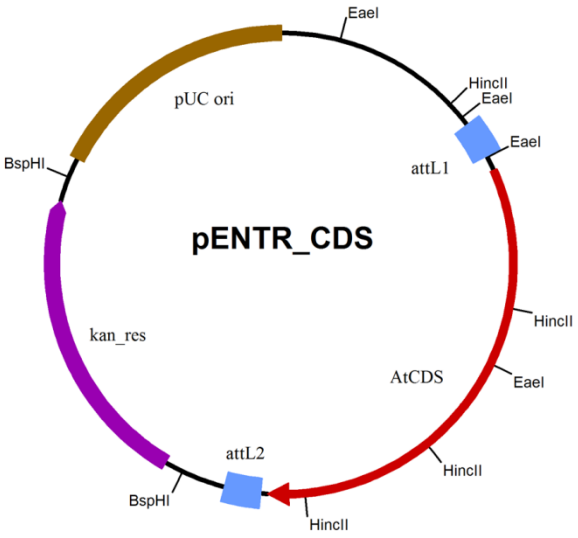

Figure A1 Map of pENTR_*CDS* construct. The enzyme sites of restriction analysis are given outside the vector. The features of the construct are shown: *AtCDS*, cDNA of *CDS* from Arabidopsis; attL1/attL2, recombination sequences for recombinational cloning of a gene of interest in the entry construct; kan_res, kanamycin resistance gene; pUC ori, pUC origin of replication that allow high-copy replication and maintenance in *E. coli*.

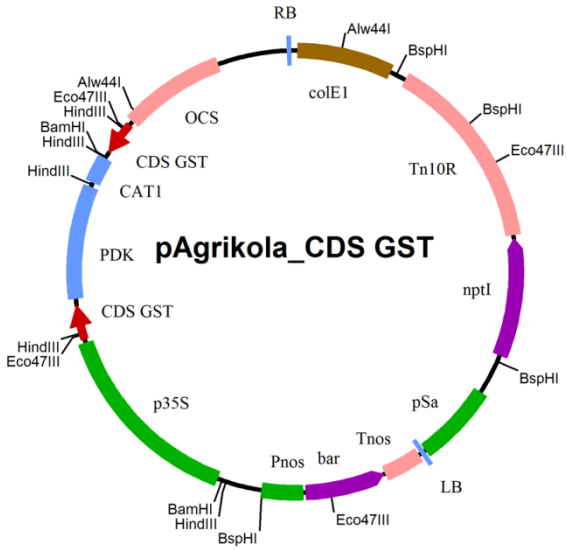

Figure A2 Map of pAgrikola_*CDS* construct. The enzyme sites of restriction analysis are given outside the vector. *CDS*_GST, gene-specific sequence tag of *CDS*; PDK and CAT1, sequence to facilitate the formation of hairpin structure; LB/RB, left/right border; nptI, kanamycin resistance gene; bar, herbicide bialaphos resistance gene; promoter p35S, pNOS and pSa are shown in green; terminator OCS, tNOS and Tn10R are shown in pink; colE1, the origin of replication.

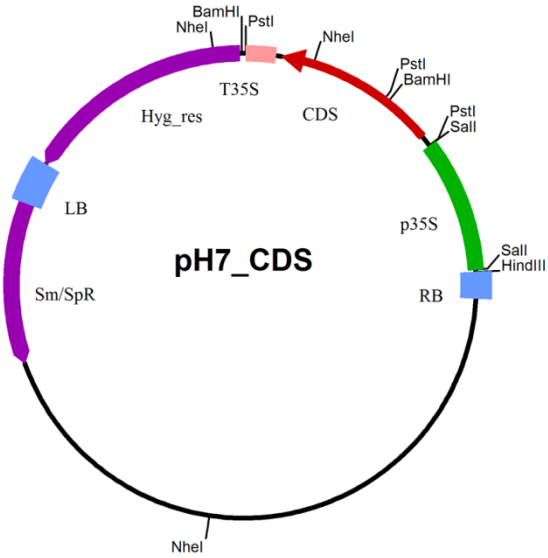

Figure A3 Map of pH7_CDS construct. The enzyme sites of restriction analysis are given outside the vector. CDS, cDNA of *CDS* from Arabidopsis; p35S, the CaMV 35S promoter; T35S, the CaMV 35S terminator; LB/RB, left/right border; Hyg_res, hygromycin resistance gene; Sm/SpR, streptomycin/ spectinomycin resistance gene.

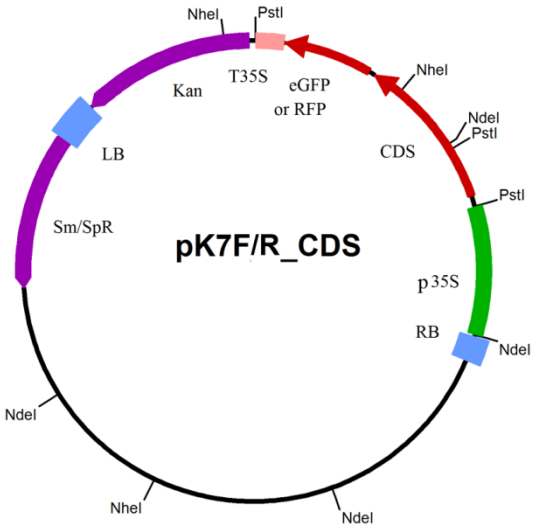

Figure A4 Map of pK7F/R_*CDS* construct. The enzyme sites of restriction analysis are given outside the vector. CDS, cDNA without stop codon of *CDS* from Arabidopsis; eGFP or RFP, enhanced green fluorescence protein gene or red fluorescence protein gene; p35S, the CaMV 35S promoter; T35S, the CaMV 35S terminator; LB/RB, left/right border; Kan, kanamycin resistance gene; Sm/SpR, streptomycin/ spectinomycin resistance gene.

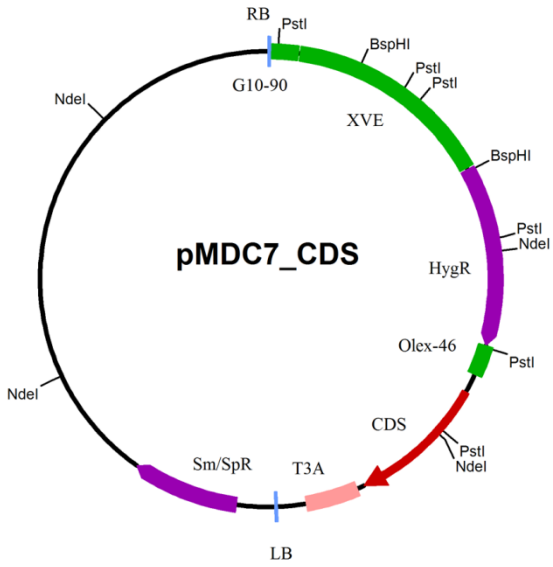

Figure A5 Map of pMDC7_*CDS* construct. The enzyme sites of restriction analysis are given outside the vector. CDS, cDNA of *CDS* from Arabidopsis; G10-90, a synthetic promoter controlling XVE; XVE, DNA sequences encoding a chimeric transcription factor containing the DNA-binding domain of LexA, the transcription activation domain of VP16 and the regulatory region of the human estrogen receptor; HygR, hygromycin resistance gene; Olex-46, eight copies of the LexA operator sequence; T3A, terminator; Sm/SpR, streptomycin/ spectinomycin resistance gene; LB/RB, left/right border.

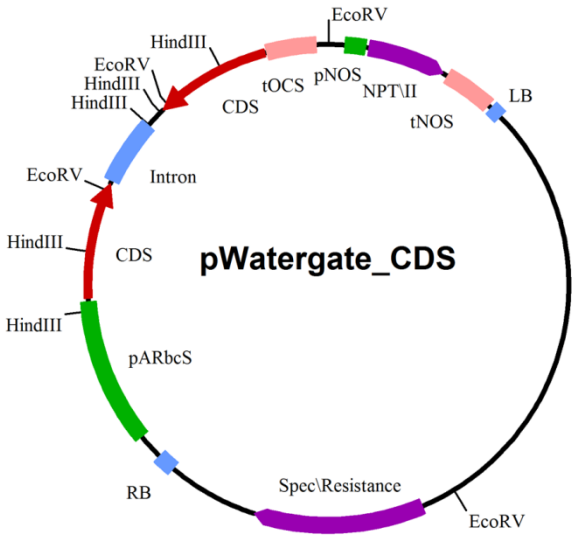

Figure A6 Map of pWatergate_*CDS* construct. The enzyme sites of restriction analysis are given outside the vector. CDS, the whole of part of cDNA of *CDS* from Arabidopsis; Intron, sequence to facilitate the formation of hairpin structure; pARbcS, Arabidopsis RbcS promoter; tOCS, OCS terminator sequence; pNOS/tNOS, the nopaline synthase promoter/terminator sequence; NPTII, kanamycin resistance gene; LB/RB, left/right border.

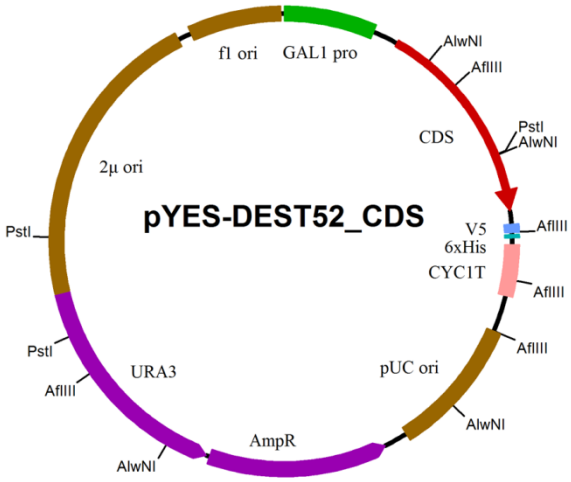

Figure A7 Map of pYES-DEST52_*CDS* construct. The enzyme sites of restriction analysis are given outside the vector. CDS, cDNA of *CDS* from Arabidopsis; GAL1 pro, galactose inducing promorter; CYC1T, CYC1 terminator sequence; URA3, uracile synthase gene; AmpR, ampicillin resistance gene; origins of replication f1 ori, 2µ ori and pUC ori are shown in brown.

3. List of tables

4. List of figures

DECLARATION

I confirm that the dissertation submitted is written independent by myself. This dissertation has not been published before and has not been submitted to any other faculty or university for examinations or accepted for any degree.

Aachen, August 2013 Yonghong Zhou

ACKNOWLEDGEMENTS

I would like to thank my supervisor Prof. Dr. Margrit Frentzen for the opportunity to work in her group and for her constant supports, patience and guidance throughout this work.

I acknowledge every former and present colleague in AG Frentzen for the helps of experiments and discussions. It is wonderful that all the members make the atmosphere in the lab so friendly and comfortable for working. Special thanks to Dr. Jens Gruber for the critical reading of the thesis.

I sincerely appreciate the help of Agnes Weth and Prof. Werner Baumgartner at Biology 2, who made the nice EM slides and photos. Thanks also go to Helga Peisker and Prof. Peter Dörmann from Institute of Molecular Physiology and Biotechnology of Plants, University of Bonn for their excellent work of steady state lipid composition.

I am grateful for the helps and support from the neighbor and other groups' members. Special thanks to Marco Löhrer for his help with laser confocal microscopy, to Prof. Nam-Hai Chua for kindly providing the vector of pMDC7, to Bo Yang and Yulei Zhao for reading the thesis.

I am deeply indebted to China Scholarship Council (CSC) for the financial support of my study in Germany.

I also would like to thank my parents and my wife Qiao for their support, keeping my mind in peace, stimulating me to pursuit what I want, and for everything…